Synthesis, Photochemical and Photophysical properties of Phthalocyanine derivatives.

A thesis submitted in fulfillment of the requirements for the degree

MASTER OF SCIENCE

By

WEZIWE THEORINE MAQANDA

December 2004

Acknowledgements

I would like to express my deepest gratitude to :

- Prof T. Nyokong and Dr D. Maree for their support and guidance through out the duration of this project.
- My family, especially my mother Oscarine Nombhedesho Nqwaba and my sister Tirry Nonzaliseko Maqanda for financial support and encouragement throughout the course of my studies.
- All my friends especially Prudence Tau, staff members and post graduate students of the Chemistry department at Rhodes University for their assistance in so many different ways.
- Above all, I give all honour to my Lord God and Savior Jesus Christ for his love, patience and guidance for being the greatest Scientist ever.
- National Research Foundation for financial support.

Contents

Abstract

Substituted zinc and magnesium phthalocyanine and porphyrazine derivatives were synthesized according to the reported procedures. The magnesium and zinc phthalocyanine and porphyrazine derivatives were synthesized by ring enlargement of subphthalocyanine and statistical condensation of the two phthalonitrile derivatives.

Characterization of the complexes involved the use of infrared spectroscopy, nuclear magnetic resonance spectroscopy, ultraviolet and visible spectroscopy, and Maldi-TOF spectroscopy (for selected compounds) and elemental analysis.

Photochemical and photophysical properties of the complexes in non-aqueous solution was then investigated. Photobleaching quantum yields are in order of 10^{-5} indicating their relative photostability. Complexes containing more electron-donating substituents were more easily oxidized. For complexes **66** and **69** (as these complexes have the same number of substituents but differ in the metal center) photobleaching quantum yield for the ZincPc complex **69** was slightly less than that of the MgPc complex **66**.

Singlet oxygen quantum yields of the various complexes in DMSO using diphenylisobenzofuran (DPBF) as a quencher in organic solvents were determined. Singlet oxygen quantum yields of the complexes range from 0.23 to 0.67.

High values of Φ_Δ ZnPc complexes was observed compared to the corresponding MgPc, complexes. This was evidenced by complexes **66** and **69** with Φ_Δ values of $\Phi_\Delta = 0.26$ and 0.40, respectively. Varying number of phenoxy substituents, complex **71** gave significantly large value of Φ_Δ compared to **70** (that is, the presence of more electron-donating substituted group, gave higher singlet oxygen quantum yields (0.67 and 0.25 for **71** and **70** repectively).

The triplet quantum yields and triplet lifetimes were determined by laser flash photolysis for selected compounds. The triplet quantum yields increase as the number of substituents increases e.g **68** > **67** > **66**.

Comparing porphyrazine complexes (**63**, **64** and **65**), **63** with benzene attached to the ring, has higher triplet state lifetime (420 μs) compared to **64** and **65** containing long alkyl chain and tertbutyl substituents, (350 and 360 μs, respectively).

The observed Φ_f values for **68** and **63** were quiet suprising, since low values are observed compared to the rest of the complexes (e.g 0.03 and 0.02 respectively). Although these values seem so low, they are sufficient for fluorescence imaging applications. The Φ_f values for the complexes under study are within the range reported for complexes currently used for PDT.

Table of contents

List of Abreviations

AlPcS	Aluminium sulphonated phthalocyanine
BCl_3	Boron trichloride
DABCO	Diazabicyclo-(2.2.2)-octane
DBU	1,8-Diazabicyclo[5.4.0]undec-7-ene
DMF	N,N-dimethylformamide
DMSO	Dimethylsulphoxide
DPBF	1,3-Diphenylisobenzofuran
^{1}HNMR	Nuclear magnetic resonance
H_2Pc	Free base or unmetalated phthalocyanine
Hp	Haematoporphyrin
HpD	Haematoporphyrin derivative
HOMO	Highest occupied molecular orbital
HPLC	High performance liquid chromatography
HVD	Hydroxylethylvinyldeuteroporphyrin
I	Intensity of light
I_{abs}	Absorbed light
$LiN(SiMe_3)_2$	Lithium bis(trimethyl)silyl amine
LUMO	Lowest unoccupied molecular orbital
MPc	Metallophthalocyanine
MS	Mass spectroscopy
m-THPC	*meta-Tetra hydroxyphenyl chlorine*
NLO	Non-linear optics

Pc	Phthalocyanine
PDT	Photodynamic therapy
Pz	Porphyrazine
Pp	Protoporphyrin
SubPc	Subphthalocyanine
TFA	Trifluoroacetic acid
THF	Tetrahydrofuran
TLC	Thin layer chromatography
UV/Vis	Ultraviolet visible
ZnPc	Zinc phthalocyanine
s	Singlet
d	Doublet
t	Triplet
q	Quartet
m	Multiplet
bs	Broad singlet
dd	Doublet of doublet

List of symbols

α	fraction of light absorbed
λ_{max}	wavelength
ν	stretching vibrations (IR)
π	pi
π^*	pi antibonding orbital
σ	sigma
Φ_{Δ}	quantum yield of singlet oxygen
Φ_T	triplet state quantum yield
Φ_{DPBF}	quantum yield of DPBF
Φ_D	Photobleaching quantum yield
Φ_{DPBF}^{MPc}	quantum yield of DPBF in the presence of MPc
Φ_{DPBF}^{ZnPc}	quantum yield of DPBF in the presence of ZnPc
τ_T	triplet lifetimes
ε	extinction coefficient
$^1O_2$	singlet oxygen
$^3O_2$	triplet oxygen
hv	light energy
nm	nanometer
$^1S^*$	excited singlet state
S0	ground state
$^3S^*$	excited triplet state

NOTE: For the sake of simplicity, schemes, figures, tables and references are numbered separately according to chapters 1, 2 and 3.

List of Schemes

List of figures

List of tables

1. Introduction

1.1 Tetrapyrrole-Macrocycles

Porphyrins (**1**), porphyrazines (**2**) and phthalocyanines (**3**) have found applications in a number of fields including pigments and dyes [1-4], photosensitization in photodynamic therapy (PDT) [5-14], electrocatalysis [15-18], materials for electrophotography [19], optical information storage systems [20], and other applications [21-25].

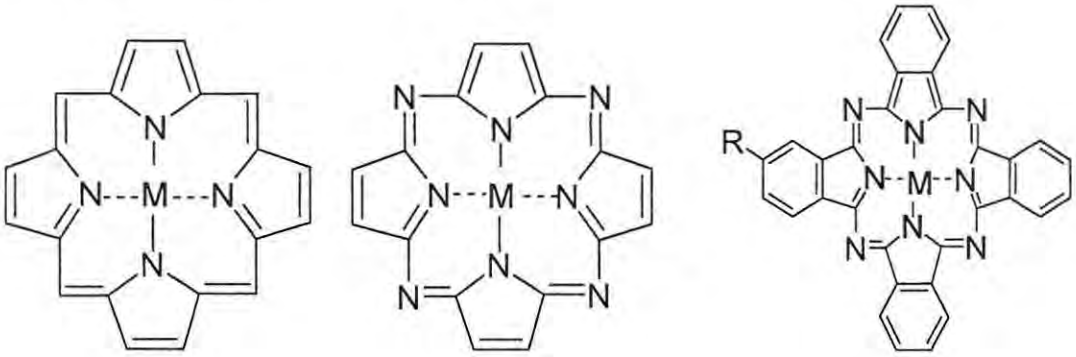

1 **2** **3**

Figure 1.1 Structures of metallated Porphyrin (**1**), Porphyrazine (**2**), and Phthalocyanine (**3**)

As can be seen in Figure 1.1 these compounds all share a similar generic structure (in that they are all tetrapyrrole compounds), hence similar characteristics are observed. Porphyrazines (**2**), are also refered to as tetraazaporphyrins [26-30]. These molecules share the core structure of the phthalocyanines (**3**) also refered to as tetrabenzoporphyrazines [29]), but have unique properties not exhibited by either porphyrins (**1**) or phthalocyanines (**3**) [27,30]. However, due to the nature of these compounds (**1**, **2**, **3**) their physical properties and characteristics required for technological applications can be manipulated by altering substituents on peripheral and non-peripheral positions, and also by coordinating various metals [1,26,28,31-34] to the central positions.

The design and synthesis of unsymmetrically substituted macrocycles enhances the technological applications of phthalocyanines and porphyrazines [35-41]. It

is therefore in our interest to be able to tailor these compounds in order to control their behaviour and characteristics, so as to make them more useful in specific applications. In the medical field, these compounds have been used as biomedical agents for diagnosis and therapy, which mainly includes photodynamic treatment of cancer [26] .

1.2 Photodynamic therapy

1.2.1 Background on photodynamic therapy

Photodynamic therapy (PDT) is a revolutionary medical technology which provides an alternative form of cancer therapy as opposed to radiotherapy and chemotherapy which are methods that can induce disabling and life threatening side effects by destroying both normal and tumour cells [42].
One of the main advantages of PDT in for example lung cancer is that, it works in places where surgery would not be feasible, such as the trachea, the major airway leading from the voice box to the lungs, as is shown in Figure 1.2.

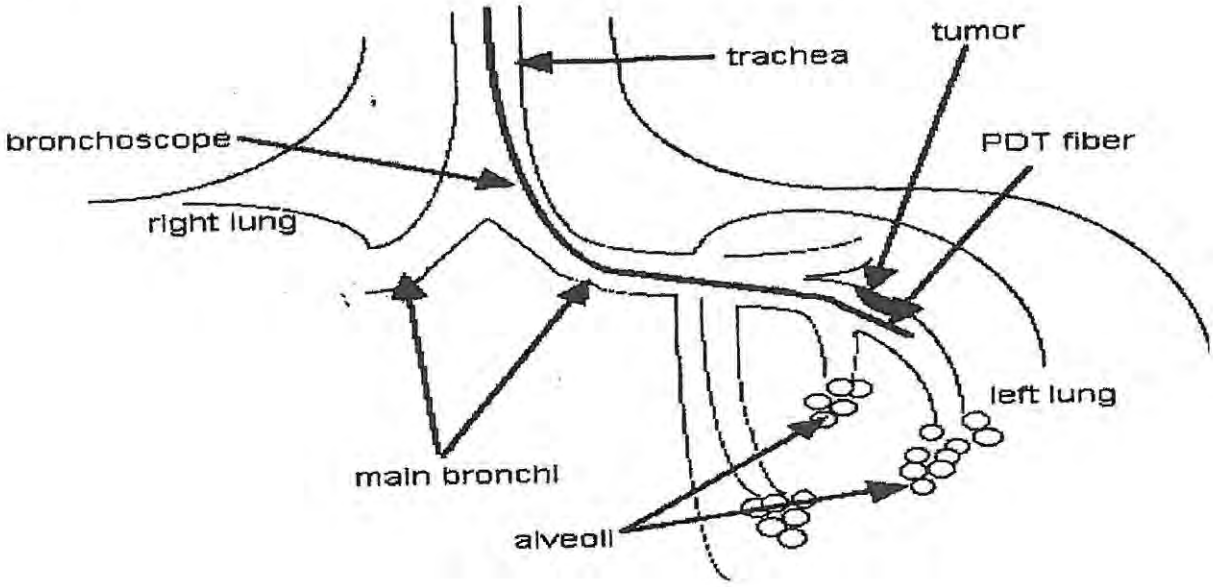

Figure 1.2 The use of PDT for lung cancer.

Where:
alveoli : tiny sacs that take in oxygen

trachea : the main airway that leads from the throat to the bronchi
bronchi : the two major airways that leads from the trachea to the right and left lungs.

The treatment is performed by inserting a bronchoscope through the patient's mouth, directed into a brochis so that when the laser is turned on, light shines from the end of the optical fiber to the tumour. Red light (> 600 nm) is used for PDT because it penetrates more deeply into tissues than other colors or wavelengths of light [43-48]. PDT can be repeated a number of times which is not the case in most other treatments. PDT utilises oxygen and light, to create a photochemical reaction that selectively destroys cancer cells [43,45-47,49-53]. In PDT, a drug or dye is administered to the patient intravenously [26]. The drug travels through the blood stream and localizes on or in cancer cells. After an appropriate time (24 -78 hours) the localized drug is activated with light. The cancer cells are destroyed, while leaving the normal cells intact. The extent of this selectivity depends on the type of drug administered [48]. Since the approval of Photofrin a number of other drugs have been studied and have shown excellent results for the PDT treatment of cancers such as lung, skin, head, neck, throat and reproductive organs [43,54-56]. New photodynamic therapy drugs are currently being studied for treatment of brain and breast cancer as well as leukemia [57]. In targeting the tumours using PDT, a number of factors must be taken into consideration, including:

>**Localization of photosensitizers in tumours**. Some sensitizers have the ability to concentrate more in tumours relative to the surrounding healthy tissue and therefore offer a beneficial therapeutic ratio for treatment.

>**Activated oxygen**. PDT is known to work through the production of activated oxygen known as singlet oxygen, which is so reactive that it does not escape from the cell in which it was produced. PDT is therefore a local technique at the cellular level and does not produce cytotoxic agents that may diffuse widely from its point of origin.

>**Lasers and fibre opticts**. It is probably developments in lasers and fibre optics more than any other factors that have led to PDT becoming a viable

clinical tool in recent years. By using fibre optics coupled with the various techniques of endoscopy it is possible to deliver light with precision to most parts of the body.

1.2.2 Sensitizers in use for photodynamic therapy

The first sensitizer used in clinical PDT was haematoporphyrin (HpD) derivative and its purified fraction, Photofrin [45-47,58]. It is prepared by acetylation of heamatoporphyrin (Hp) (Figure 1.3) [45], followed by neutralisation prior to alkaline hydrolysis to give the mixture that contains heamatoporphyrin, hydroxyethylvinyldeuteroporphyrin (HVD) and protoporphyrin (Pp), as well as a complex dimeric and oligomeric fractions containing esters, ethers and carbon-carbon linked heamatoporphyrin derivatives. HpD [43,51] is typically 45% monomeric/dimeric porphyrins and 50% oligomeric material. However, this is a disadvantage of HpD, since some compounds are PDT inactive and it is difficult to reproduce the same properties from batch to batch [43,53]. HpD localises in both healthy and tumour cells and is cleared slowly from the body and thus patients have to be kept in the dark for long periods of time. Additionally, HpD has a low fluorescence quantum yield and a low efficiency for generation of singlet oxygen [53]. Photofrin shows a large absorption band around 400 nm (the Soret band) with progressively smaller bands out towards the red region (> 600 nm) of the electromagnetic spectrum. As mentioned above penetration of light into tissue is strongly wavelength dependant, with red light penetrating much more effectively than blue or violet light. PDT using Photofrin is perfomed at 630 nm [46]. New drugs are sought for PDT due to the imperfections of Photofrin, such as the fact that it is a complex mixture, that it has a relatively low absorption at the treatment wavelength and has a very long lifetime in the body which causes prolonged skin photosensitivity. Illumination is usually carried out 48hr after systematic administration of Photofrin, when the accumulation of sensitizer by tumour tissue is thought to be optimal [8,59,60].

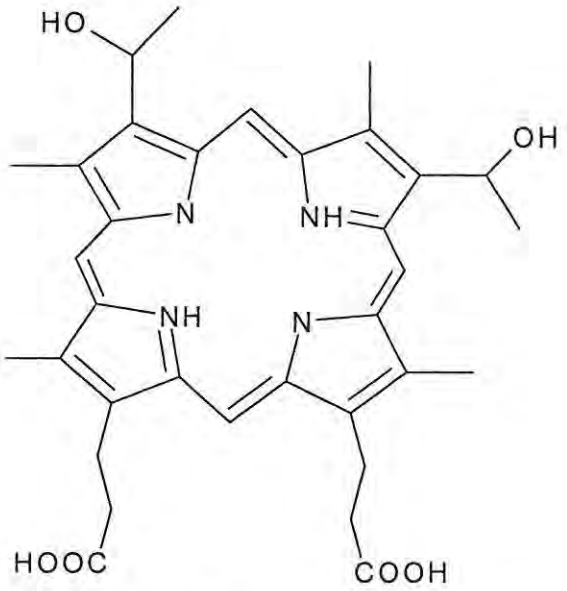

4

Figure 1.3 Structure of heamatoporphyrin (4)

New photosensitizers have been synthesised that have better properties than HpD. Following the success of PDT a number of so called "second generation" photosensitizers [61,62] have been developed. These include modified porphyrins [43,47,48], chlorins [63-66], bacteriochlorins, phthalocyanine (**3**) [67], pheophorbides [68], pupurins [69,70] and benzoporpyhrins [71,72]. These photosensitizers show increased efficacy in PDT for many different reasons, such as improved photophysical properties as demonstrated by their longer wavelengths, thus increasing tissue penetration. The properties of some of the photosensitizers are summarised below.

1.2.2.1 Chlorins and Bacteriochlorins

In chlorins one of the exo-pyrrole double bonds of the porphyrin (**1**) ring is hydrogenated, resulting in an intense absorption at wavelengths greater than 650 nm [73]. In bacteriochlorins, two of the exo-pyrrole double bonds of the porphyrin (**1**) ring are hydrogenated, yielding compounds with maximum absorption at even longer wavelength. Because of these improved optical

properties, chlorins and bacteriochlorins are being intensively studied as potential new drugs for PDT.

meta-Tetra hydroxyphenyl chlorin (m-THPC)

The first clinical study with m-THPC (Figure 1.4) began in 1990 for the treatment of human mesothelioma and it is currently in clinical trials [48,60, 74-76] for gyneocological, respiratory and head and neck cancers in USA, Europe and the UK. m-THPC is a second generation photosensitizer, developed for clinical use by Scotia QuantaNova. m-THPC has a hydrophobic chlorin core and hydroxyphenyl groups at the meso position to increase solubility of the photosensitizer [46]. m-THPC is a single pure compound, rather than a mixture of porphyrins. It is excited at a wavelength longer than that of Photofrin [76] and the molar absorbance coefficient for m-THPC is also much higher than that of Photofrin. m-THPC has a longer half life than Photofrin in the triplet state generating more cytotoxic oxygen species, and is more selective between tumour and normal tissue [45]. m-THPC is more hydrophobic than Photofrin which increases cellular uptake leading to higher efficacy *in vitro* [45,77].

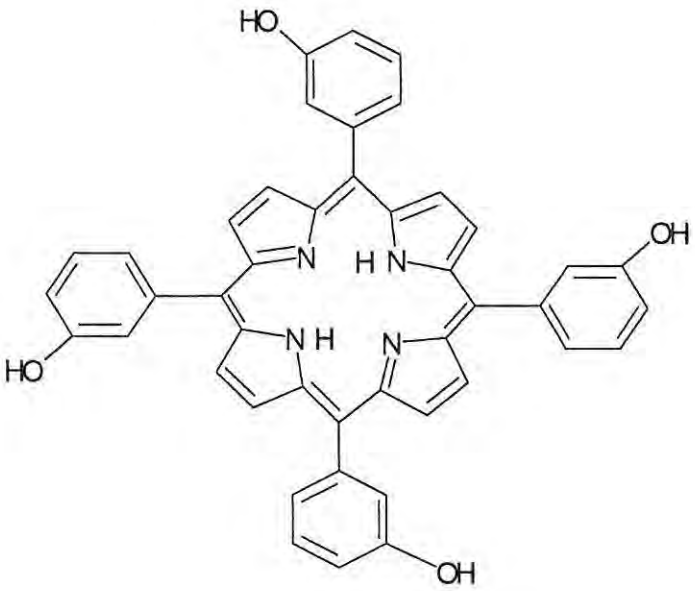

5

Figure 1.4 Structure of m-Tetra hydroxyphenyl chlorin (m-THPC) (**5**).

Mono-L-aspartyl chlorin e6

Mono-L-aspartyl chlorin e6 [71] (Figure 1.5) is a highly water soluble chlorin-type photosensitizer. It has an absorbance peak at 654 nm and is effective *in vitro* and *in vivo*. Efficient photodynamic damage with little skin phototoxicity [71] characterise this compound.

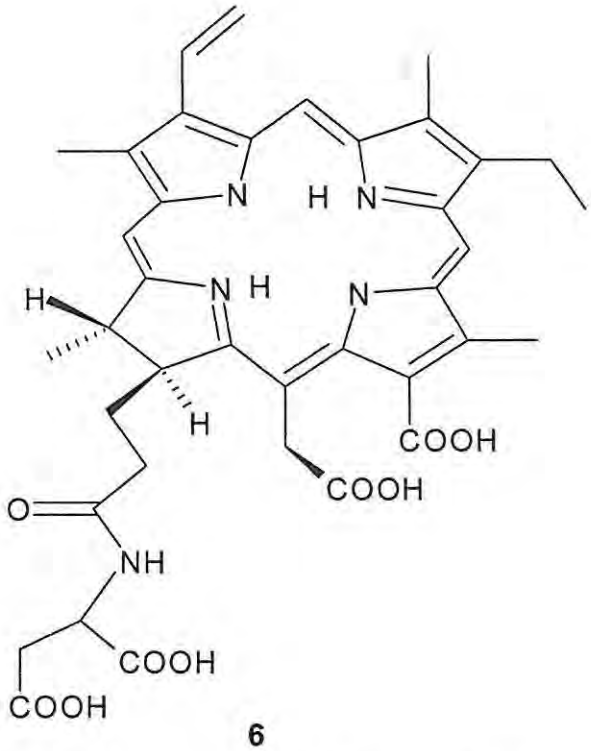

6

Figure 1.5 Structure of Mono-L-aspartyl chlorin e6 (**6**)

1.2.2.2 Phthalocyanines

Remarkable progress has been made over the years in the use of metallophthalocyanines (MPc) as sensitizers for PDT. Phthalocyanines [8,46,47, 78] are generally hydrophobic compounds although water-soluble derivatives can be readily synthesised through substitution of the ring with moieties such as sulphonic acid, carboxylic acid and amine groups [8,26,78]. The sulphonated compounds, and in particular hydroxy aluminium sulphonated phthalocyanine (OHAlPcS) complexes (Figure 1.6) have received the most

attention with regard to photodynamic efficacy. The sulphonated compounds have been observed to aggregate at relatively low concentrations in aqueous media which results in loss of photochemical activity. OHAlPcS exhibits selective retention in some tumours. This coupled with negligible dark-toxicity, minimal cutaneous photosensitivity, and excellent photodynamic activity at longer wavelengths has led to the clinical evaluation of OHAlPcS for PDT [46,48].

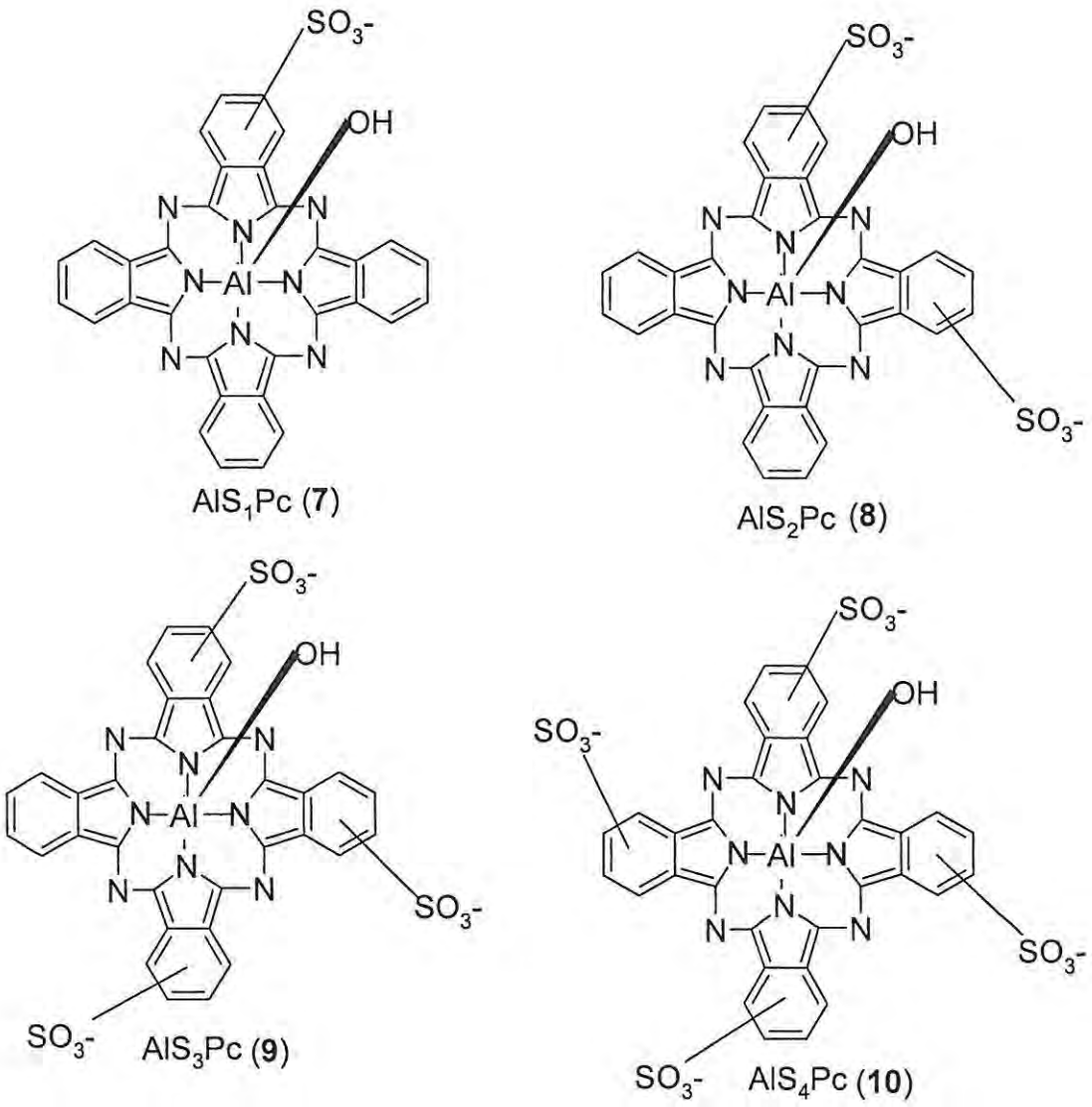

Figure 1.6 Mono- (7), di- (8), tri- (9) and tetra-sulphonated aluminium phthalocyanines (**10**) .

1.2.3 Mechanisms of photodynamic therapy

The cytotoxic agent in PDT is produced by one of two different processes, which in photochemistry are referred to as Type I or Type II processes [79]. Type I, (Scheme 1.1.) involves electron / hydrogen transfer directly from the photosensitizer producing ions, or electron / hydrogen abstraction from a substrate molecule to form a free radicals [52,80,81]. These radicals then react rapidly, usually with oxygen, resulting in the production of highly reactive oxygen species [46-48]. These radicals then attack the cellular target.

$S + h\nu \longrightarrow {}^1S^*$ Absorption of light to give singlet state

${}^1S^* \longrightarrow {}^3S^*$ Intersystem crossing to give long lived triplet state

${}^3S^* + {}^1O_2 \longrightarrow S^{+\cdot} + O_2^{-\cdot}$

${}^3S^* + Sub \longrightarrow Pc^{-\cdot} + Sub^{+\cdot}$

$S^{-\cdot} + {}^1O_2 \longrightarrow S + O_2^{-\cdot}$

$O_2^{-\cdot} \xrightarrow{H+} HO_2^{\cdot}$

$HO_2^{\cdot} + Sub\text{-}H \longrightarrow H_2O_2 + Sub^{\cdot}$

$Sub^{+\cdot}, Sub^{\cdot}, H_2O_2 \longrightarrow$ tumour necrosis.

Scheme 1.1 Type I mechanism, where S = sensitizer, Sub = substrate.

Type II mechanism (Scheme 1.2) involves energy transfer from the sensitizer, to the ground state oxygen. A molecule of the drug / sensitizer absorbs a photon of red light and is excited to the first excited singlet state. Energy can be transferred from the singlet state to the triplet state through intersystem crossing. This triplet state can react with local oxygen molecules,

creating an excited state of oxygen called singlet oxygen, which will destroy tumour cells [26,47,48].

$S + h\nu \longrightarrow {}^1S^*$ Absorption of light to give singlet state

${}^1S^* \longrightarrow S + h\nu_F$ Fluorescence

${}^1S^* \longrightarrow {}^3S^*$ Intersystem crossing to give long-lived triplet state

${}^3S^* + O_2 \longrightarrow S + {}^1O_2$ Energy transfer to give singlet oxygen

${}^1O_2 + \text{Tissue} \longrightarrow \text{necrosis}$

Scheme 1.2 Type II mechanism

Both Type II and Type I mechanisms result in cytotoxic species causing oxidative destruction of tissue [46,48]. Type I and Type II mechanisms are in competition with each other depending on the magnitude of the rate constants, it is of importance for us to investigate the physical and chemical properties of the sensitizer to be used.

Oxygen is unique in that its ground state is the triplet state (Figure 1.7). Ground state oxygen has two unpaired electrons in the antibonding orbitals, hence it is described as a triplet state. The interaction of this oxygen with the excited sensitizer causes the spin of one of the electrons to invert. The electrons pair together into the π^*2p antibonding orbital, thus generating the extremely reactive singlet oxygen due to the destabilization of the molecule [45].

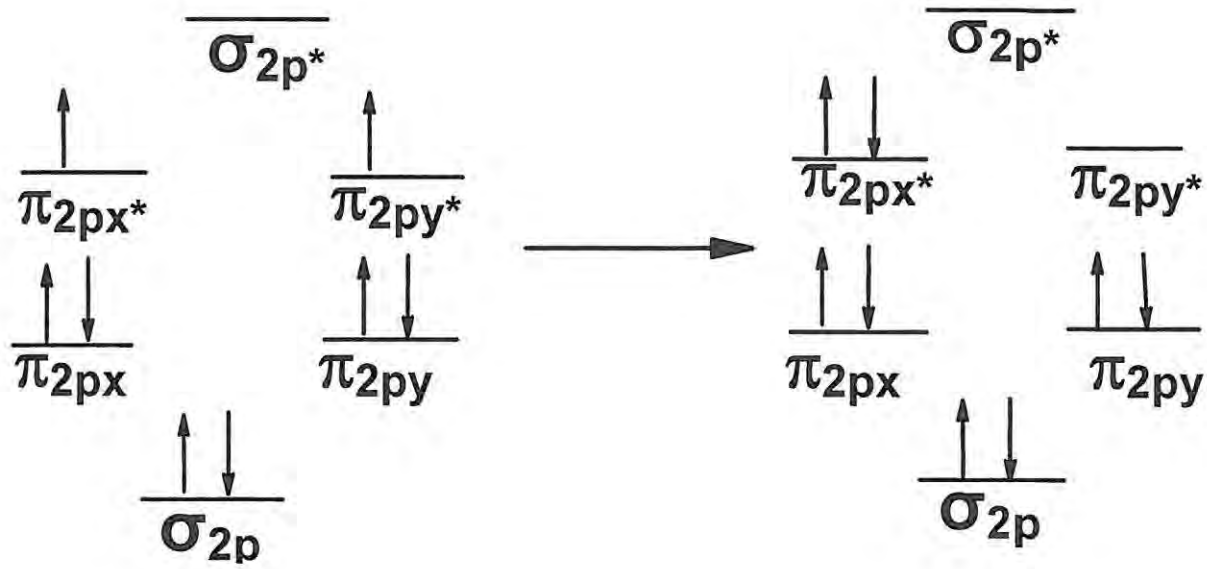

Figure 1.7 The molecular orbital diagrams of oxygen, with electron distribution in triplet oxygen and singlet oxygen.

1.2.4. The fate of the excited sensitizer (Jablonski diagram, Figure 1.8)

Photosensitizers have a stable electronic configuration which is in a singlet state in their ground state. Absorption of a photon of light, results in an excited state molecule, which is also a singlet state and is short lived. The molecules returns to the ground state through any of the following processes:

1. **Radiative transitions** (Figure 1.8) including ***fluorescence*** photon emission occurs between states of the same multiplicities, i.e. $S_1 \rightarrow S_o$, where S denotes the singlet state, ***phosphorescence***, when the photon emission occurs between states of different multiplicities,i.e $T_1 \rightarrow S_o$ (triplet to singlet state). Fluorescence is much more likely to occur than phosphorescence, The former generally has a shorter lifetime, i.e. $1x10^{-5}$ - $1x10^{-8}$ seconds. Phosphorescence is a spin-forbidden transition and its probability of occurring is low [82].

2. **Radiationless transitions** (Figure 1.8) occur through ***internal conversion*** (IC) (transition between states of the same multiplicities) or ***intersystem crossing*** (ISC) (transition between states of different multiplicities). ISC is also a spin-forbidden transition, it occurs due to a small energy separation between the states. ***Vibrational relaxation*** (VR), which occurs due to molecular collisions, resulting in the loss of energy to the environment, e.g. solvents. These processes are demonstrated by a Jablonski diagram of an organic molecule such as metallophthalocyanine (Figure 1.8).

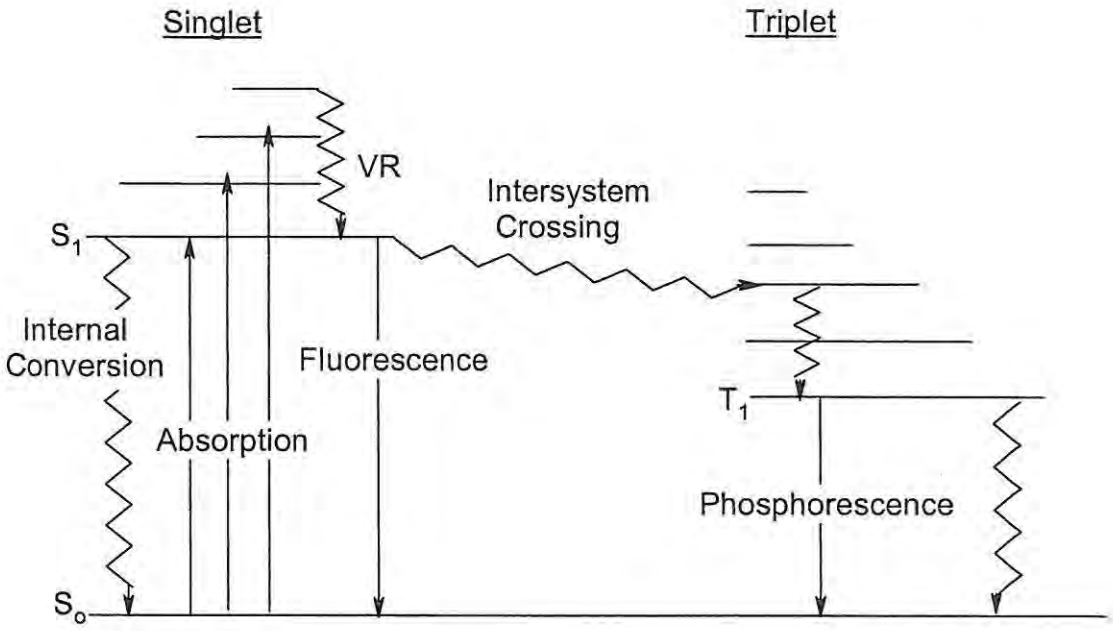

Figure 1.8 A Jablonski diagram, showing photophysical processes taking place upon irradiation with light.

The tendency of a photosensitizer to populate the triplet state is measured by the triplet state quantum yield, which measures the probability of formation of the triplet state per photon absorbed [83].

1.3 Determination of photochemical and photophysical parameters

1.3.1 Singlet oxygen determination

The ability to produce singlet oxygen is measured as the singlet oxygen quantum yield [84-88], denoted by Φ_Δ, which has been defined as the number of singlet oxygen molecules generated per photon absorbed by the sensitizer [86]. One way of determining singlet oxygen quantum yield is by using a chemical quencher such as 1,3-diphenylisobenzofuran (DPBF). DPBF is an efficient $^1O_2$ quencher in organic solvents and its disappearance can readily be monitored by following its absorption peak at 416 nm (in dimethylsulphoxide, DMSO for example). Scheme 1.3. shows the fate of $^1O_2$ in the presence or absence of DPBF.

$$^3O_2 \xrightarrow[^3MPc^*]{h\nu} {}^1O_2 \qquad \text{... 1}$$

$$^1O_2 \xrightarrow{k_d} {}^3O_2 \quad \text{(Natural decay)} \qquad \text{... 2}$$

$$^1O_2 + DPBF \xrightarrow{k_q} \text{Oxidation products (Chemical quenching)} \qquad \text{... 3}$$

$$^1O_2 + DPBF \xrightarrow{k_p} {}^3O_2 + DPBF^* \quad \text{(Physical quenching)} \qquad \text{... 4}$$

$$^1O_2 + MPc \longrightarrow {}^3O_2 + MPc^* \quad \text{(Physical quenching)} \qquad \text{... 5}$$

$$^1O_2 + MPc \longrightarrow \text{Chemical reaction (Chemical quenching)} \qquad \text{... 6}$$

Scheme 1.3 Physical and chemical reaction on $^1O_2$ determination.

DPBF acts exclusively as a chemical quencher in DMSO and other organic solvents [86,87,89], thus equation 4 is not important and can be ignored. Physical quenching through equation 5 can also be ignored since Φ_Δ does not depend on the concentration of the sensitizer (MPc). Futhermore, the reaction rate of the sensitizer with the $^1O_2$ according to equation 6 is negligible compared to

the rate of the reaction with the DPBF. Only equations 1, 2 and 3 are relevant to the decay of singlet oxygen.

The rate of disappearance of DPBF in the presence of singlet oxygen is given by equation 7 :

$$\text{Rate} = \frac{-d[DPBF]}{dt} = kq\ [\text{DPBF}][^1\text{O}_2] \qquad \ldots 7$$

By applying the steady state approximation for singlet oxygen and rearranging gives :

$$I_{abs} = k_d[^1\text{O}_2] + k_q[\text{DPBF}][^1\text{O}_2]$$
$$= [^1\text{O}_2](k_d + k_q[\text{DPBF}])$$

since

$$\Phi_\Delta = \frac{\text{rate of formation of } [^1\text{O}_2]}{I_{abs}}$$

then

$$\Phi_\Delta \,.\, I_{abs} = \text{rate of formation of } [^1\text{O}_2]$$
$$= [^1\text{O}_2](k_d + k_q\,[\text{DPBF}])$$

and

$$[^1\text{O}_2] = \frac{\Phi_\Delta . I_{abs}}{k_d + k_q[DPBF]} \qquad \ldots 8$$

substitution of equation 8 into 7 gives 9

$$\frac{-d[DPBF]}{dt} = \frac{k_q[DPBF].\Phi_\Delta.I_{abs}}{k_d + k_q[DPBF]} \qquad \ldots 9$$

where I_{abs} is the amount of light absorbed by the sensitizer and Φ_{Δ} the singlet oxygen quantum yield.

Since equation 10 applies.

$$\Phi_{DPBF} = \frac{-d[DPBF]/dt}{I_{abs}} \quad \text{... 10}$$

$$\Phi_{DPBF} \cdot I_{abs} = \frac{-d[DPBF]}{dt} \quad \text{... 11}$$

then sustitution of 11 into 9 gives 12

$$\Phi_{DPBF} = \frac{k_d[DPBF]\Phi_{\Delta}}{k_d + k_q[DPBF]} \quad \text{... 12}$$

At low concentrations of DPBF, $k_d >> k_q[DPBF]$ and equation 12 becomes 13

$$\Phi_{[DPBF]} = \frac{k_d[DPBF]\Phi_{\Delta}}{k_d} \quad \text{... 13}$$

The reaction kinetics at these low concentrations are first order, whereas they obey zero-order law at high [DPBF]. At high [DPBF] the rate of the reaction becomes independent of the concentration of the DPBF, which is not wanted in this case. Thus at low DPBF concentration, equation 13 applies for porphyrazine and phthalocyanine complexes, and may be represented by equation 14.

$$\Phi_{DPBF}^{MPc} = \frac{k_q}{k_d}[DPBF]^{MPc}\Phi_{\Delta}^{MPc} \quad \text{... 14}$$

Where Φ_{DPBF}^{MPc} is the DPBF quantum yield in the presence of MPc sensitizer,

Φ_{Δ}^{MPc} is the quantum yield of singlet oxygen in the presence of MPc and $[DPBF]^{MPc}$ is the concentration of DPBF in the presence of MPc.

$$\Phi_{DPBF}^{ZnPc} = \Phi_{\Delta}^{ZnPc} . \frac{k_q}{k_d} [DPBF]^{ZnPc} \quad \text{...15}$$

Where Φ_{DPBF}^{ZnPc} is the quantum yield of DPBF in the presence of ZnPc (used as standard) and Φ_{Δ}^{ZnPc} is the quantum yield of singlet oxygen in the presence of the ZnPc standard and $[DPBF]^{ZnPc}$ is the concentration of DPBF in the presence of ZnPc. Taking the ratio of equation 14 over 15, Φ_{Δ} of the unknown MPc can be determined through equation 16.

$$\Phi_{\Delta}^{MPc} = \Phi_{\Delta}^{ZnPc} . \frac{\Phi_{DPBF}^{MPc} . [DPBF]^{ZnPc}}{\Phi_{DPBF}^{ZnPc} . [DPBF]^{MPc}} \quad \text{... 16}$$

Φ_{DPBF} may also be defined by eq 17 :

$$\Phi_{DPBF} = \frac{(C_0 - C_t)V}{I_{abs} . t} \quad \text{... 17}$$

Where V is the volume of the sample in the cell, t is the photolysis time and C_o and C_t are the initial and final concentrations of DPBF during photolysis, respectively. I_{abs} is the light absorbed which is determined by equation 18.

$$I_{abs} = \frac{\alpha SI}{N_a} \quad \text{... 18}$$

Where α is the fraction of light absorbed, S is the cell area irradiated, N_a is Avogadro's constant and I the light intensity. Equation 19 can be obtained by substituting equation 18 into 17, then 17 into 16.

$$\Phi_{\Delta}^{MPc} = \Phi_{\Delta}^{ZnPc} \cdot \frac{(C_o - C_t)^{MPc} \cdot [DPBF]^{ZnPc} \cdot (\alpha t)^{ZnPc}}{(C_o - C_t)^{ZnPc} \cdot [DPBF]^{MPc} \cdot (\alpha t)^{MPc}} \quad \text{... 19}$$

where $(C_o\text{-}C_t)^{MPc}$, $(C_o\text{-}C_t)^{ZnPc}$, are the changes in the concentration of DPBF, in the presence of MPc and the ZnPc standard, respectively. t^{ZnPc} and t^{MPc} are the photolysis times in the presence of ZnPc and MPc respectively. S, V, and Na are the same for both the MPc and the ZnPc hence they cancel in equation 19.

1.3.2 Photobleaching quantum yield

Photobleaching (Φ_P) of the MPc is the loss of absorbance due to the degradation of the Pc ring on the exposure to light [90,91]. The quantum yield of photobleaching for the compounds can be determined using equation 20.

$$\Phi_P = \frac{(C_o - C_t)V}{I_{abs} \cdot t} \quad \text{.... 20}$$

C_0 and C_t represent the concentration of the sensitizer before and after the irradiation respectively, V is the sample volume and I_{abs} is the absorbed light which is determined by equation 18 [92-94]. The concentrations of the sensitizer are obtained using Q-band extinction coefficients. The concentrations may be obtained from Beer's law using $A = \varepsilon cl$, with ε the extinction coefficient, c the concentration and 1 the pathlength of the cell. Factors such as the central metal, axial ligands attached to the central metal, aggregation, medium temperature and solvents affect the photobleaching rates.

1.3.3 Determination of triplet lifetimes and triplet quantum yields

Deactivation of the triplet state, M*, to the ground state, S_0, can be described by equation 21:

$$\frac{d[M^*]}{dt} = k_1[M^*] + k_2[M^*][S_o] + 2k_3[M^*]^2 \text{-d[M*]} \quad \text{... 21}$$

where k_1 is the measured first order rate constant and is the sum of the radiative and non-radiative unimolecular decay processes. In most cases, for molecules in solution, the radiative process from the triplet state, i.e phosphorescence, is negligible. The second term in the equation is due to quenching of the excited triplet state by ground state molecules, i.e. self-quenching and the final term is due to quenching of the triplet by another triplet state i.e. triplet-triplet annihilation. At low concentrations of the sensitizer and low laser powers, only the first term in the equation is important and the rate constant k_1 is obtained from a first-order plot, equation 22.

i.e $\ln\frac{[M^*]_o}{[M^*]_t}$ vs t from $\ln\frac{[M^*]_o}{[M^*]_t} = k_1 t$ **...22**

where $[M^*]_o$ and $[M^*]_t$ are the triplet concentrations at time 0 and t respectively. The change in triplet concentration with time is directly proportional to the transmittance and hence the voltage change measured on the oscilloscope. Hence the change in absorbance, ΔA, can be calculated using the Beer-Lambert law, equation 22:

$$\Delta A = \varepsilon \Delta c l = \ln\frac{I_o}{I} = \ln\frac{V_\infty}{V_\infty - \Delta V} \quad \textbf{...23}$$

Where $l = 1$ cm pathlength, V_∞ is the 0 – 100% voltage and ΔV is the change in voltage observed on the oscilloscope. A linear plot of ln(A) versus time thus gives a gradient k_1 and its reciprocal, the triplet lifetime, $\tau_t = 1/k_1$.

Triplet quantum yields may be determined by the relative method (singlet depletion method) [92-95] using ZnPc as a standard [96], equation 24.

$$\Phi_T^{Sample} = \Phi_T^{Sample} \cdot \frac{\Delta A_S^{Sample} . \varepsilon_S^{STD}}{\Delta A_S^{STD} . \varepsilon_S^{Sample}} \quad \text{... 24}$$

where Φ_T^{Sample} and Φ_T^{Std} are the triplet yields for the sample and the standard respectively. ΔA_s^{Sample} and ΔA_s^{STD}, ε_s^{Sample} and ε_s^{STD} are the singlet absorbance and the singlet extinction coefficients of the unknown and standard, respectively.

1.3.4 Determination of fluorescence quantum yields

Fluorescence quantum yield (Φ_F) is the number of emitted photons related to the number of the absorbed photons, which can be determined by a relative method using a reference material. Typically phthalocyanines have fluorescence lifetimes ranging between 1 and 7 ns [93,94].

Fluorescence quantum yields may be determined using a reference material such as ZnPc whose fluorescence quantum yield is known (Φ_F = 0.18) in dimethylsulphoxide [93,94]. Low concentrations are essential to avoid quenching of fluorescence, this requires absorbance of the sample to be less than 0.2. The fluorescence quantum yield may thus be determined using equation 25 [94].

$$\Phi_f = \Phi_{f(std)} \cdot \frac{F_{area(s)} . A_{area(std)} . \eta^2_{(s)}}{F_{area(std}) . A_{area(s)} . \eta^2_{(std)}} \quad \text{... 25}$$

Where $F_{area}(s)$ and $F_{area}(std)$ are the respective areas of the unknown sample and standard under their respective emission spectra, $A_{area}(s)$ and $A_{area(std)}$ are the absorbance areas of the sample and standard under their respective absorption spectra, and the refractive indexes of the solvents used for the sample and standard are given by $\eta_{(s)}$ and $\eta_{(std)}$ respectively.

1.4 Synthesis

1.4.1 Porphyrins

Since the synthesis and characterization of phthalocyanine and porphyrazine derivatives constitute the heart of this research program, it is important to highlight some aspects of synthesis in this literature survey. Many porphyrins are naturally occurring compounds, such as chlorophyll and haemoglobin [61]. Although all these macrocyclic compounds share similar structure, their synthetic routes differ drastically in that porphyrin structures can be assembled piece by piece, unlike phthalocyanines and porphyrazines which are usually macrocyclized in a one pot reaction without the option of isolating the intermediates. Scheme 1.4 shows an approach used to synthesise porphyrin dimers [75,95].

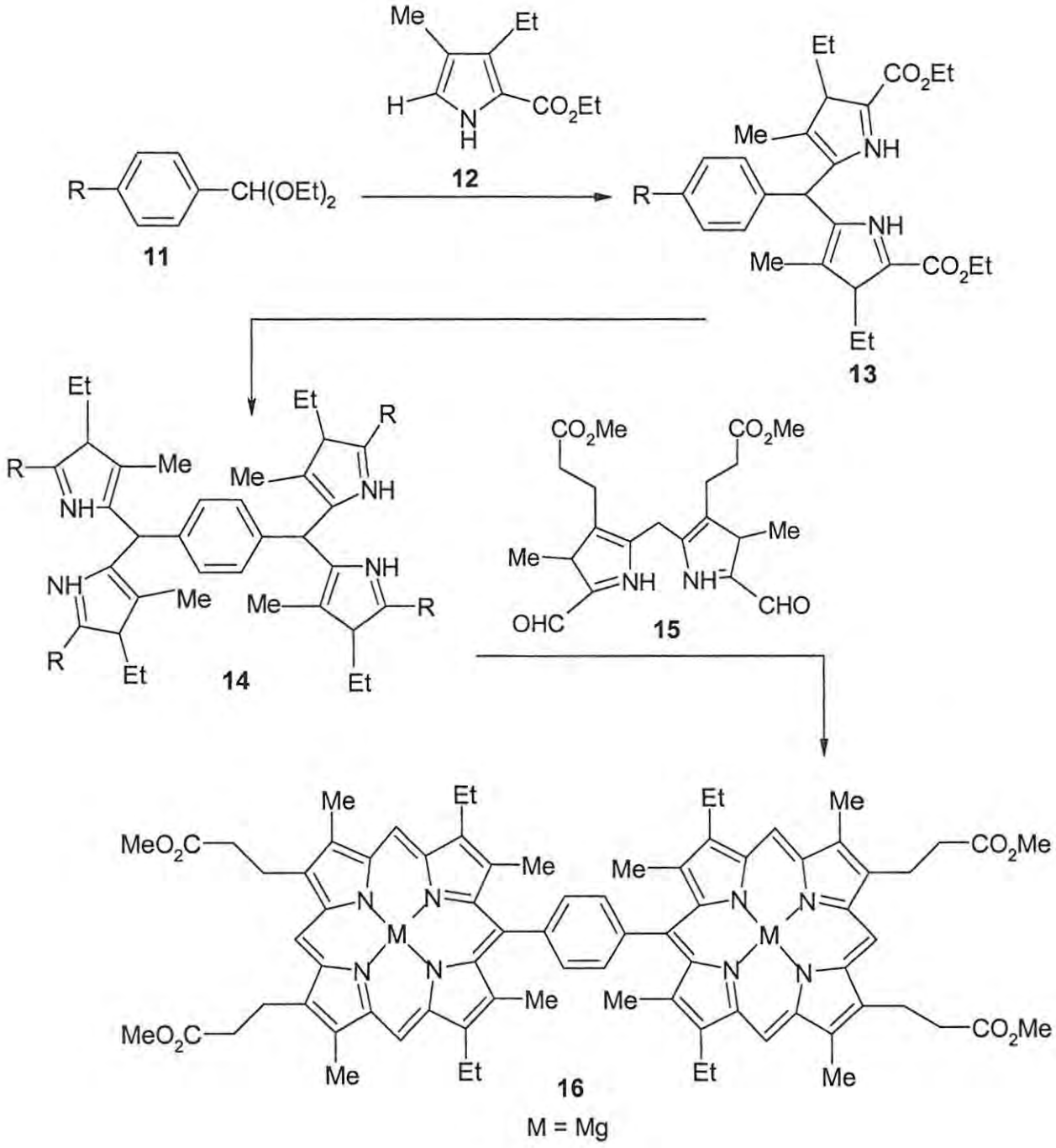

Scheme 1.4. Synthesis of the porphyrin dimer (**16**)

Scheme 1.4 also shows how porphyrin synthesis is advantageous over phthalocyanine and porphyrazine synthesis due to the molecular approach. The intermediates **14** and **15** were condensed to form **16** [76].

1.4.2 Phthalocyanines

Phthalocyanines also known as tetrabenzotetraazaporphyrins [29] are generally more stable than porphyrins and more commonly used in industry. When compared with the structure of porphyrins (Figure 1), the Pc has a similar inner backbone with the nitrogen aza bonds replacing the methane linkages of the porphyrins. Pc's were discovered accidentally in 1928 during the industrial preparation of phthalimide in the Grange mouth works of Messrs Scottish Dyes, Ltd [61]. During this process, the phthalimide prepared from phthalic anhydride and was ammonia contaminated with a stable dark blue insoluble complex which was later shown to be ferrous phthalocyanine. The phthalocyanine was reported by Linstead in 1934 who was able to characterize the complex, and that was followed by elucidation of their structure using X-ray diffraction analysis [97,98]. Linstead was also able to determine the molecular weight of these compounds through an ebullioscopic method using platinum-resistance thermometer. Using all this information Linstead was able to determine the molecular structure of the phthalocyanines which was similar to that of the porphyrin. Phthalocyanines and porphyrins exhibit similar properties in that both of them are found to be stable to alkali, but less stable to acids. Both are highly coloured, can form complex metallic compounds and can be degraded by oxidation to the imides of dibasic acids.

1.4.2.1 Synthesis of substituted Pcs : statistical condensation

Scheme 1.5 shows an example of this statistical condensation by reaction of equimolar amounts of tetraphenylphthalonitrile (**18**) and the appropriate 2,3-dicyanonaphthalene (**17**) respectively with metal salt in hexanol in the presence of catalytic amounts of 1,8-diazabicyclo [5.4.0]undec-7-ene (DBU) [99]. The mixtures of the obtained phthalocyanine complexes may be separated by common chromatography.

If we regard A (**18**) and B (**17**) as two different phthalonitriles then six different compounds are expected, AAAA (**24**), BBBB (**19**), AAAB (**23**), ABBB (**20**), ABAB (**21**) and AABB (**22**), which are difficult to separate by common chromatographic methods due to their tendency towards aggregation [99,100]. Bulky or rigid groups can be attached to phthalonitriles to avoid aggregation [99-101]. When one of the starting phthalonitriles bears rigid groups at the 1,4-position (see Figure 1. for numbering) a reduced number of products is obtained, mainly due to the steric hindrance between the bulky groups and the Pc macrocyclic rings [99].

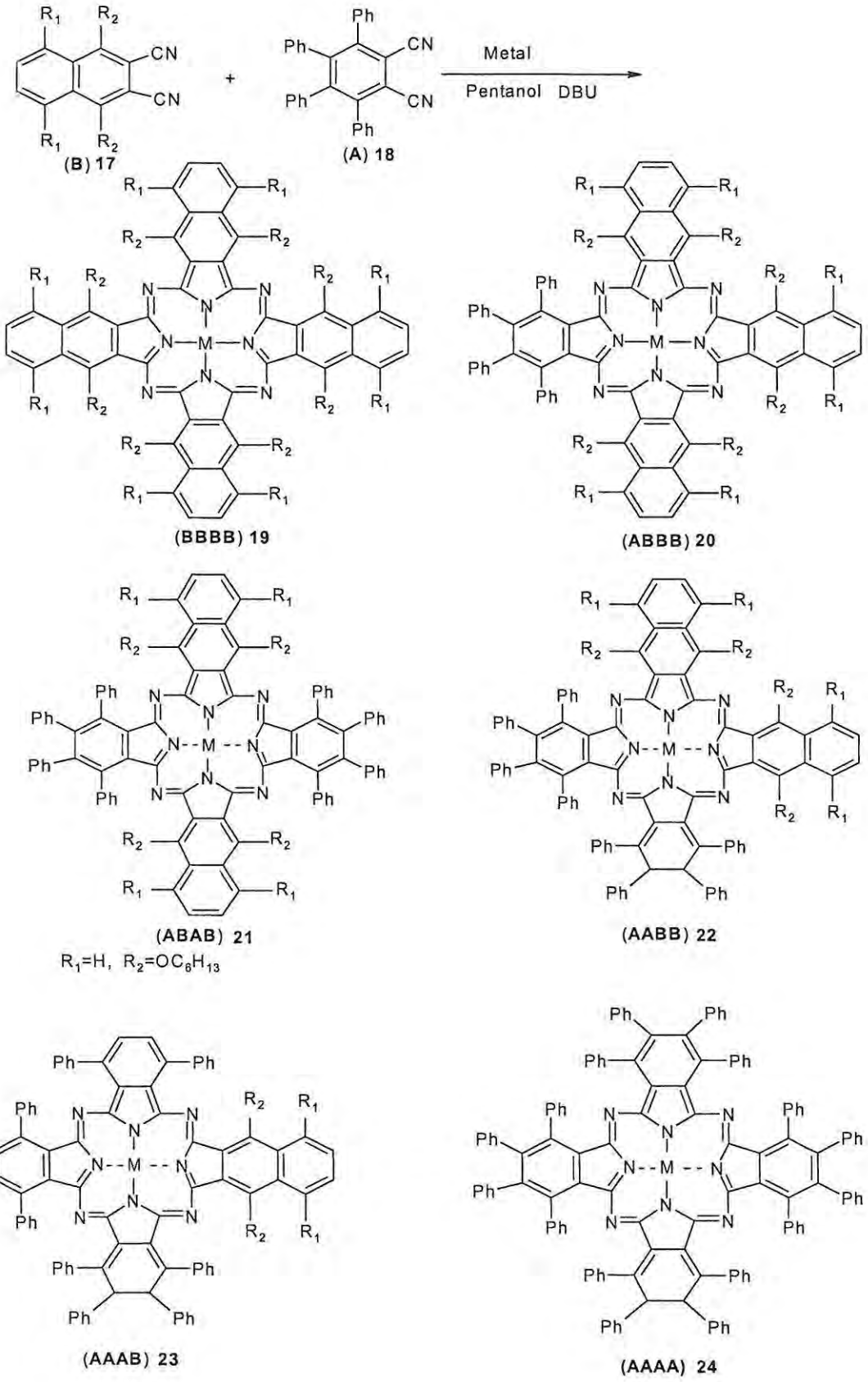

Scheme 1.5. Synthesis of variously substituted phthalocyanine complexes.

1.4.2.2 Synthesis of unsymmetrical Pc's : Ring expansion of SubPc.

Subphthalocyanines [102-105] are composed of three diiminoisoindole rings *N*-fused around a boron centre and have a C_{3v} symmetry, and a Hückel aromatic delocalised 14π– electron system, along with their non-planar cone shape structure, making them very attractive compounds for applications as chromophores for second order non-linear optics (NLO) [106-114] and thin film formation. They have recently received considerable attention in the chemistry of phthalocyanines for the preparation of unsymmetrically substituted phthalocyanines. The subphthalocyanine synthesis was firstly carried out by Meler *et al* [104] by condensing boron trichloride (BCl_3) with phthalonitrile (**25**) and heating to 250°C yielding 40% of product (**26**). However, the procedure has been improved with milder conditions and approximately 20% higher yield by employing boron chloride in hexane solution and using a high boiling point solvent (Scheme 1.6).

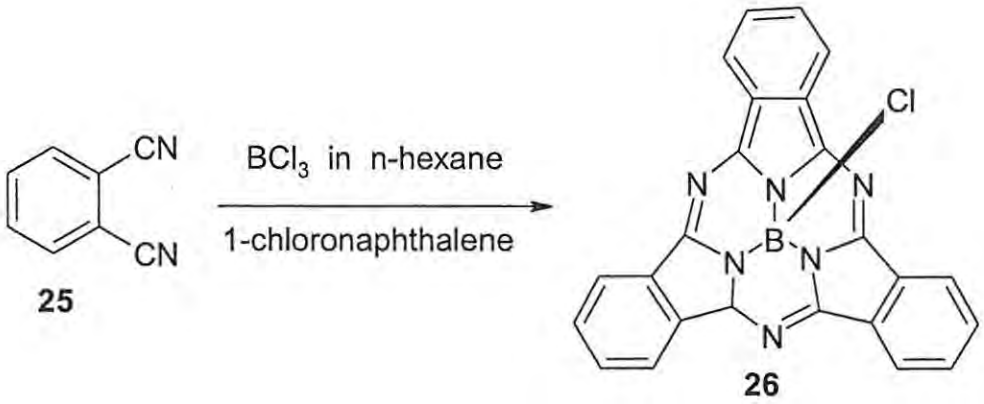

25 **26**

Scheme 1.6. Synthesis of unsubstituted subphthalocyanine.

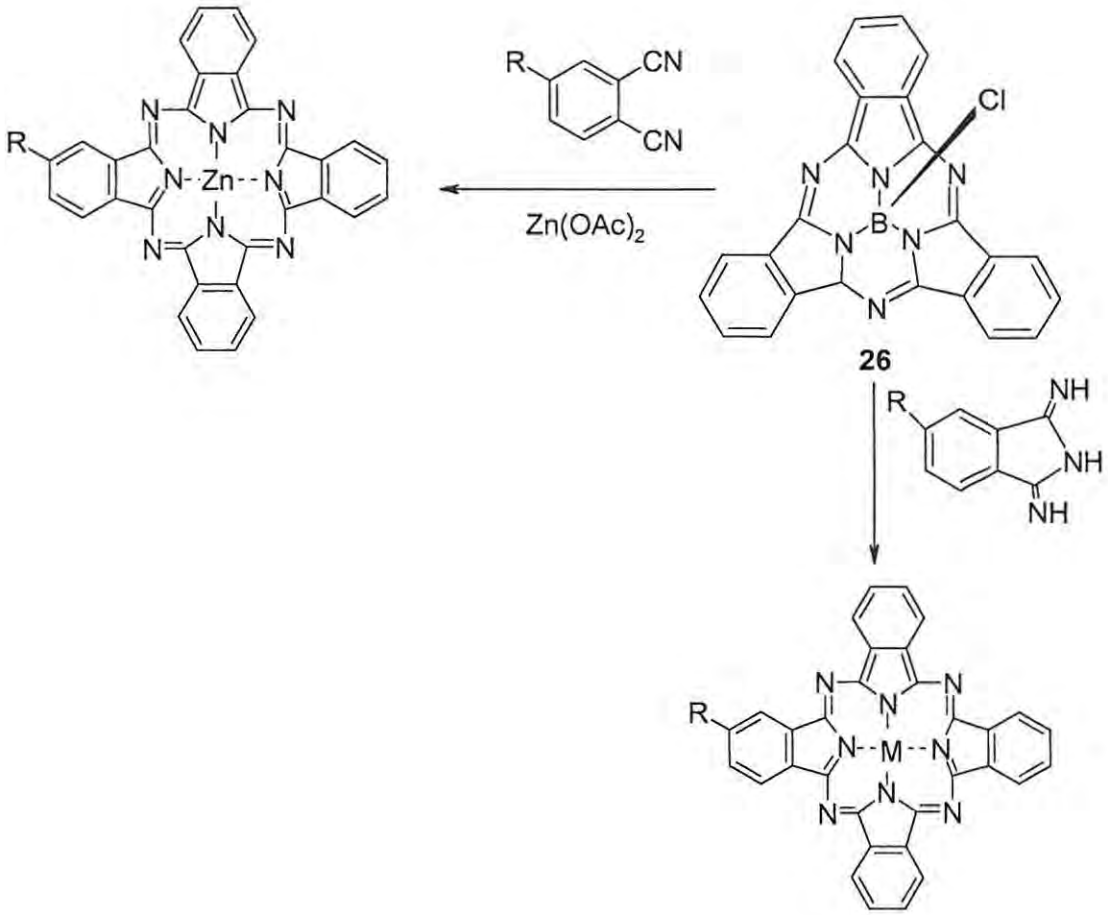

Scheme 1.7. Synthesis of unsymmetrically substituted phthalocyanines by the ring enlargement method.

The synthesis of monosubstituted phthalocyanines from subphthalocyanines (Scheme 1.7) results in not only monosubstituted phthalocyanines but also a mixture of unsubstituted, differently substituted, and ring chlorinated phthalocyanines. It has been reported that the unmetallated products formed from the ring enlargement method are highly insoluble in organic solvents, and difficult to separate [115,116]. For this reason, metallation of the formed phthalocyanines mixture is required in most cases. However, it has been found that zinc metallation during ring expansion cannot be done in the presence of diiminoisoindolines, due to the tendency of diiminoisoindolines to cyclotetramerise with zinc salts, thus the less reactive phthalonitriles are used for direct metallation [104,105]. Different substituents have been introduced to the peripheral positions of the Pc ring in order to increase the solubility of these

compounds and to fine-tune their photophysical and photochemical properties [117].

1.4.3 Porphyrazines

The porphyrazine (Pz) macrocycle is isoelectronic with porphine and has the same shape. The synthetic route to porphyrazines involves the metal-templated cyclization of maleonitrile derivatives (Scheme 1.8), allowing for the direct preparation of macrocycles with functional groups attached directly at the β-positions of the pyrrole rings [33,118-129]. Functional groups attached in this way may have stronger couplings to the macrocyclic core than those attached to the fused benzo-rings to Pc, and therefore, exert a greater effect on the physical properties of these compounds. Scheme 1.8 shows a typical synthetic strategy employed for the preparation of the Pz's involving the co-cyclization of bis(dimethylamino)maleonitrile (**27**), and 1,2-dicyanobenzene (**25**). A number of products (**28-33**) are formed by this reaction [130] in the presence of Mg^{2+}. The products may readily be separated by thin layer chromatography (TLC) and column chromatography. The Mg^{2+} may be removed from the formed Pz's by treatment with trifluoroacetic acid (TFA).

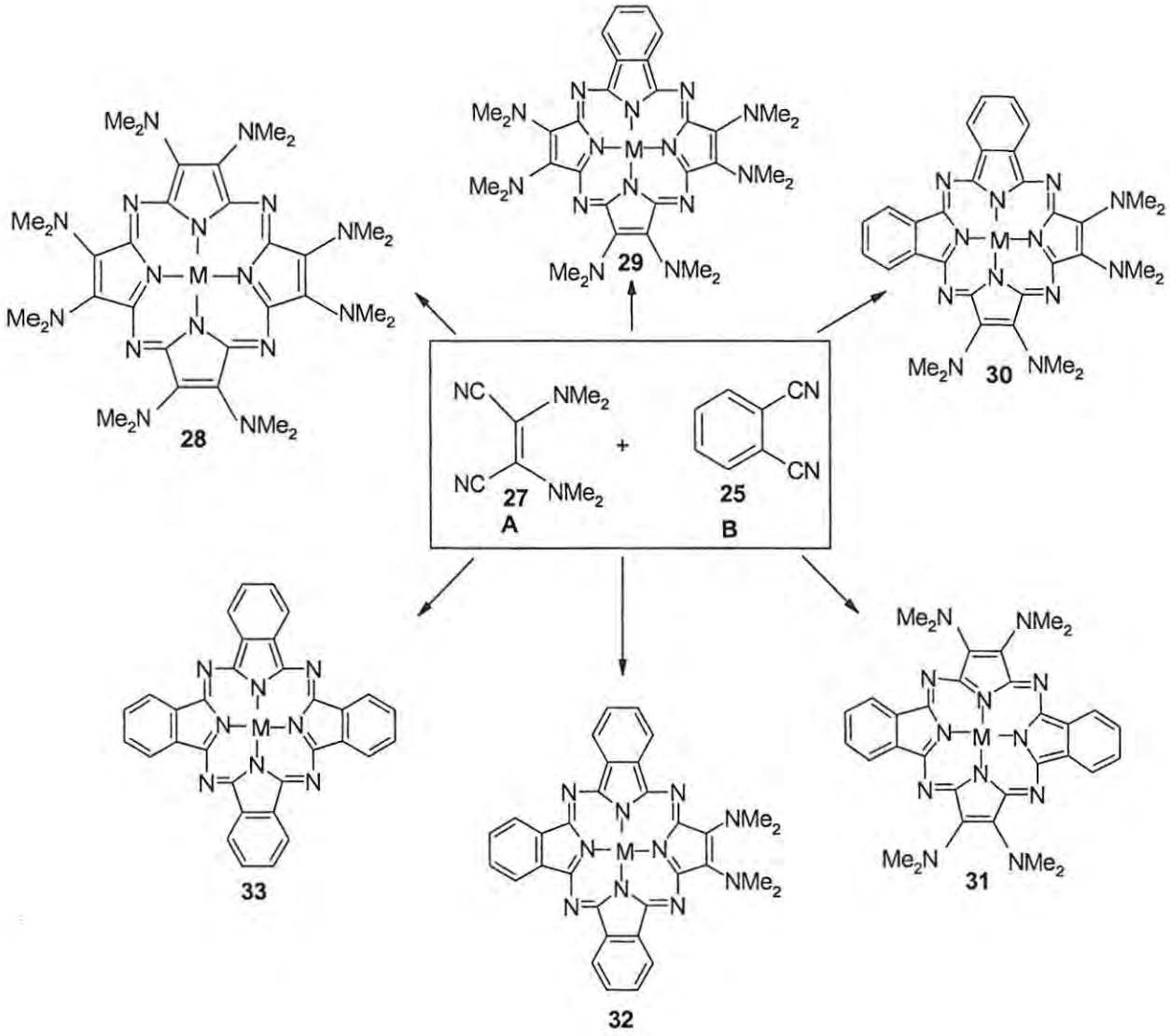

Scheme 1.8 Synthesis of porphyrazines by statistical condensation [130]

Methods of metallation

Porphyrazines and related macrocycles can bind many metal ions. In statistical condensation using Linstead macrocyclization, the use of a magnesium alkoxide in the presence of alcohol is preferred. Since in this form the metal is readily co-ordinated in the centre during the synthesis of these macrocycles. Prior to metallation with a metal other than magnesium, the formed Pz needs to be demetallated with acetic acid or trifluoroacetic acid [30-31,33].

As can be seen in Scheme 1.9, Linstead macrocyclization of **27** using magnesium propoxide in propanol, provided **28** in up to 48% yield, and traces of a less polar purple pigment. Demetallation of **28** with acetic acid gave the expected free base porphyrazine **34**. Further reaction with zinc(II) acetate resulted in selective metallation within the macrocyclic cavity to provide the corresponding zinc complex **35** in high yield.

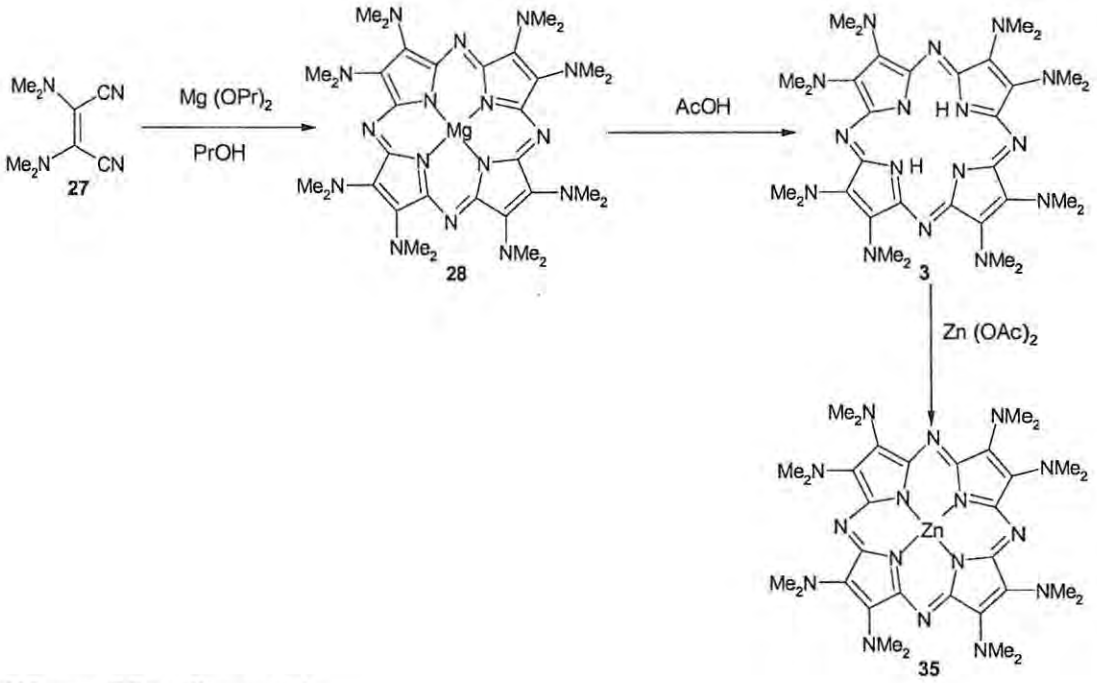

Where OPr = Propoxide

Scheme 1.9. The reaction path to the zinc substituted porphyrazine (**35**)

However, this is not the only method of metallating these compounds, peripheral metal binding is also possible as shown in Scheme 1.10. The porphyrazines can easily be metallated on the peripheral positions after deprotection of the sulphur moieties, however this also depends on the protecting group used. Deprotection of the thioether (**36**) generates the porphyrazine thiolate (**37**). Due to the air-sensitivity of the unprotected porphyrazine, Schlenk-techniques had been used for this process. The nickel product (**39**) is isolated by venting off the ammonia and removing the tetrahydrofuran (THF) *in vacuo*. However, it has been noted that the peripheral metal and core metal can communicate electronically through the

extensive conjugated porphyrazine core. Using this information one can therefore make use of core metallation and peripheral metallation [130-133] of these tetrapyrrole compounds to fine-tune their characteristics for specific applications [134,135].

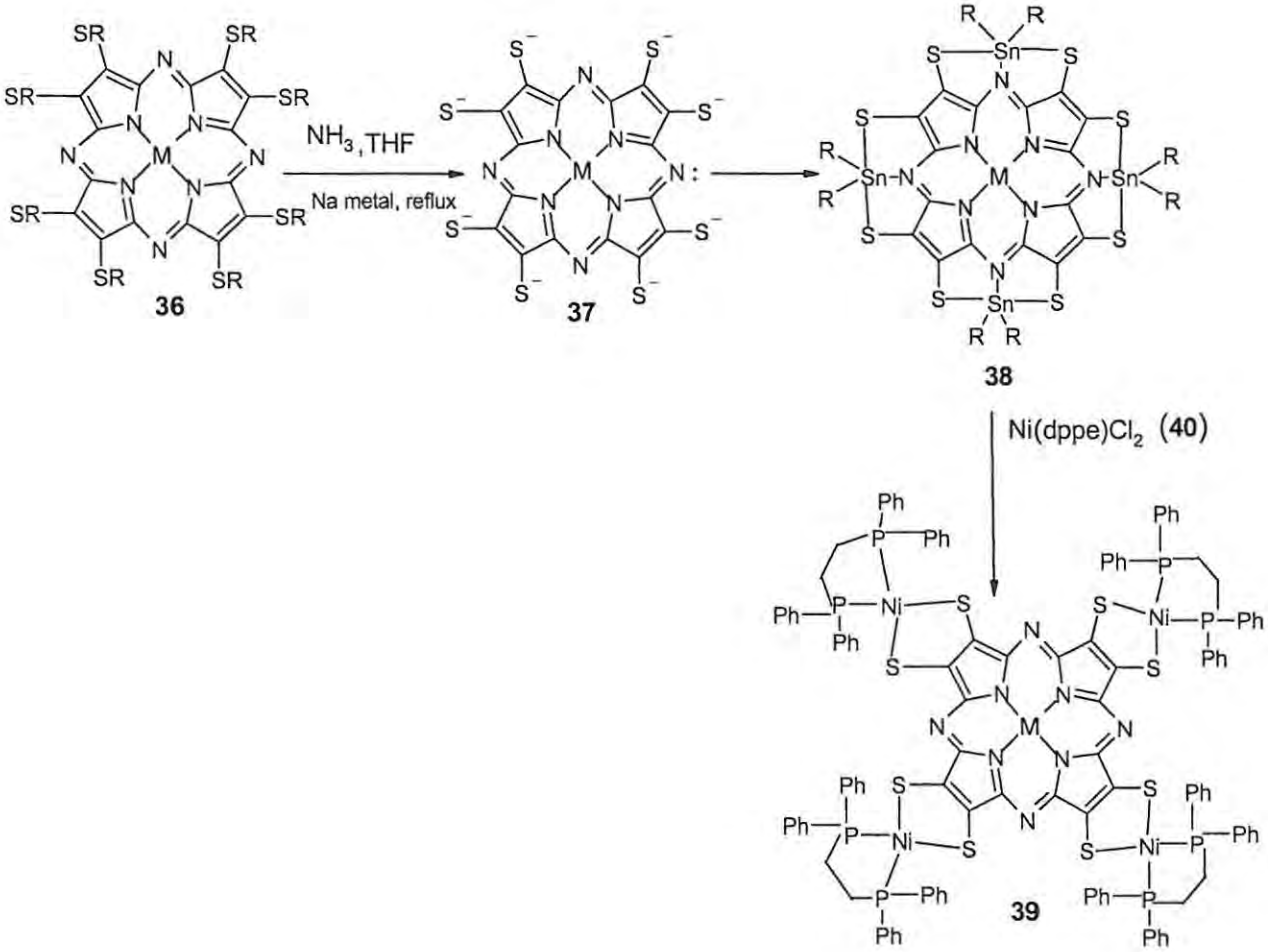

where R = *t*-butyl

Dppe = 1,2-bis(diphenylphosphine)ethane

Scheme 1.10 Peripheral metallation of a porphyrazine

1.5 Spectral properties of phthalocyanines and porphyrazines

1.5.1 ^{1}H-NMR spectroscopy

Phthalocyanines and related macrocyclic compounds are known to show a strong diamagnetic ring current effect [136]. The aromatic protons give multiple signals due to structural isomers at low field, and the peaks of the ring substituents appear at higher field. Protons in the axial area (just above or below the planar phthalocyanines ring) are more effectively shielded due to the extended pi conjugation of the phthalocyanine ring [137]. Typically the Pc non-peripheral protons (1,4 in Figure 1) give ^{1}H-NMR signals in the range $\delta = 9 - 11$ ppm and the peripheral protons $8 - 9$ ppm as can be seen for tetra-3-pyridoporphyrazinatosilicon in Figure 1.9. The diamagnetic shifts of the Pc π system are similar to those of the porphyrin π system due to perturbations of ring current by the meso nitrogens and benzo π system [138]. The peaks at higher field are due to the ring substituents.

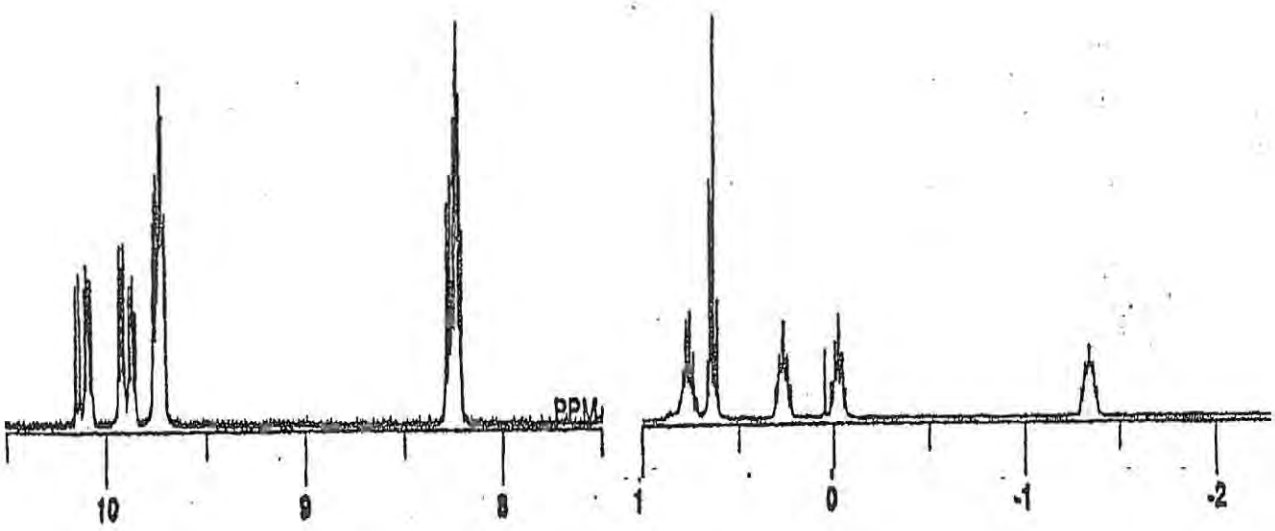

Figure 1.9 ^{1}H-NMR spectra of tetra-3-pyridoporphyrazinatosilicon (400 MHz in $CDCl_3$) [137].

1.5.2 UV-visible spectroscopy

Due to the extended electronic conjugation of the tetrapyrrole compounds, it is obvious that UV-visible spectroscopy would provide interesting and vital information about the electronic structure of these compounds. A model that may be used to understand the electronic absorption behaviour was proposed by Gouterman's group (Figure 1.10), describing a highly simplified four orbital model [21]. This model describes the top two occupied molecular orbitals (a_{1u} and a_{2u}) and the degenerate, lowest unoccupied orbital (e_g), to set up the states that account well for the first two or three allowed transition in the visible UV region of the spectrum [26].

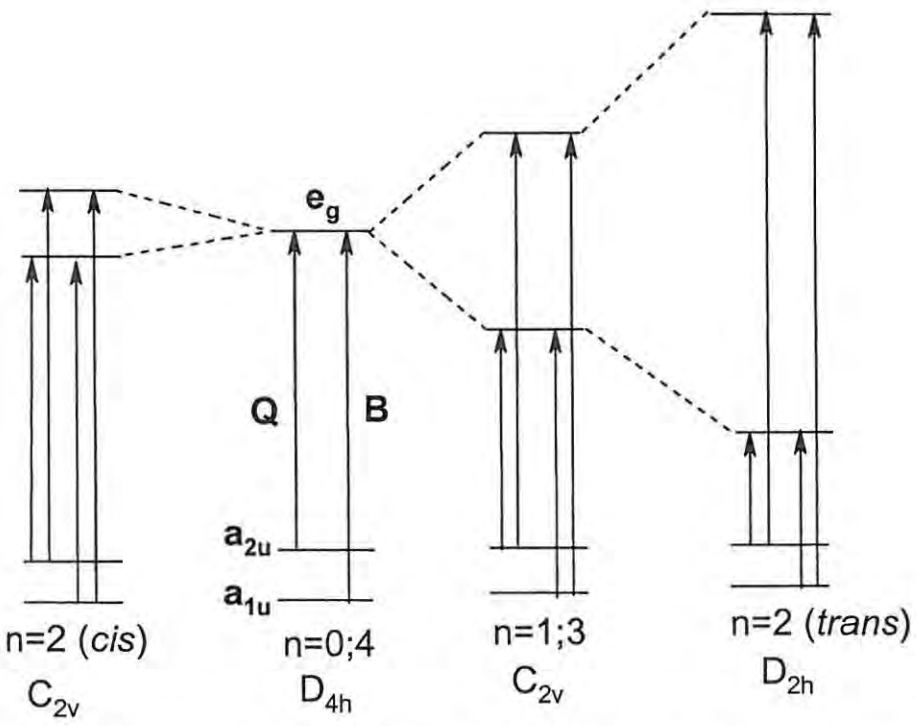

Figure 1.10 Qualitative orbital energy diagram for the Q and B (Soret) bands of porphyrazines, showing the effect that the symmetry of the conjugated porphyrazine core has on the electronic structure of the macrocycle.

Pigments such as porphyrazines and phthalocyanines exhibit similar electronic spectra. They both have UV-visible spectra with a strong characteristic band in red end of the visible spectra at wavelengths between 600 – 800 nm called the Q band and a weaker absorption in UV region at wavelengths between 300 - 400 nm called the B band (Soret band) [32,139]. In a D_{4h}-symmetric macrocycle, the lowest unoccupied molecular orbital (LUMO) is doubly degenerate (e_g) and a first approximation of the Q and B bands are associated with transitions from the two highest occupied molecular orbitals (HOMO) (a_{1u}, a_{2u}) into the LUMO (Figure 1.10). In reducing the symmetry from, example, D_{4h} to D_{2h}, the degeneracy of the e_g (LUMO) is removed and this gives rise to two possible transitions of varying energy and subsequently a split in Q-band [31,139] (Figure 1.10). Metal-free phthalocyanines (H_2Pc) characteristically show a split Q-band [140-143] due to loss of symmetry. Loss of symmetry was also found to cause a shift in the Q band of porphyrazine when forming a diseco-porphyrazine. Here the peaks at 709 and 679 nm correspond to the red-shifted split Q band, and the n-π^* peak was reduced to a small shoulder at 470 nm [143]. The splitting reflects the overall C_{2v} symmetry of the molecules and can be rationalized with Gouterman's four-orbital model [144-148]. Metallation changes the symmetry from D_2h (split Q band) to D_4h (single Q band) in cases where the polarity is maintained, Figure 1.11.

It is known that the Q bands of Pcs which have peripheral substituents on the carbons furthest from the Pc core (peripheral substituents, 2,3 in Figure 1.) generally appear at shorter (blue-shifted) wavelengths, while those which have non-peripheral substituents appear at longer wavelengths [30]. Shifts of the Q band positions in the films compared to those in solution [4,32,139,150-153] have been explained by differences in aggregation behaviour, the longer-wavelength shift observed for thin films has been ascribed to an presence of face-to-face type stacking of the Pc planes.

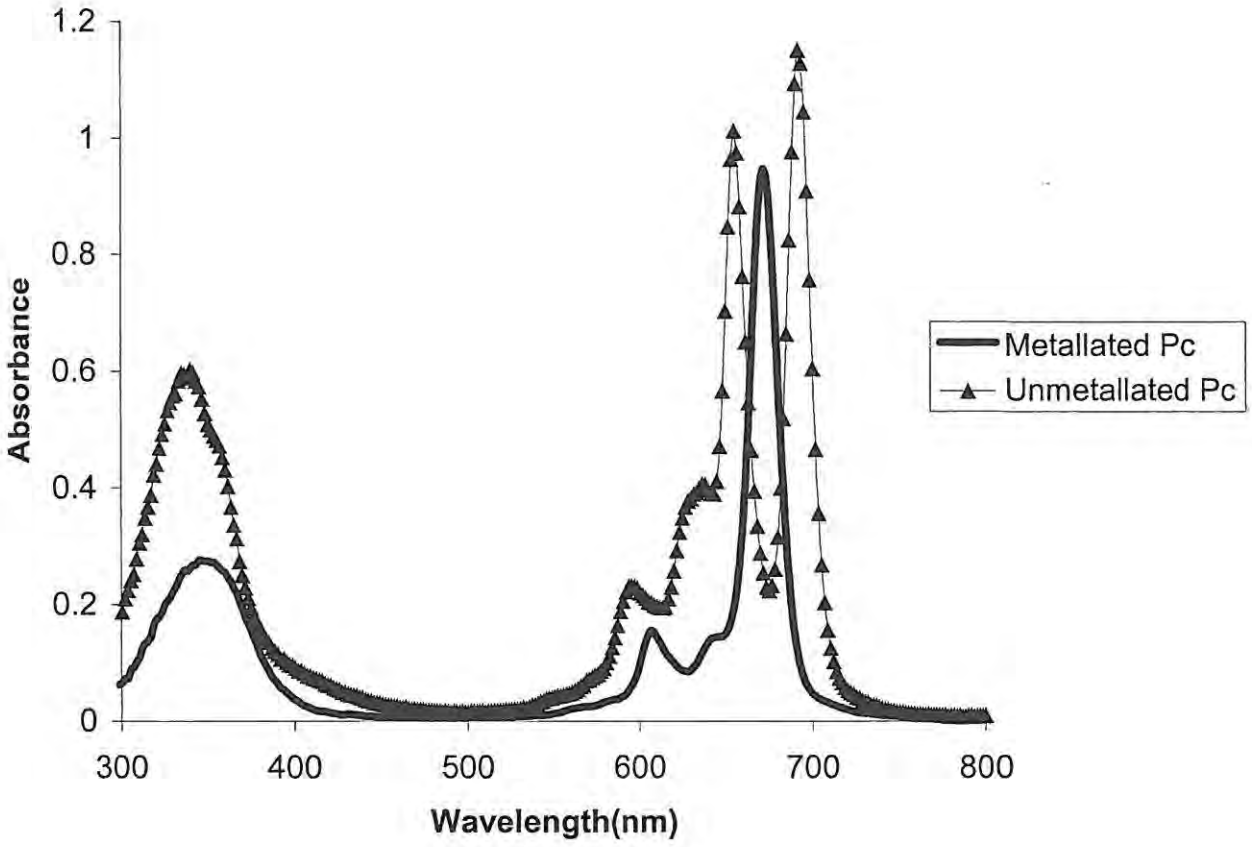

Figure 1.11 Absorption spectra of unmetallated and metallated phthalocyanines.

1.5.3 IR spectroscopy

The characteristic vibration bands common to metallated phthalocyanines (Figure 1.12) are observed at 670 – 700, 750 – 790 cm^{-1} (C-H out of plane bending), 840 – 850, 940 –945, 1090 –1120 cm^{-1} (C-H in plane bending), 1140 – 1147, 1200 – 1210, 1240 – 1290, 1305 – 1320, 1400 –1430, 1490 –1540 and 1600 – 1625 cm^{-1} (benzene ring vibrations). The bands at 670 – 700, 750 – 790, 1240 – 1300 and 1400 – 1430 cm^{-1} are well-defined doublets and those at 1090 – 1120 cm^{-1} quite intense [28].

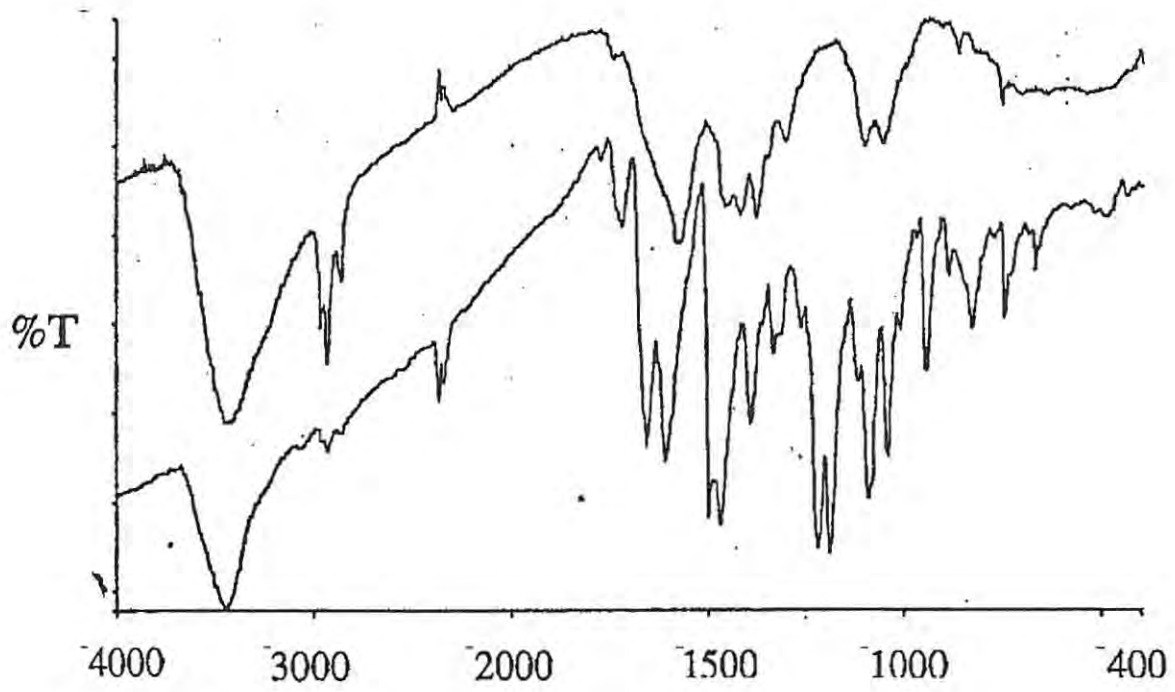

Figure 1.12 Typical IR spectra of the phthalocyanines [28].

The near IR electron absorption bands in the 850 –2000 nm region may be attributed to charge transfer, a_{1u} (π) --- e_g (dxz, dyz), or N(aza) ---π^* (Pc) transitions except for a band near 1660 (ν (C-H) overtone) and another around 1000 (irradiation damaged Pc). Influences of the central metal on the bands directly attributed to the ligand can also be detected [153].

1.6 Aims of the project

1) To synthesize and characterize a series of soluble substituted phthalocyanines containing Zn and Mg metal : bis-1,2-di-benzamide porphyrazine Zn(II) (**63**, Scheme 2.7), bis-1,2-di-octamide porphyrazine Zn(II) (**64**, Scheme 2.7), bis-1,2-di-tertbutylacetamide porphyrazine (**65**, Scheme 2.7), bis-1,4-pentoxy phthalocyanato Mg(II) (**66**, Scheme 2.8), tetra-1,4,9,12-pentoxy phthalocyanato Mg(II) (**67**, Scheme 2.8), octa-1,4,5,8,9,12,13,16-pentoxy phthalocyanato Mg(II) (**68**, Scheme 2.8), di-1,4-pentoxy phthalocyanato Zn(II) (**69**, Scheme 2.8), di-1,4-naphthaloxy phthalocyanato Mg(II) (**70**, Scheme 2.9), tetra-1,4,9.12-naphthaloxy phthalocyanato Mg(II) (**71**, Scheme 2.9), di-1,4-hexyl phthalocyanato Mg(II) (**72**, Scheme 2.10), di-1,4-hexyl phthalocyanato Zn(II) (**73**, Scheme 2.10).

2) To investigate the photochemical (singlet oxygen quantum yield, photodegradation quantum yield) and photophysical properties (fluorescence quantum yield, triplet quantum yield and triplet life time) of the above mentioned compounds:

References:

1. R. Faust. *J. Org.Chem.* 1999, **64**, 2571.
2. P. Gregory. High-Technology Applications of Organic Colorants, Plenum Press: New York. 1991.
3. P. Gregory. *J. Porphyrins Phthalocyanines.* 2000, **4**, 452.
4. M. J. Cook, A. J. Dunn, S. D. Howe, A. J. Thomason, and K. J. Harrison. *J.Chem. Soc. Perkin Trans.* 1. 1998, 2453.
5. R. Bonnet. *Chem. Soc. Rev.* 1995, **24**, 19.
6. I. Rosenthal, in Phthalocyanines: Properties and Applications; C. C. Leznoff and A. B. P. Lever. Eds. VCH: New York. 1996, **4**, 485.
7. C. J. Gomer, N. Rucker, A. Ferraro, and S. Wong. *Radiat. Res.* 1989, **120**, 1.
8. E. A. Luk'yanets. *J. Porphrins Phthalocyanines.* 1999, **3**, 424.
9. H. Hastrat and J. E. van Lier. *Chem Rev.* 1999, **99**, 2379.
10. V. Cuomo, G. Jori, B. Rihter, M. E. Kerry, and M. A. J. Rdgers. *Br. J. Cancer.* 1990, **62**, 966.
11. N. C. Yates, J. Moan, and A. Western. *J. Photochem. Photobiol. B: Biol.* 1990, **4**, 379.
12. B. Paquette, H. Ali, R. Langlois, and J. E. van Lier. *Photochem. Photobiol.* 1990, **51**, 313.
13. D. Wöhrle, M. Shopova, S. Müller, A. D. Milev, V. N. Mantareva, and K. K. Kranstev. *J. Photochem. Photobiol. B: Biol.* 1993, **21**, 155.
14. W. E. Ford, M. A. J. Rodgers, L. A. Schechtman, J. R. Sounik, B. D. Rihter, and M. E. Kenney. *J. Am. Chem. Soc.* 1992, **31**, 3371.
15. P. Vasunedan, N. Poughat, and A. K. Shuklat. *Appl. Organomet. Chem.* 1996, **10**, 591.
16. J. Oni and T. Nyokong. *Anal.Chim.Acta.* 2001, **434**, 9.
17. S. Vilakazi and T. Nyokong. *J. Electroanal.Chem.* 2001, **512**, 56.
18. S. Maree and T. Nyokong. *J. Electroanal.Chem.* 2000, **492**, 120.
19. R. O. Loufty, A. M. Hor, C. K. Hsiao, G. Baranyi, and P. Kazmaier. *Pure Appl.Chem.* 1988, **60**, 1047.
20. J. E. Kuder. *Imag. Sci.* 1988, **32**, 51.

21. C. C. Leznoff in Phthalocyanine : Properties and applications, C. C. Leznoff, A. B. P. Lever. Eds. VCH Publishers. Cambridge. 1989, vol.1, chapter 1.

22. J. S. Shirk, R. G. S. Pong, S. R. Flom, H. Heckmann, and M. Hannack. *J .Phys .Chem. A.* 2000, **104**, 1438.

23. M. Hanackan, T. Schneider, M. Barthel, J. S. Shirk, S. R. Flom, and R. G. S. Pong. *Coord. Chem. Rev.* 2001, **219**, 235.

24. D. Dini, M. Barthel and M. Hanack. *Eur. J. Org. Chem.* 2001, 3759.

25. N. Q. Wang, Y. M. Cai, J. R. Heffin, and A. F. Garito. *Mol.Cryst.Liq.Cryst.* 1990, **189**, 39.

26. I. Rosenthal, E. Ben-Hur in Phthalocyanines : Properties and Application, C. C. Leznoff and A. B. P. Lever. Eds. VCH. New York. 1989, vol.1, chapter.6.

27. H. Miwa, E. A. Makarova, K. Ishii, E. A. Luk'yanets, and N. Kobayashi, *Chem. Eur. J.* 2002, **8**, 1082.

28. N. Kobayashi. Synthesis and Spectroscopic properties of Phthalocyanine Analogues In C. C. Leznoff and A. B. P. Lever. Phthalocyanines, properties and applications. VCH. New York. 1993, vol.2, chapter.3.

29. M. J. Stillman and T. Nyokong. Phthalocyanines-Properties and Applications; C. C. Leznoff, A. B. P. Lever. Eds. VCH. New York. 1989, vol.1, chapter.3.

30. S. J. Lange, J. W. Sibert, A.G.M. Barrett, and B. M. Hoffman, *Tetrahedron*, 2000, **56**, 7371.

31. S. J. Lange, H. Nie, C. L. Stern, A. G. M. Barrett, and B. M. Hoffman. *Inorg. Chem.* 1998, **37**, 6436.

32. P. A. Stuzhin, E. M. Bauer, and C. Ercolani. *Inorg. Chem.* 1998, **37**, 1536.

33. H. Nie, A. G. M. Barrett, and B. M Hoffman. *J. Org. Chem.* 1999, **64**, 6791.

34. K. I. Ozoemena, T. Nyokong, P. Westbroek. *Electroanalysis*. 2003, **14**, 1762.

35. C. M. Che, L. G. Butler, P. J. Grunthaner, and H. B. Gray. *Inorg. Chem.* 1985, **24**, 4662.

36. W. B. Hever, M. Totten, G. S. Rodman, E. J. Herbert, H. J. Tracy, and J. K. Nagle. *J. Am. Chem. Soc.* 1984, **106**, 1163.

37. G. P. Gupta, G. Lang, L. A. Koch, B. Wang, W. R. Scheidt, and C. A. Reed. *Inorg. Chem.* 1990, **29**, 4234.

38. J. S. Miller, C. Vazquez, J. C. Calabrese, R. S. Mclean, and A. J. Epstein. *Ad. Mater.* 1994, **6**, 217

39. J. S. Miller, J. C. Calabrese, R. S. Mclean, and A. J. Epstein. *Ad. Mat.* 1992, **4**, 498.

40. C. C. Leznoff and A. B. P. Lever. Phthalocyanines, Properties and Applications, VCH : New York, 1996, vol.4, chapter.1.

41. R. O. Loufty and J. H. Sharp. *J. Chem. Phys.* 1979, **71**, 211.

42. S. B. Brown. *J. Photochem. Photobiol. B : Biol.* 1990, **6**, 12.

43. S. B. Brown and T. G. Truscott. *Chem. Br.* 1993, 956.

44. R. W. Boyle and J. E. van Lier. *Synlett.* 1993, 351.

45. I. J. MacDonald and T. J. Dougherty. *J. Porphyrins Phthalocyanines.* 2001, **5**,105.

46. C. M. Allen, W. M. Sharman, and J. E. Van Lier, *J. Porphyrins Phthalocyanines.* 2001, **5**, 162.

47. D. Phillips. *Pure & Appl. Chem.* 1995, **67**, 119.

48. D. Phillips. *Science Progress.* 1993/94, **77**, 295.

49. T. Theodossiou, V. Hovhannysian, P. Kastaniotis, K. Politopoulos, and D. Yova. *Proc. SPIE.* 2001, **4433**, 1606.

50. A . J. MacRobert, S. G. Brown, and D. Phillips. *Med. Laser.Appl,* 1992, **51**, 1131.

51. T. J. Dougherty. *Photochem. Photobiol.* 1987, **45**, 879.

52. N. A. Kuznetsova and O. L. Kaliya. *Russ. Chem. Rev.* 1998, **42**, 424.

53. J. Miller. *J. Chem. Ed.* 1999, **76**, 593.

54. L. H. P. Murrer, J. P. A. Marijnissen, and W. M. Star. *J. Cancer.* 1999, **88**, 744.

55. H. B. Ris, H. J. Alternatt, and R. Inderbitzi. *Br. J. Cancer.* 1999, **60**, 64 .

56 A. Kuebler, T. Haase, and C. Staff. *Laser. Surg. Med.* 1999, **60**, 25.

57. S. B. Brown. *J. Photochem. Photobiol.* B : Biol. 1990, **12**, 4.

58. W. Baumler, C. Abels, and R. Szeimies. *Med. Laser. Appl.* 2003, **18**, 47.

59. R. W. Boyle and J. E. van Lier. *Synthesis.* 1995, 1078.

60. M. J. Abrahams. *Platinum Metal Rev.* 1995, **39**, 14.

61. R. L. Milgram in Colours of life : *An introduction to Chemistry of porphyrins and related compounds*. Oxford University Press,1st Ed, 1977.
62. J. Z. Li, X. Y. Pang, D. Gao, and R. Q. Yu. *Talanta*. 1995, **42**, 1775.
63. C. Grewer, G. Schermann, R. Schmidt, A. Vöiollker, H. D. Brauer, A. Meier, and F. P. Montforks. *J. Photochem. Photol. B: Biol.* 1991, **11**, 285.
64. H. B. Ris, H. J. Alternatt, R. Inderbitzi, R. Hess, B. Nachbur, J. C. M. Sterwart, Q. Wang, C. K. Lim, R. Bonnett, M. C. Berenbaun, and U. Althaus. *Br. J. Cancer*. 19991, **64**, 1116.
65. T. G. Truscott. *J. Chem. Soc. Faraday Trans. 2*. 1986, **82**, 2177.
66. J. K. Hoober, T. W. Sery, and N. Yamamoto. *Photochem. Photobiol.* 1988, **48**, 579.
67. N. Brasseur, H. Ali, R. Wagner, R. Langlois, J. Rousseau, and J. E. van Lier. *Photochem. Photobiol.* 1987, **45**, 583.
68. R. K. Pandey, D. A. Bellnier, K. M. Smith, and T. J. Dougherty. *Photochem. Photobiol.* 1991, **53**, 65.
69. C. F. Borland, D. J. Mc Garvey, A. R. Morgan, and T. G. Truscott. *Phochem. Photobiol. B: Biol.* 1988, **2**, 427.
70. A. R. Morgan, G. M. Garbo, R. W. Keck, and S. H. Selman. *Cance. Res.* 1988, **48**, 194.
71. A. M. Richter, S. Cerruti-Sola, E. D. Sternberg, D. Dolphin, and J. G. Levy. *J. Photochem. Photobiol. B : Biol.* 1990, **5**, 231.
72. A. R. Morgan, V. S. Pangka, and D. Dolphin. *J. Chem. Soc. Chem. Commun.* 1984, 1047.
73. T. S. Mang, R. Allison, and G. Hewston. *Cancer J. Sci. Am.* 1998, **4**, 378.
74. J. L. Sessler, N. A. Tvermoes, J. Davis, P. Anzenbucher Jr, K. Jursikova, W. Sato, D. Seidel, V. Lynch, C. B. Black, A. Try, B. Andioletti, G. Hemmi, T. D. Mody, and D. J. Magda, V. Kral. *Pure. Appl. Chem.* 1999, **71**, 2009.
75. G. Kosterich, T. Babushkina, A. Lavi, V. Langzam, Malik, A. Orestein, B. Ehrenberg. *J. Porphyrins. Phthalocyanines*. 1998, **2**, 383.
76. R. K. Pandey. *J. Porphyrins. Phthalocyanines*. 2000, **4**, 368.
77. T. D. Mady. *J. Porphyrins Phthalocyanines*. 2000, **4**, 362.
78. M. Ambroz, A. Beeby, J. MacRoberts, M. S. Simpson, R. K. Svesson, and D. Phillips. *J. Photochem. Photobiol*. 1991, **9**, 87.

79. P. W. Atkins, Physical Chemistry (5th Ed), Oxford University Press, Oxford. 1994, 211.

80 N. B. McKeown. *Chem. Industr.* 1999, **1**, 92.

81 I. Rosenthal. *Photochem. Photobiol.* 1991, **54**, 859.

82. C. H. DePuy, and O. L.Chapman. *Molecular reactions and Photochemistry.* 1972, 35.

83. H. H. Selizer, and W. D. Mc Elroy. *Physical and biological action.*1965, 86.

84. A. Mayeda and A. J. Bard. *J. Am. Chem. Soc.* 1974, **96**, 4023.

85. R. Zimmerman, L. Flohe, U. Weser, and H. Hartman. *FEBS Lett.* 1973, **29**, 117.

86. W. Spiller, H. Kliesch, D. Wohrle, S. Hackbarth, B. Roder, and G. Scnurpfeil. *J.Porphyrins Phthalocyanines.* 1998, **2**, 146.

87. X. Zhang and H. Xu. *J. Chem. Soc. Faraday Trans.* 1993, **89**, 3847.

88. E. E. Wegner and A. W. Adamson. *J. Am. Chem. Soc.* 1966, **88**, 394.

89. M. G. Lagorio, L. E. Dicelio, E. A. San Romory. *J. Photochem. Photobiol. B. Biol.* 1989, **3**, 615.

90. R. Bonnet. Chemical aspects of Photodynamic therapy : Gordon and Breach, 2000, London.

91. D. R. Arnold, N. C. Baird, J. R. Bolton, J. C. D. Brand, P. W. M. Jacobs, P. de Mayo, and W. R. Ware. Photochemistry : An Introduction. Academic Press. New York. 1974.

92. R. Bensasson, C. R. Goldschmidt, E. Land, and T. G. Truscott. *Photochem. Photobiol.* 1978, **28**, 277.

93. P. Jacques and A. M. Braun. *Helv. Chim. Acta.* 1981, **64**, 1800.

94. J. A. Lacey, D. Phillips, L. R. Milgram, G. Yahioglu, and R. D. Recs, J. G. Dalton, and N. J. Turro. *Mol. Photochem.* 1970, **2**, 133.

95. A. D. Pomogailo, V. F. Razumov, and I. S. Voloshanovski. *J.Pophyrins Phthalocyanines.* 2000, **4**, 45.

96. X. Zhang and H. Xu. *J. Chem. Soc. Faradays Trans.* 1993, **89**, 3347.

97. J. M. Roberts. *J. Chem. Soc.* 1936, **1**, 1195.

98. R. P. Linstead. *J. Chem. Soc.* 1984, **136**, 1016.

99. R. K. Polley, T. G. Linben, P. Stihler, and M. Hanack. *J.Porphyrins Phthalocyanines.* 1997, **1**, 169.

100. N. Kobayashi, T. Ashida, and T. Osa. *Chem. Lett.* 1992, 2031.

101. M. Brewis and G. Clarkson. *J. Chem. Commun.* 1998, 969.

102. M. Geyer, F. Plenzig, J. Rauschnabel, M. Hanack, B. del Rey, A. Sastre, and T. Torres. *Synthesis.* 1996, 1139.

103. C. G. Claessens, D. Gonzalez-Rodriguez, and T. Torres. *Chem. Rev.* 2002, **102**, 835.

104. A. Meler and A. Osko. *Monatch. Chem.* 1972, **103**, 150.

105. A. Weitemeyer, H. Kliesch, and D. J. Wöhrle. *Org. Chem.* 1995, **60**, 4900.

106. P. Margaro, R. Langlois, J. E. van Lier, and S. Gaspard. *J. Photochem.Photobiol. B : Biol.* 1992, **14**, 187.

107. H. Ali, S. K. Sim, and J. E. van Lier. *J. Chem. Research.* 1999, 496.

108. K. Kuninobu, I. Tsutomu, and H. Makoto. *Inorg. Chim. Acta.* 1992, **196**, 127.

109. S. Nonell, N. Rubio, B. del Rey, and T. Torres. *J. Chem. Soc. Perkin Trans.2.* 2000, 1091.

110. N. Kobayashi, T. Tshizaki, K. Ishii, and H. Konami. *J. Am. Chem. Soc.* 1999, **121**, 1091.

111. B. del Rey, U. Keller, T. Torres, G. Rojo, F. Agullo-Lopez, S. Nonel, C. Marti, S. Brasselet, I. Ledoux, and J. Zyss. *J. Am. Chem. Soc.* 1998, **120**, 12808.

112. S. H. Kang, K. Kim, Y. S. Kang, W. C. Zim, G. O. Lbrechts, K. Wostyn, K. Clays, and A. Perssons. *Chem. Commun.* 1999, 1661.

113. M. J. Cook, M. F. Daniel, K. J. Harrisson, and A. J. Thomson. *J.Chem. Soc, Chem. Commun.* 1987, 1148

114. C. Feucht, T. Linssen, and M. Hanack. *Chem. Ber.* 1994, **127**, 113.

115. D. Wöhrle, G. Schnurpfeil, and G. Knothe. *Deys and Pigments.* 1992, **18**, 97.

116. M. Hanack and M. Geyer. *J. Chem. Soc. Chem. Commun.* 1994, 2253.

117. G. Torre and T. Torres. *J. Porphyrins. Phthalocynines.* 2002, **6**, 274.

118. O.Kahn, J. Galy, Y. Journaux, J. Jaud, I. Morgenstem-Badarau. *J. Am. Chem. Soc.* 1982, **104**, 2165.

119. C. G. Pierpant, L. C. Francesconi, D. N. Hendrickson. *Inorg. Chem.* 1977, **16**, 2367.

120. Y. Pei, Y. Journaux, and O. Kahn. *Inorg. Chem.* 1989, **28**, 100.

121. P. D. W. Boyd, Q. Li, J. B. Vincent, K. Folting, H. R. Chang, W. E. Streib, J. C. Huffman, G. Criston, and D. N. Hendrickson. *J. Am. Chem. Soc.* 1988, **110**, 8537.

122. G. P. Gupta, G. Lang, C. A. Koch, B. Wang, W. R. Scheidt, C. A. Reed. Inorg. Chem. 1990, **29**, 4234.

123. C. M. Che, L. G. Butler, and H. B. Gray. *J. Am. Chem. Soc.* 1981, **103**, 7796.

124. W. A. Fordyce, J. G. Brummer, G. A. Crosby. *J. Am. Chem. Soc.* 1981, **103**, 7061.

125. T. V. O'Halloran, M. M. Roberts, and S. J. Lippard. *Inorg. Chem.* 1986, **25**, 957.

126. M. K. Dickson, S. K. Pettee, and D. M. Rounhill. *Anal. Chem.* 1981, **53**, 2159.

127. L. Guo, D. E. Ellis, B. M. Hoffman, and Y. Ishikawa, Inorg. Chem. 1996, **35**, 5304.

128. D. Astruc. Electron Transfer and Radical Processes in Transition Metal Chemistry. VCH. New York. 1995.

129. O. Kahn, Molecular Magnestism. VCH. New York. 1993.

130. C. S. Velázquez, T. F. Baumann, M. M. Olmstead, H. Hope, A. G. M. Barrett, and B. M. Hoffman. *J. Am. Chem. Soc.* 1993, **115**, 9997.

131. C. S. Velázquez, G. A. Fox, W. E. Broderick, K. A. Andersen, O. P. Andersen, A. G. M. Barrett, and B. M. Hoffman. *J. Am. Chem. Soc.* 1992, **114**, 7416.

132. D. P. Goldberg, S. L. J. Michel, A. J. P. White, D. J. Williams, A. G. M. Barrett, and B. M. Hoffman. *Inorg. Chem.* 1998, **37**, 2100.

133. H. Nie, C. L. Stern, A. G. M. Barrett, and B. M. Hoffman. *J. Chem. Soc.*, Chem. Commun. 1999, 703.

134. A. G. Mantalban, S. J. Lange, L. S. Beal, N. S. Mani, A. J. P. White, D. J. Williams, A. G. M. Barrett, and B. M. Hoffman. *J. Org. Chem.* 1997, **62**, 9284.

135. S. J. Lange. *Tetrahedron.* 2000, **56**, 7371.

136. B. L. Wheeler, G. Nagasubramanien, A. J. Bard, L. A. Schechtman, D. R. Dininny, and M. E. Kenney. *J. Am. Chem. Soc.* 1984, **106**, 7404.

137. J. A. Ibers. *J. Porphyrins Phthalocyanines*. 2000, **4**, 425.

138. J. R. Darwent, P. Douglas, A. Harriman, G. Porter and M. Richoux. *Chem. Rev.* 1982, **44**, 83.

139. J. W. Sibert, T. F. Baumann, D. J. Williams, A. J. P. White, A. G. M Barrett, and B. M. Hoffman. *J. Am. Chem. Soc.* 1996, **118**, 10487.

140. T. P. Forsynth, D. B. G. Williams, A. G. Montalban, C. L. Stern, A. G. M. Barrett, and B. M. Hoffman. *J. Org. Chem.* 1998, **63**, 331.

141. T. F. Bauman, M. S. Nasir, J. W. Sibert, A. J. P. White, M. M. Olmstead, D. J. Williams, A. G. M. Barrett, and B. M. Hoffman. *J. Am. Chem. Soc.* 1996, **118**, 10479.

142. C. S. Velázquez, W. E. Broderick, M. Sabat, A. G. M. Barrett, and B. M. Hoffman. *J. Am. Chem. Soc.* 1990, **112**, 7408.

143. A. S. Cook, D. B. G. Williams, A. J. P. White, D. J. Williams, S. J. Lange, A. G. M. Barrett, and B. M. Hoffman. *Angew. Chem. Int. Ed Engl.* 1997, **36**, 760.

144. T. F. Bauman, A. G. M. Barrett, and B. M. Hoffman. *Inorg. Chem.* 1997, **36**, 5661.

145. M. Gouterm. In The Porphyrins; D. Dolphin, Ed.; Academic Press; New York. 1978, vol. 3, chapter 1.

146. J. Mack, S. Kirby, E. A. Ough, and M. J. Stillman. *Inorg. Chem.* 1992, **31**, 1717.

147. M. G. Cory, H. Hirose, and M. C. Zerner. *Inorg. Chem.* 1995, **34**, 2969.

148. X. L. Liang, S. Flores, D. E. Ellis, B. M. Hoffman, and R. L. Murselman. *J. Chem. Phys.* 1991, **95**, 403.

149. V. A. Kuzmitski, K. N. Solov'yov, M. P. Tsvirko. In Porphyrins : Spectroscopy, Electrochemistry and Application; N. S. Ersikolopyan, Ed. Nauka . Moscow. 1987, 37.

150. A. B. P. Lever., S, R. Pickens, P. C. Minor, S. Licicciа, B. S. Ramswamy, and K. Mangnal, *J. Am. Chem. Soc.* 1981, **103**, 6800.

151. W. A. Nevin, M. R. Hempstead, W. Liu, C. C. Leznoff, and A. B. P. Lever. *Inorg. Chem.* 1987, **26**, 540.

152. A. W. Dale. *Trans. Faraday. Soc*, 1969, **65,** 311.

153. W. J. Kroenke and M. E. Kenney. *Inorganic Chemistry.* 1964, **3**, 697.

2. Results and Discussion

2.1 Synthesis and characterisation of phthalocyanine and porphyrazine precursors

2.1.1 Substituted phthalonitrile derivatives

This section describes the synthesis of the starting materials as described in the literature (check chapter 3 for references) with modifications. The pre-cursors needed for this project were derived from 3,6-dicyanohydroquinone (**41**), unsubstituted furan (**42**), phthalic acid (**51**), diaminomaleonitrile (**44**), and 1,2-dicyanobenzene (**25**) (all of these were commercially available). Modification of the hydroxyl moieties of the 3,6-dicyanohydroquinone (**41**) with 1-bromopentane (**45**) or 1-chloronaphthalene (**46**) was necessary, Scheme 2.1. This modification was done to enhance the solubility of the resultant phthalonitriles (**47** and **48**). These reactions are generally very slow, and were completed after 5 days. K_2CO_3 was used as a base to abstract a hydroxyl proton from 3,6-dicyanohydroquinone (**41**). This nucleophile then reacts with 1-bromopentane or 1-chloronaphthalene to give **47** and **48** respectively. All the phthalonitriles were synthesized in good yields as reported in the experimental section.

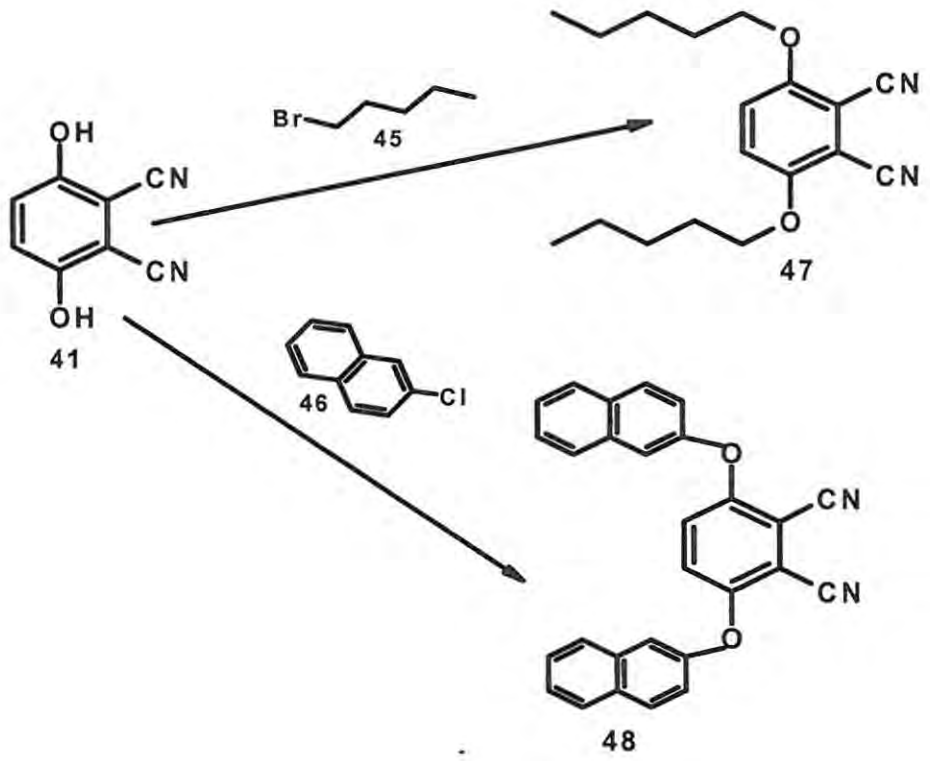

Scheme 2.1 Synthesis of phthalonitriles **47** and **48**

Compound **47** was synthesised in 92% yield and ^{1}H NMR spectroscopy showed slightly deshielded peaks (CH_2) at δ = 4.25-1.5 ppm, and at δ = 1.09-1.15 ppm the terminal methyl groups peak were observed. A singlet at δ = 7.45 ppm was also present and corresponds to protons that are attached directly to the benzene ring. IR spectroscopy also confirmed the presence of the nitrile group due to a stretch at 2228 cm^{-1} as well as an ether stretch at 1290 cm^{-1}. To increase the reactivity of compound **47**, NH_3 gas was bubbled through a suspension of this compound in hot ethylene glycol which allowed the synthesis of the diiminoisoindoline (**49**) (Scheme 2.2). Compound **48** (Scheme 2.1) was purified by recrystallization from methanol to yield 90% of product. The ^{1}H NMR spectrum showed deshielded peaks at δ = 7.35-7.93 ppm which correspond to the naphthalene ring substituents attached to the phthalonitrile. IR spectroscopy showed a nitrile stretch at 2225 cm^{-1} and a prominent ether band at 1315cm^{-1}.

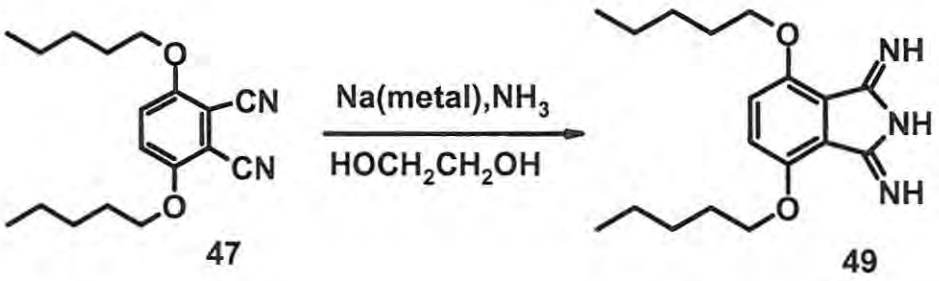

Scheme 2.2 Synthesis of diiminoisoindoline (**49**)

A direct carbon-carbon linked dihexyl phthalonitrile (**50**) was also synthesized for comparative purposes. The approach used is shown in Scheme 2.3. Conversion of commercially available furan (**42**), into dialkyl furan (**43**) was confirmed by the ^{1}HNMR which shows the expected methyl groups at ~ δ = 1.5-1.6 ppm and the -CH_2 groups of the long chain was also observed at ~ δ = 3.0-5.5 ppm. IR spectroscopy, in agreement with ^{1}HNMR, also confirmed the presence of a long alkyl chain at 1483 cm^{-1} and the aryl ether at 1288 cm^{-1}. The reaction of fumalonitrile with compound **43**, formed intermediate ether which was later converted to a 3,6-dihexylphthalonitrile (**50**) using lithium bis (trimethylsilyl) amide as a strong base. The formation of the compound **50** was also confirmed by ^{1}HNMR and IR spectroscopy. The shift of the proton peaks from the ^{1}HNMR spectroscopy to higher field was observed, and the peaks intergrated correctly. The IR spectroscopy showed the presence of C≡N vibration at 2135 cm^{-1}, which also confirms the formation of the phthalonitrile (**50**).

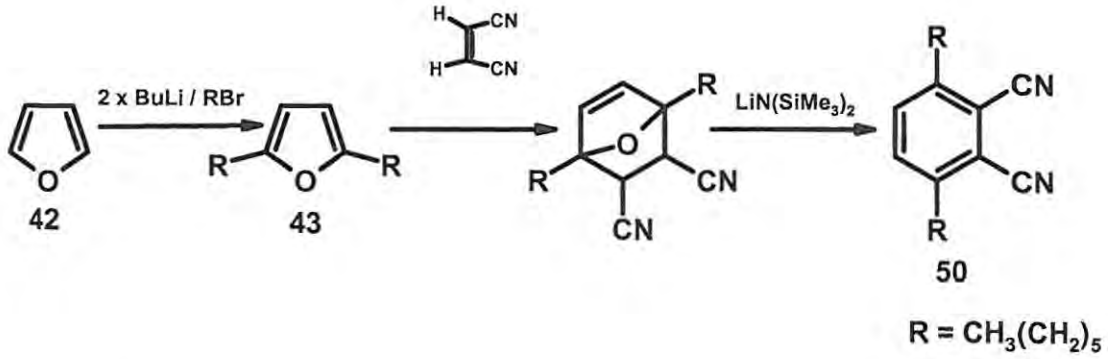

Scheme 2.3 Synthesis of 3,6-dihexylphthalonitrile (**50**) [1].

4-Nitrophthalonitrile was also required for the synthesis of an unsymmetrically substituted phthalocyanine and was prepared from phthalic acid (**51**), according to Scheme 2.4

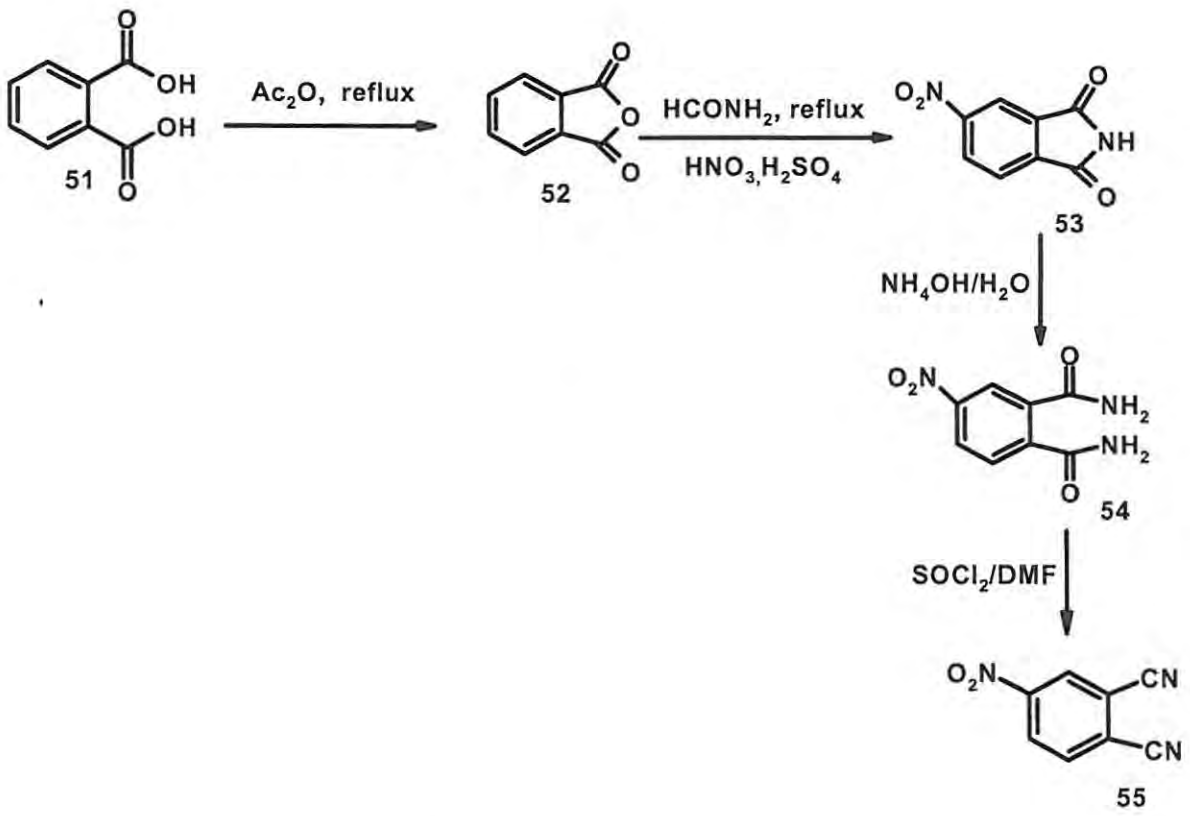

Scheme 2.4 Synthesis of 4-nitrophthalonitrile (**55**).

2.1.2 Substituted maleonitrile derivatives

Starting with maleonitrile (**44**), three compounds were made using acid chlorides to form amides according to Scheme 2.5 following reported methods (see experimental section).

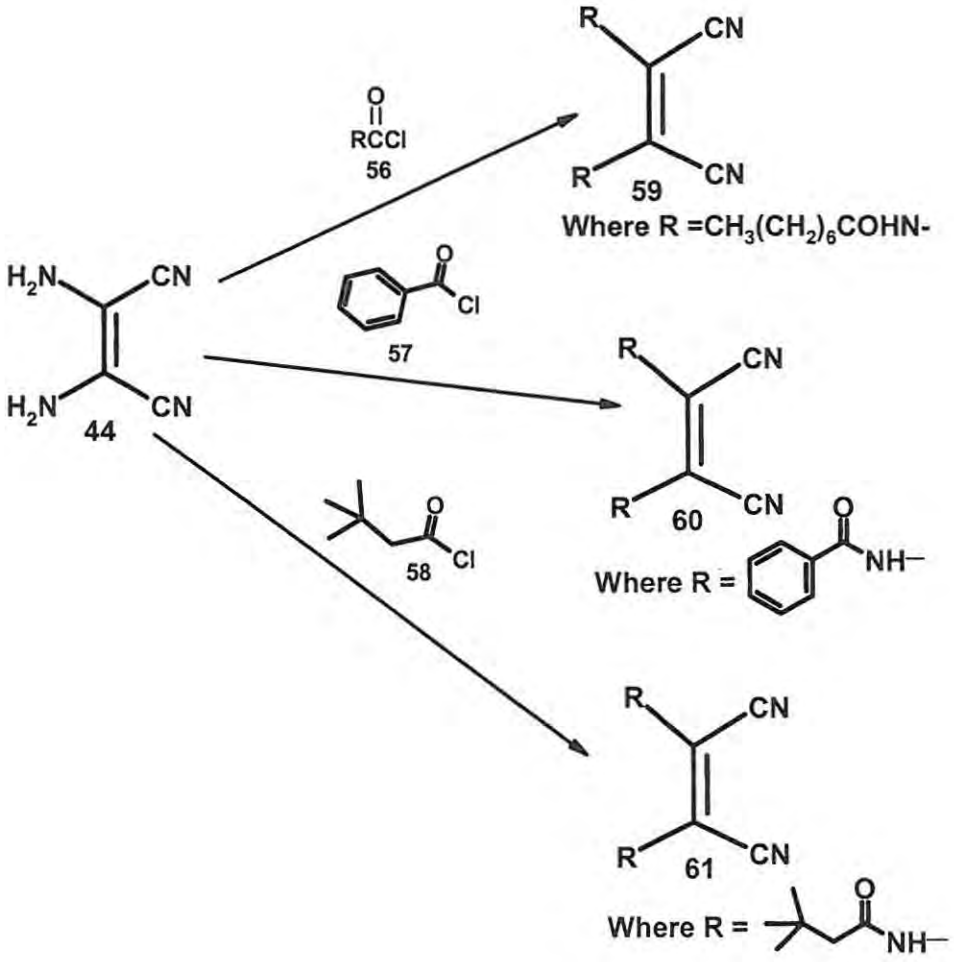

Scheme 2.5 Summary of the synthesis of maleonitrile derivatives (**59**, **60** and **61**)

The synthesis of these substituted maleonitriles was done using a standard acid chloride condensation with an amine. In the first reaction shown on Scheme 2.5 octanoyl chloride (**56**) was added to a solution of diaminomaleonitrile (**44**) and the reaction proceeded at room temperature to give **59**. The yield of the reaction was satisfactory at 67%. The reactions to produce compounds **60** and **61** were also performed at room temperature and the yields were 40% and 65%, respectively.

The acetyl chloride (**58**) was observed to react immediately and often violently with the maleonitrile (**44**). Benzoyl chloride (**57**) is much less reactive than both alkane derivatives (**56** and **58**) due to the decreased electrophilic character of the carbonyl carbon which is the point of attack for the amine nucleophile. The products were characterized by ^{1}H NMR and IR studies as shown in the experimental section. The IR spectra of all these substituted amide derivatives (**59**, **60** and **61**) showed strong stretches at ~ 3460 cm^{-1} which are characteristic N-H stretches. C≡N stretches are also present at 2359 cm^{-1}. Bands at ~ 1682 cm^{-1} are characteristic of carbonyl stretches. Compound **60** was found to be highly insoluble in many organic solvents but was soluble in MeOH, and only sparingly soluble in DMSO. The insolubility problem is probably due to the extended linear congugation due to the benzene rings.

2.1.3 Subphthalocyanine (SubPc)

Subphthalocyanine (**26**) (Scheme 2.6) was prepared according to the literature (see section 3.3.3). The SubPc was synthesized from commercially available 1,2-dicyanobenzene (**25**) and boron trichloride in a mixture of 1-chloronaphthalene/ dimethylsulphoxide (1:1) to yield a violet product, which was further purified by Soxhlet extraction using MeOH as a solvent, to form a brown product, and was employed as starting material for the formation of unsymmetrically substituted MPc complexes by ring expansion using substituted phthalonitriles and maleonitriles.

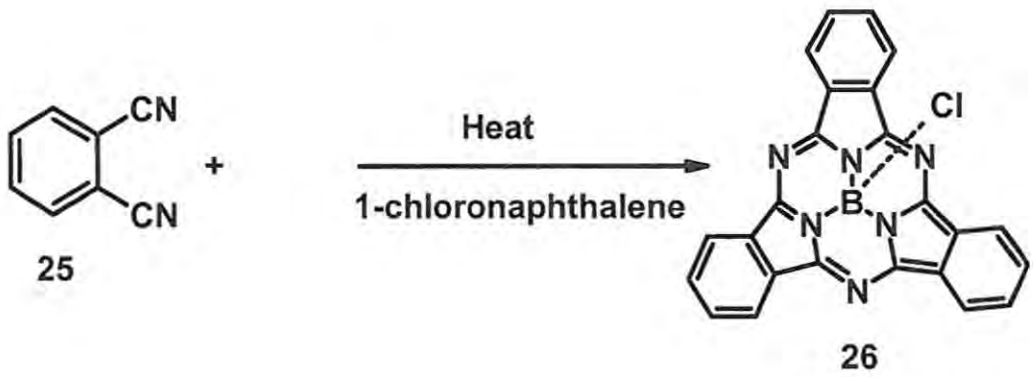

Scheme 2.6 Synthesis of unsubstituted subphthalocyanine (**26**)

2.2 Synthesis and charactarization of zinc phthalocyanine and porphyrazine derivatives

2.2.1 Synthesis

Subphthalocyanine (**26**) was used to synthesise the title compounds as shown in Scheme 2.7. The compounds are zinc(II)nitrophthalocyanine (**62**) as well as the three zinc(II) hemiporphyrazines (**63**, **64** and **65**)

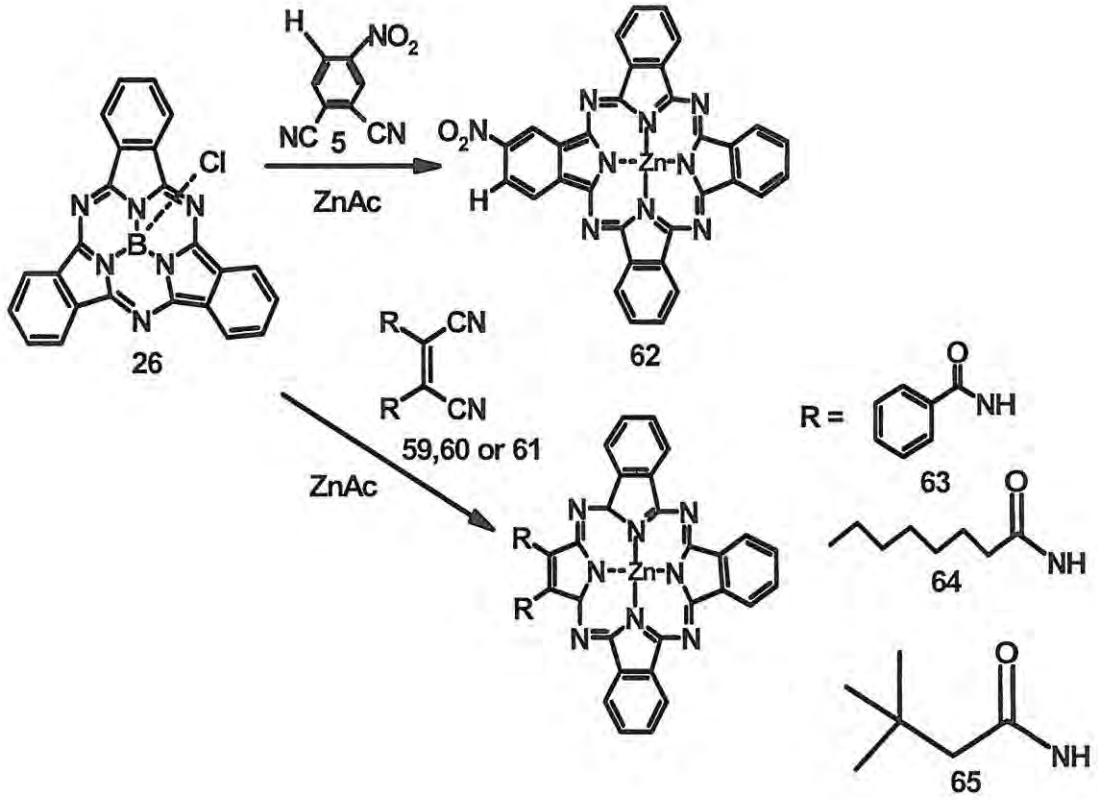

Scheme 2.7 Schematic represantation for the synthesis of compounds **62** to **65**

Statistical condensation and ring enlargement of subphthalocyanine, have been the most commonly used routes for synthesizing variously ring substituted phthalocyanines. The ring enlargement of subphthalocyanine [2,3] has been favoured over statistical condensation in that it generally results in higher compound yields [4]. A disadvantage of using this method is that some ring halogenated compounds are formed (< 1%) which are difficult to separate from

the desired compounds. In this study, thin layer chromatography (TLC) was employed for the separation of the compounds. These complexes gave satisfactory spectroscopic analysis, confirming the absence of chlorinated derivatives. The reaction times varied, depending on the complex synthesized (~1.5- 2 hrs) (see experimental). These compounds were characterized using IR, UV-visible spectroscopy, ^{1}H NMR and elemental analysis. The obtained yields of the Zn porphyrazine derivatives (**63**, **64** and **65**) Scheme 2.7 were lower than those reported in the literature [5], while that of zinc(II)nitrophthalocyanine (**62**) was comparatively higher (70%) than the reported literature value. Complexes **64** and **65** were also soluble in most organic solvents. Statistical condensation reaction of **49** and **25** (Scheme 2.8) (**66-68**), which were separated by column chromatography on silica gel using a 1:1 mixture of CH_2Cl_2/hexane as eluent. The separation of the compounds of this nature by common chromatographic methods is not easy due to their tendency to form aggregates [6]. These compounds were further purified by Soxhlet extraction. In all the formed compounds, the magnesium was removed by trifluoroacetic acid and the complex remetallated with zinc.

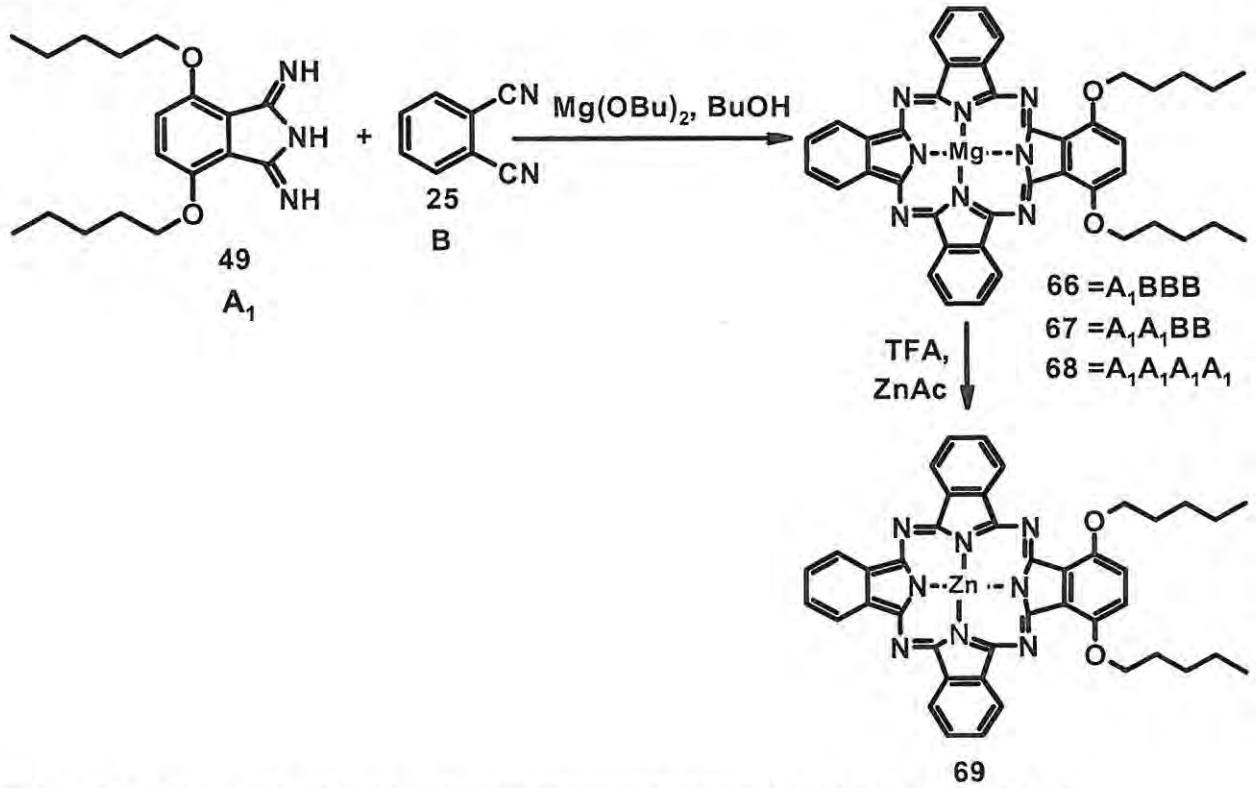

Scheme 2.8 Synthesis of zinc and magnesium phthalocyanines from the statistical condensation of **49** and **25**.

The main product among **66**, **67** and **68**, is compound **66**, which was converted to the zinc phthalocyanine (**69**) derivative. The abbreviations used represent the obtained compounds and the A_1A_1BB represents 2 compounds where the B groups are cis or trans to each other. The complexes show good solubility in common organic solvents. The yield of the compounds ranged from 15 - 33%. IR, ^{1}H NMR, UV-visible and Maldi-TOF mass spectrometry were used to characterize the compounds. Similarly from the condensation of 3,6-dinaphthaloxyphthalonitrile (**48**) and phthalonitrile (**25**), compound **70** and **71** were isolated (Scheme 2.9).

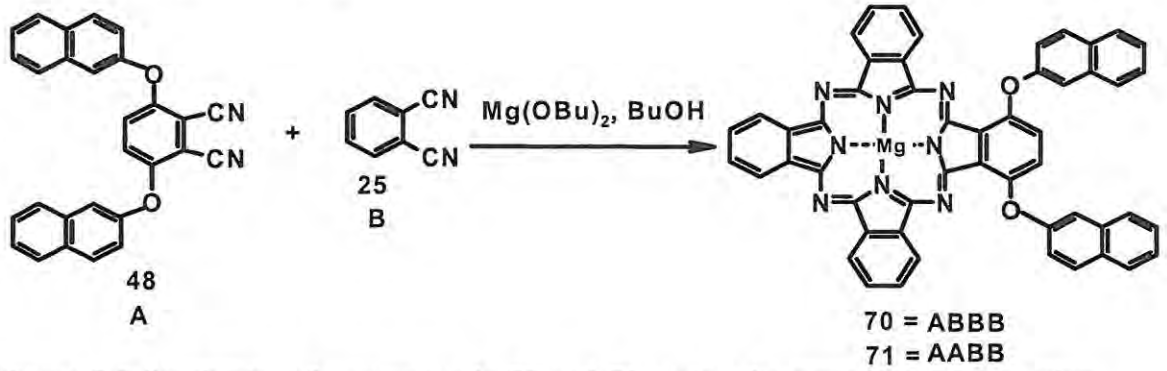

Scheme 2.9 Synthesis of compounds **70** and **71** using the statistical condensation method

In order to synthesise compounds **72** and **73** with direct carbon-carbon linkages, compounds **25** and **50** were condensed to form a mixture of magnesium phthalocyanines of which our interest was in the separated compounds **72** and resultant zinc phthalocyanine **73** (Scheme 2.10).

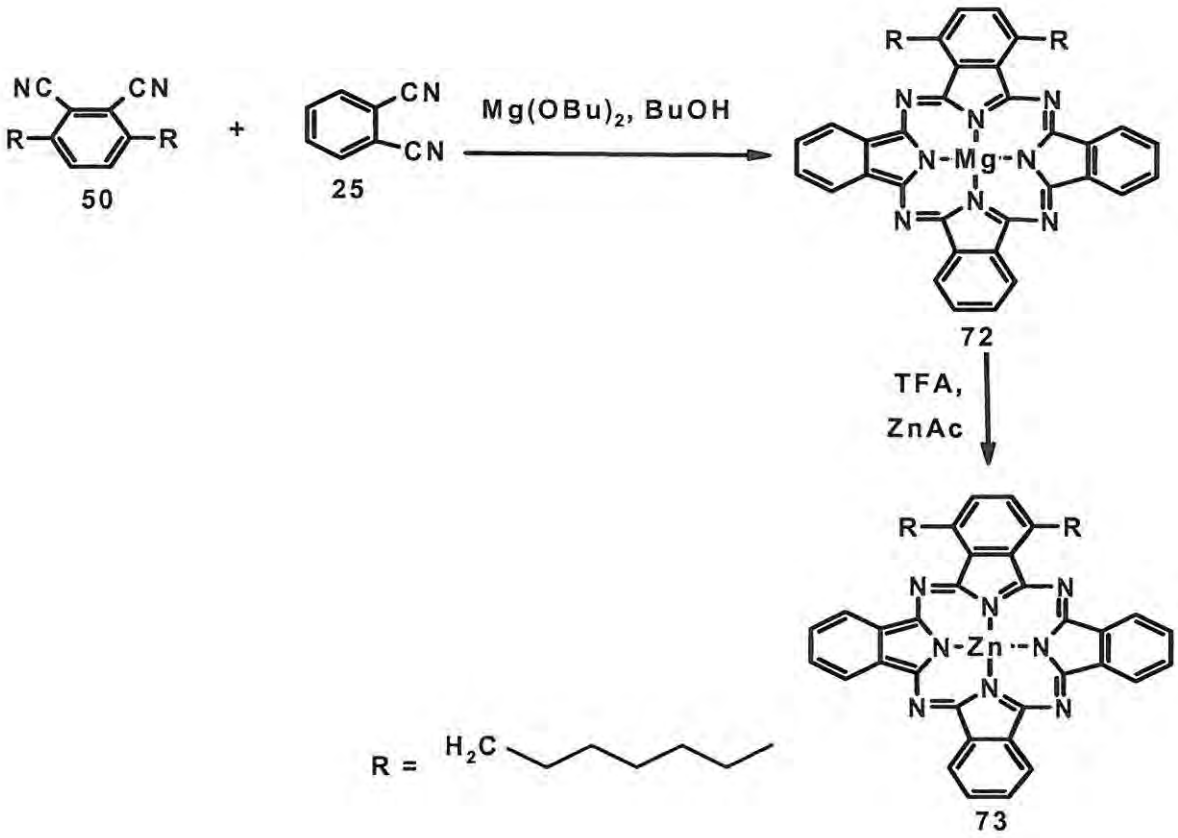

Scheme 2.10 Synthesis of compounds **72** and **73** using the statistical condensation of phthalonitrile (**25**) and dihexylphthalonitrile (**50**) [7,8].

The product **72** was isolated using thin layer chromatography (TLC) using CH_3OH / $CHCl_3$ (1:3) as eluent. Demetallation using TFA and subsequent metallation using zinc acetate gave the zinc phthalocyanine **73**. The yield obtained for complexes **72** and **73** were 49 and 42%, respectively. Both these compounds were soluble in aliphatic and aromatic hydrocarbon solvents i.e tetrahydrofuran, chloroform, and dichloromethane.

2.2.2 Spectroscopic characterization

The electronic spectra of all synthesised phthalocyanines and porphyrazines generally show no aggregation at concentrations lower than 1×10^{-5} mol dm^{-3}, and Beer's law was obeyed below this concentration (Figure 2.1)

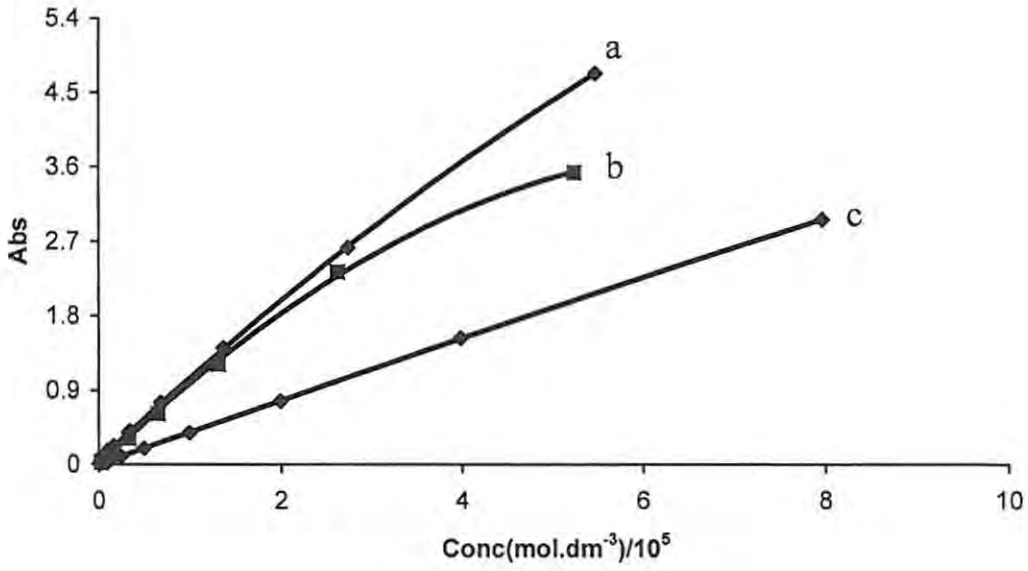

Figure 2.1. Beer's law dependence for complexes in DMSO, where a = **64** , b= **66**, and c = **70**.

The absorption spectral data of (**66, 67** and **68**) (Table 2.1) show λ_{max} of the Q band at 674, 693 and 696 nm respectively, with a weaker shoulder to the blue due to the vibrational modes within the electronic transition, Figure 2.2. The shoulder observed in the spectra of (**66, 67** and **68**) are located at 624, 622 and 625 nm respectively. The B bands were found at ~ 347 nm. It is clear that the number substituents have a dramatic effect (shifting) [9] on the Q band absorptions (compounds **66-68**).

The long alky chain groups increase the solubility properties of Pcs (**66** , **67** and **68**) i.e the more alkyl substituted the compound, the higher the solubility. The sequence of solubility is **68** > **67** > **66**.

The electronic absorption spectrum of compound **70** and **71** show split Q bands normally observed for macrocycles of less than D_{4h} symmetry [10].

Table 2.1. Electron absorption spectral data in DMSO for zinc and magnesium complexes. Where λ = wavelength in nm and ε = extinction coefficient in $dm^3\ mol^{-1}\ cm^{-1}$.

Complex	λ_{max} (log ε)	
	Q-bands	**B-bands**
63	672 (5.03), 607 (4.24)	342 (4.57)
64	672 (5.05), 607 (4.00)	340 (4.22)
65	672 (4.95), 607 (4.24)	338 (4.41)
66	674 (4.74), 624 (4.06)	347 (4.41)
67	693 (5.14), 622 (4.39)	347 (4.70)
68	696 (4.96), 625(4.82)	348 (4.43)
69	673 (5.02), 606 (4.84)	345 (4.23)
70	696 (4.92), 673 (4.29),606(4.45)	347 (4.53)
71	738(5.15),697(5.07)	347 (4.76)
72	672 (5.02), 607 (4.32)	348 (4.58)
73	673 (4.87), 607 (4.01)	347 (4.20)

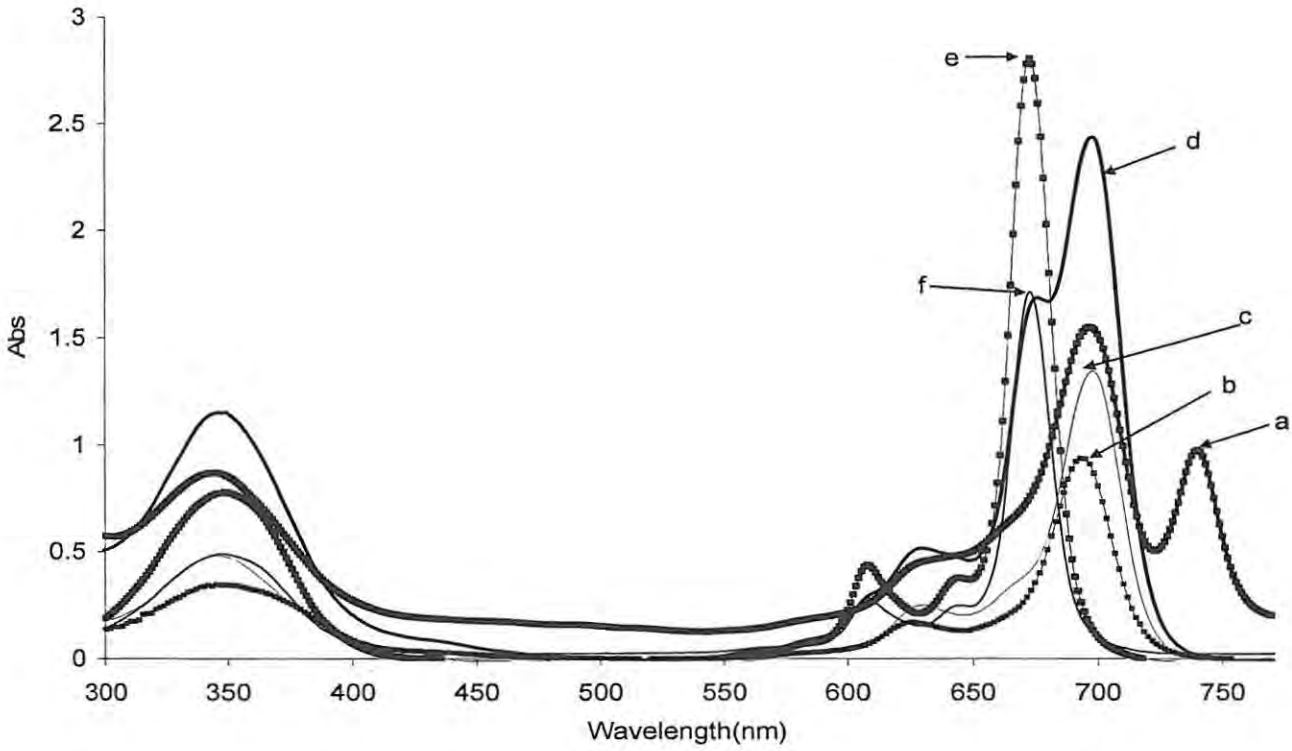

Figure 2.2. Electron absorption spectra of selected complexes in DMSO. Concentration ~$6x10^{-6}$ where a = **71**, b = **67**, c = **68**, d = **70**, e = **66**, f = **72** mol dm^{-3}.

Compound **69** shows a distinct Q band at 673 nm, which is the same as **66** within instrumental error.

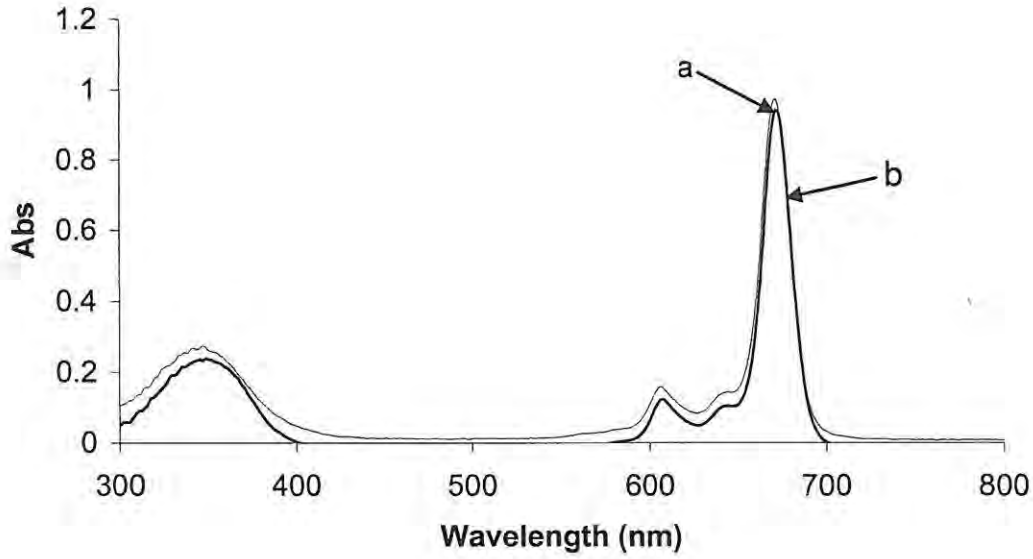

Figure 2.3. Electronic absorption spectra of the phthalocyanines complexes, a = **66** and b = **69**.

^{1}HNMR spectra of complexes (Figure 2.4) were recorded in d_6-DMSO and the values are given in Table 2.2. ^{1}HNMR was found to be a very useful tool of determining the structure of unsymmetrically substituted phthalocyanines [11]. All compounds gave satisfactory spectroscopic analysis of ^{1}HNMR to confirm their formation.

Strong and well resolved resonances are observed for methyl groups of the alkyl chain for both compounds **66** and **69** at $\delta = 0.30$ to 0.40 and 0.80 to 1.00 respectively, and $-CH_2$ groups ranging from $\delta = 0.80$ to 2.70 (**66**) and 1.30 to 5.06 (**69**), respectively.

Characteristic resonances in complexes **66** and **69** due to the non-peripheral (1,4-positions, see Figure.1 for labelling) protons of the phthalocyanines were observed as multiplets ranging from $\delta = 9.30$ to 9.41 (**66**) and 9.40 to 9.70 (**69**) and resonances due to the peripheral (2,3-positions) protons were observed as multiplet in separately enviroment ranging from $\delta =$ 7.50 to 8.50 (**66**) and 7.60 to 8.90 (**69**). The peaks were observed as multiplets probably due to the lack of symmetry of the compounds.

The ^{1}HNMR of compounds **66** and **69**, showed that the signals of the latter were slightly shifted to the down field than the former. This may probably due to a large diamagnetic ring current of Zn (as they are the same, and only differ in the metal center).

Complex **68** is octa-substituted hence contained no protons at 1,4-positions. Characteristic resonances due to the peripheral protons (2,3-positions) were observed as doublet at $\delta = 7.52$-7.89. The $-CH_3$ groups of the alkyl chain were observed at $\delta = 0.50$-1.00, and the $-CH_2$ groups at $\delta = 1.10$-4.30 were observed.

The 1,4-position protons of the Pc ring were observed downfield at δ ranging from $\delta = 9.75$ to 9.85 and $\delta = 9.83$ to 9.95 for both complexes **70** and **71** respectively, due to the ring current effects of the substituted benzene ring. Characteristic resonances due to the peripheral (2,3-positions) and non-peripheral (1,4-positions) protons of compound **71** and **70**, were observed as mainly singlets. The substituents on the phthalocyanine ring showed proton resonance peaks at $\delta = 7.10$ to 7.73 and $\delta = 7.00$ to 8.05 respectively, due to the aromatic rings for **70** and **71** and these intergrated correctly (Table 2.2.).

The structures of the compound **72** and **73** were also determined based on ^{1}HNMR, Figure 2.4. The most characteristic ^{1}HNMR spectra of these phthalocyanines showed resonances of the $-CH_2$ groups of the side chains ranging from $\delta = 1.00$ to 4.50 (**72**) and 1.40 to 5.40 (**73**). The methyl groups were also observed for these compounds ranging from $\delta = 0.80$ to 0.90 (**72**) and $\delta = 0.90$ to 1.20 (**73**). Again a slightly shift of the signals of the ZnPc (**73**) compared to that of the MgPc (**72**) was observed, due to a large diamagnetic ring current shift of Zn. The resonance peaks which were due to the Pc ring itself were observed ranging from $\delta = 9.40$ to 9.50 (**72**) and $\delta = 9.60$ to 9.70 (**73**) for non-peripheral (1,4-position). For peripheral (2,3-position) peaks were ranging from $\delta = 7.80$ to 8.50 (**73**) and $\delta = 7.60$ to 8.30 (**72**).

The side chains which exists in two magnetically similar environments, were observed as singlets and multiplets (compounds **72** and **73**). The signals of the protons of the $-CH_2$ groups which are closer to the benzene ring of the Pc were observed at a down field in contrast to the $-CH_2$ protons which are further apart from the ring. The shift of the protons of the side chains (in compounds **72** and **73**) to down field depends on their distance to the heteroaromatic core. The shorter the distance between the side chain protons and the center of the macrocycle, the larger the shift of the proton resonance to down field (compared to the rest of the molecules with long alkyl chain) [11].

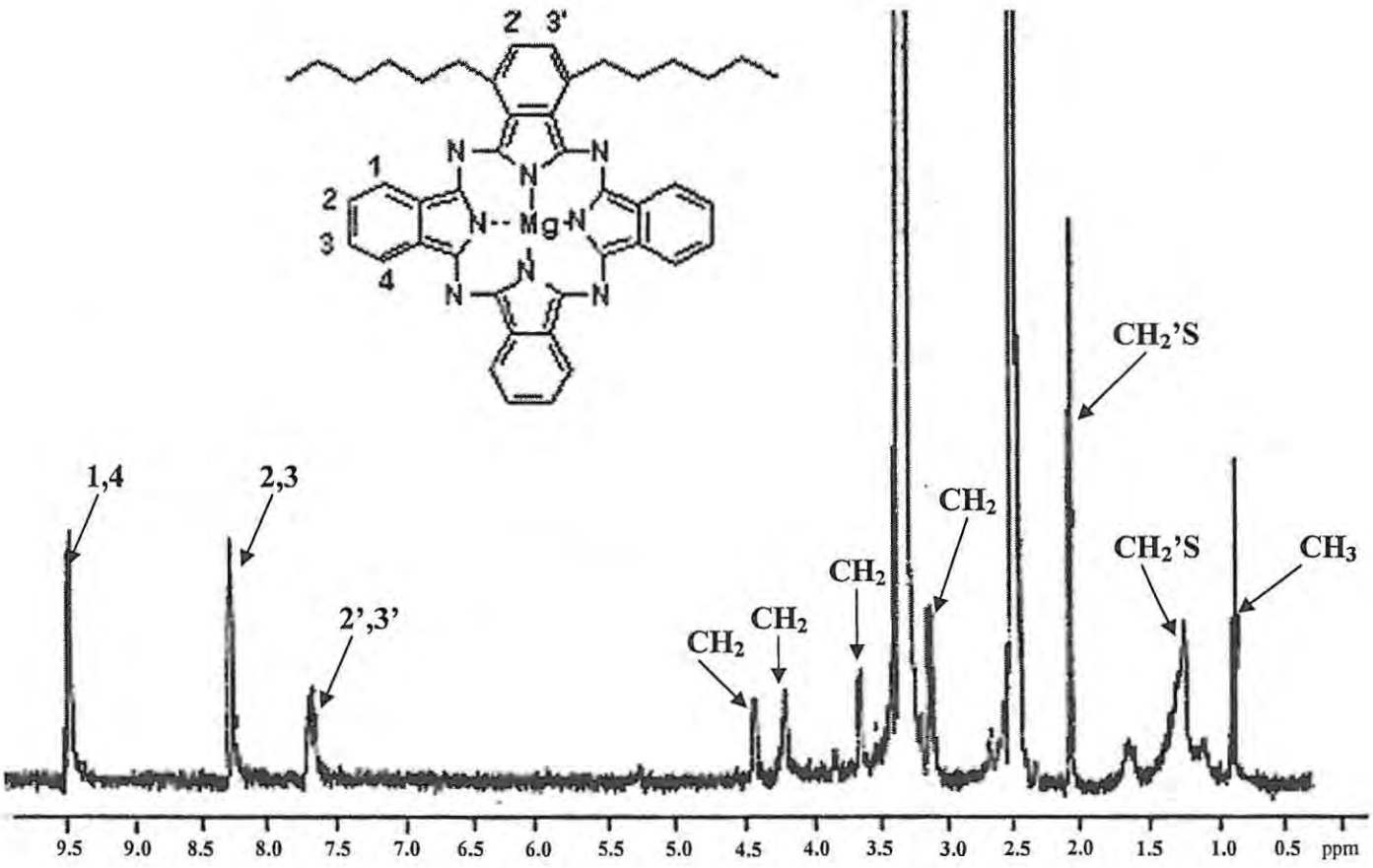

Figure 2.4 ^{1}HNMR spectra of complex **72** in d_6-DMSO

Table 2.2. ^{1}HNMR spectral data of the complexes in d_6-DMSO.

Complex	^{1}H NMR		
	1,4-Pc	**2,3-Pc**	**Ring substituents**
63	9.37-9.52 (m,6H)	8.21-8.30 (m,6H)	11.89-12.05 (s,1H,H_{-NH});10.40-10.55(s,1H,H_{-NH}) 7.45-8.20 (m,10H, H-benzene ring substituents)
64	9.30-9.38 (m,6H)	8.20-8.35 (m,6H)	12.65-12.85 (s,1H,H_{-NH}); 10.30-10.50(s,1H,H_{-NH}); 1.10-2.75 (m, 24H, H-long alkyl chain); 0.70-0.92 (t, 6H, H_{-CH3})
65	8.60-8.80 (m, 6H)	7.40-7.60 (m, 6H)	12.85-12.92 (s,1H, H_{-NH}); 10.40-10.60 (s,1H,H_{-NH}); 2.40-2.50 (m,4H,H_{CH2}); 1.70-1.90 (t,18H,H_{-CH3}).
66	9.30-9.40 (br s, 6H)	8.20-8.50 (m,2H); 7.50-7.90 (m,6H)	0.80-2.70 (m,16H,H-long alkyl chain); 0.30-0.40 (t, 6H, H_{-CH3}).
67	9.52-9.38 (m, 4H)	8.34-8.20 (m, 4H); 7.60-7.75 (m, 4H)	1.15-4.23 (m, 32H, H-long alkyl chain); 0.73-0.92 (t, 12H, H-$_{CH3}$).

68	-	7.52-7.89 (m, 8H)	1.10-4.30 (m, 64H, $H_{\text{-long alky chain}}$); 0.51-1.00 (t, 24H, $H_{\text{-CH3}}$).
69	9.40-9.70 (br s),6H)	8.40-8.90 (m,2H); 7.60-8.50 (m,6H)	1.30-5.06(m,6H,$H_{\text{-CH2}}$); 0.80-1.00(t,6H,$H_{\text{-CH3}}$).
70	9.75-9.85 (s , 6H)	8.01-8.33 (d , 8H)	7.25-7.73 (m,7H,H-Naphthaloxy ring substituents); 7.10-7.22 (m, 7H,H-Naphthaloxy ring substituents)
71	9.83-9.95 (s,4H)	8.15-8.32 (s, 4H); 8.47-8.95 (s, 4H)	7.00-8.05 (m, 28H, H-Naphthaloxy ring substituents)
72	9.40-9.50 (m, 6H)	8.20-8.30(m, 6H); 7.60-7.70(d, 2H)	4.40-4.50 (s, 2H, $H_{\text{-CH2}}$); 4.20-4.30 (s, 2H, $H_{\text{-CH2}}$); 2.60-2.70 (m, 4H, $H_{\text{-CH2}}$); 2.21-2.30 (m, 4H, $H_{\text{-CH2}}$); 2.00-2.10 (d, 4H, $H_{\text{-CH2}}$); 1.60-1.80 (s, br, 2H, $H_{\text{-CH2}}$); 1.00-1.50 (m, 6H, $H_{\text{-CH2}}$); 0.80-0.90 (t, 6H, $H_{\text{-CH3}}$).
73	9.60-9.70 (m, 6H)	8.00-8.50 (m, 6H); 7.80-7.90 (d, 2H)	5.20-5.40 (s, 2H, $H_{\text{-CH2}}$); 4.80-4.90 (m, 2H, $H_{\text{-CH2}}$); 4.50-4.70 (s, 2H, $H_{\text{-CH2}}$); 2.50-

			2.54 (m, 4H, H_{-CH2}); 2.30-2.40 (d, 4H, H_{-CH2}); 1.80-2.10 (s, br, 4H, H_{-CH2}); 1.40-1.50 (m, 6H, H_{-CH2}); 0.90-1.20 (t, 6H, H_{-CH3}).

br = broad, s = singlet and m = multiplet.

For complex **66**, Maldi-Tof mass spectra showed an intense isotopic cluster assignable to the protonated molecular ion [MH^+]. Its molecular mass of m/z = 709.098 corresponding to its structure. Figure 2.6. shows the experimental molecular ion region of complex **66** in which the isotopic distribution can be clearly resolved.

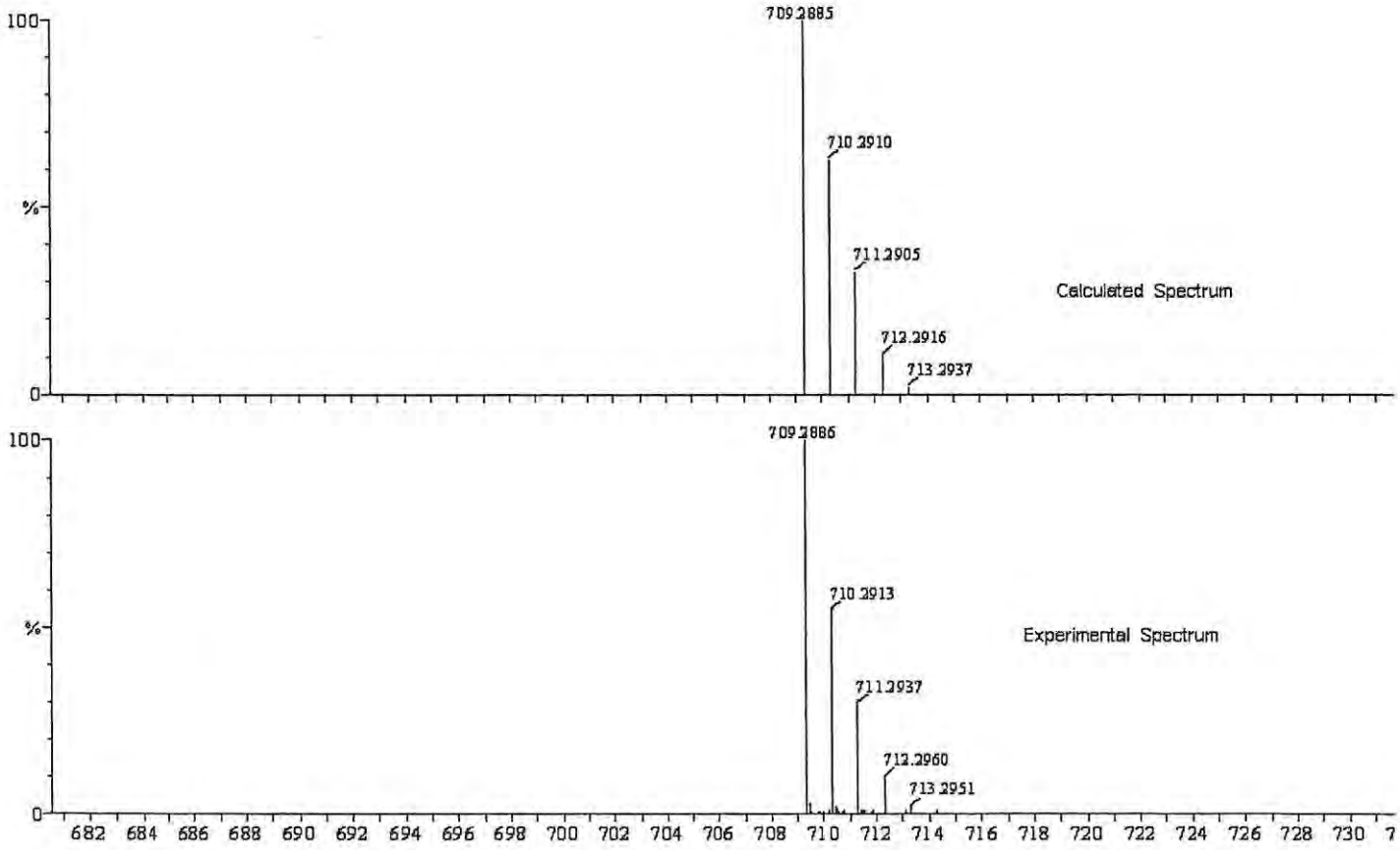

Figure 2.5. Maldi-Tof mass spectra for complex **66**.

IR spectra of the complexes are similar in pattern, Figure 2.7 (Table 2.3). Compounds show a band at ~1200 cm^{-1} (C-O-C vibration) which is a characteristic of an alkyl ether functionality [12]. The disappearance of the N-H of the diaminoisoindoline (**49**) at ~ 3228 cm^{-1} confirm the formation of the phthalocyanine.

IR spectra of all the compounds, showed the disappearance of C≡N vibration, as evidence of the formation of the complexes. The elemental analysis for the complexes gave satisfactory results. See Experimental, Chapter 3.

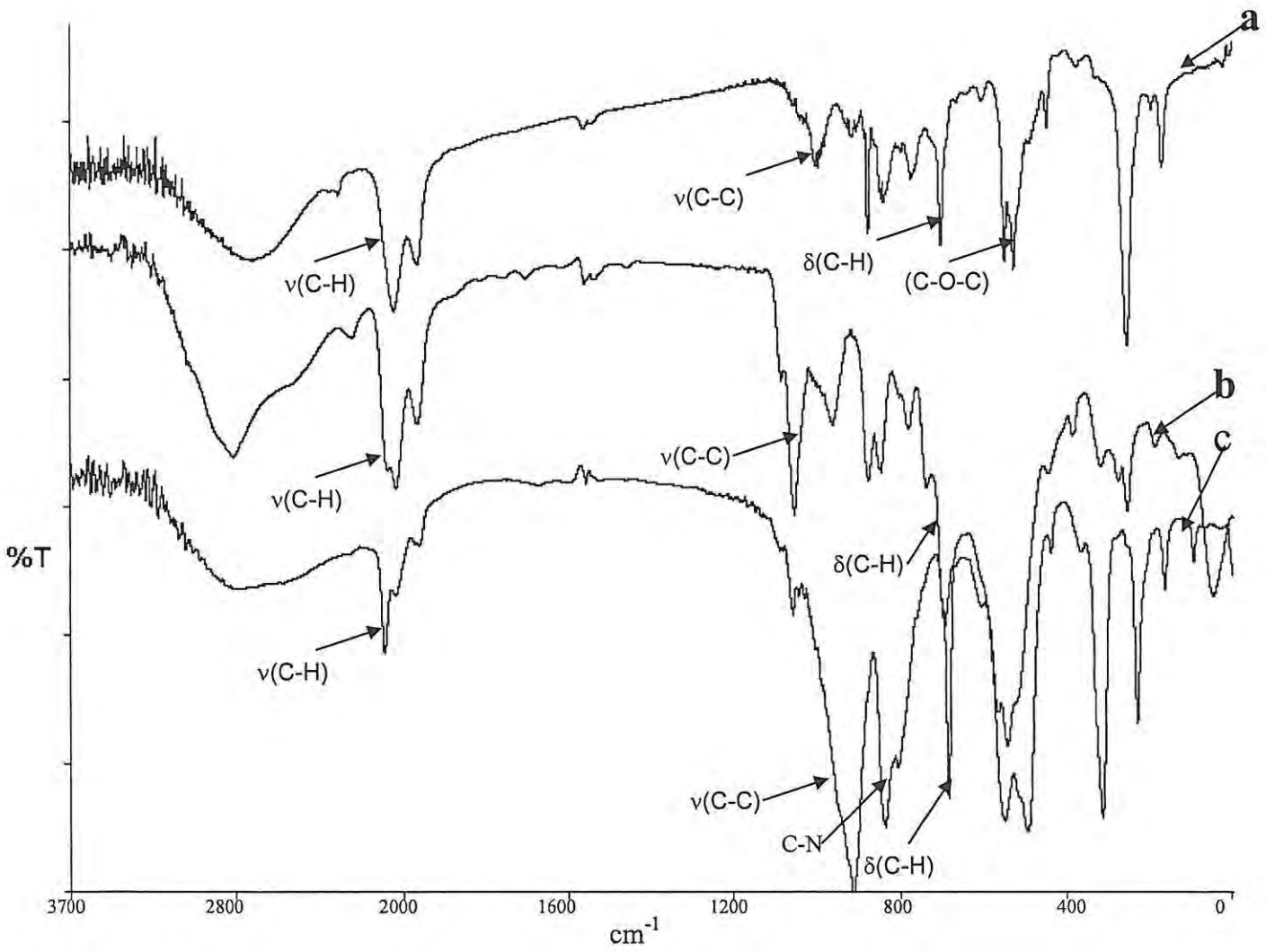

Figure 2.6. IR Spectra of the compounds, where a = **66**, b = **72** and c = **65**.

Table 2.3. Infrared spectroscopic data for zinc and magnesium phthalocyanine and porphyrazine complexes.

Complex	IR (KBr) (cm^{-1})	
	Characteristic bands	**Other bands**
63	3436 ν(N-H), 2234 (C-N),1676 ν(C=O), 1483 ν(C-C), 729 π(C-H)	3051, 1331, 1116, 1083, 1059, 889, 776, 754
64	3435 ν(N-H), 2357 ν(C-N), 1677 ν(C=O), 1467 ν(C-C), 1103(C-C), 743 π(C-H)	3046, 2931, 2336, 2218, 1192, 884, 648, 507
65	3460 ν(N-H), 3441 ν(C-H), 2359 ν(C-N), 2977 ν(C-H), 1648 , 1682 ν(C=O)	3370, 2731, 1366, 1319, 1247, 733, 625, 520, 466
66	3418 ν(C-H), 2929 ν(C-H), 1464 ν(C-C), 1274 (C-O-C), 724 π(C-H)	2865, 1725, 1608, 1502, 1380, 1085, 890, 804, 640, 463
67	3412 ν(C-H), 2954, 2924 ν(C-H), 1470, 1383 ν(C-C), 1276 (C-O-C), 1086 (C-C), 720 π(C-H)	2863, 1764, 1729, 1505, 1326, 1116, 1051, 880, 796, 747, 640, 461
68	3434 ν(C-H), 2973 ν(C-H), 1274 (C-O-C), 1153 (C-C), 718 π(C-H)	1728, 1373, 1213, 1059, 907
69	3394 ν(C-H), 2964 ν(C-H), 1454 ν(C-C), 1094, 1026 ν(C-C), 1262 (C-O-C), 696 π(C-H)	1553, 956, 802, 612, 523
70	3469 ν(C-H), 2962 ν(C-H), 1620 ν(C-C), 1501ν(C-C), 1261(C-O-C), 1099(C-H), 734 π(C-H)	1440, 1328, 1008, 803, 314
71	3057ν(C-H), 1607ν(C-C), 1506 ν(C-C), 1283 (C-O-C), 729 π(C-H)	2959, 2623, 2435, 2231, 1958, 1718,

		1486, 1458, 1409, 1333, 1246, 1165, 1114, 1093, 956, 886, 830, 796
72	3415 ν(C-H), 2966 ν(C-H), 1484 ν(C-C), 725 π(C-H)	3049, 1609, 1456, 1331, 1115, 1080, 1058
73	3473 ν(C-H), 2878 ν(C-H), 1470 ν(C-C), 750 π(C-H)	3053, 1638, 1569, 1398, 1310, 1150, 1093, 1023

2.3 Photochemical studies

2.3.1 Photobleaching studies

In photobleaching a compound is irradiated in the Q band region, which results in the degradation of it's macrocycle. Photobleaching were perfomed as described in the Experimental, Section 3.3. Photobleaching studies of the complexes were undertaken in order to determine the effects of different ring substituents on the stability of zinc and magnesium phthalocyanine and porphyrazine complexes in the presence of light. A typical specral change observed during degradation is shown in Figure 2.7, using compound **70**.
Photobleaching quantum yields of the complexes are listed in Table 2.4. All photobleaching studies were perfomed in DMSO, the quantum yields are in the order of 10^{-5} for all the complexes.

Table 2.4. Singlet oxygen and photobleaching quantum yields for zinc and magnesium phthalocyanines and porphyrazines DMSO.

Complex	λ_Q/nm(log ε)	Φ_Δ	Φ_p
63	673(4.93)	0.24	$2.58x10^{-5}$
64	673(5.05)	0.23	$1.9x10^{-5}$
65	673(4.95)	0.24	$2.48x10^{-5}$
66	693(5.02)	0.26	$1.33x10^{-5}$
67	674(5.14)	0.30	$2.88x10^{-5}$
68	674(4.82), 696(4.96)	0.50	$78.7x10^{-5}$
69	696(4.95)	0.40	$4.31x10^{-5}$
70	673(4.92)	0.25	$12.0x10^{-5}$
71	673(4.79), 695(4.65)	0.67	$1.33x10^{-5}$
72	672(5.02)	0.26	$0.22x10^{-5}$
73	673(4.87)	0.67	$4.29x10^{-5}$

Complexes containing more electron-donating groups are expected to be more easily oxidized, hence the observation of high photobleaching rates for some complexes like **65** compared to **64** confirms that the photobleaching mechanism involves oxidative degradation of the ring.

Comparing complexes **66**, **67**, and **68** with the same metal center but different number of the same substituents, the higher the number of the substituents, the higher the photobleaching quantum yield of the compound (hence lower stability). Whereas in **66** and **69** (as these complexes have the same number of substituents but differ in the metal center) photobleaching quantum yield for the Zn complex (**69**) was slightly less stable than that of the Mg complex (**66**). Complex **70** (which is di-substituted) showed less stability compared to **71** (which is tetra-substituted). High photostability reflect a strong π conjugation in **71** compared to **70**.

For porphyrazine complexes (**63**, **64**, and **65**) photobleaching quantum yields are not too different, while for different **72** and **73**, Mg complex more stable than Zn.

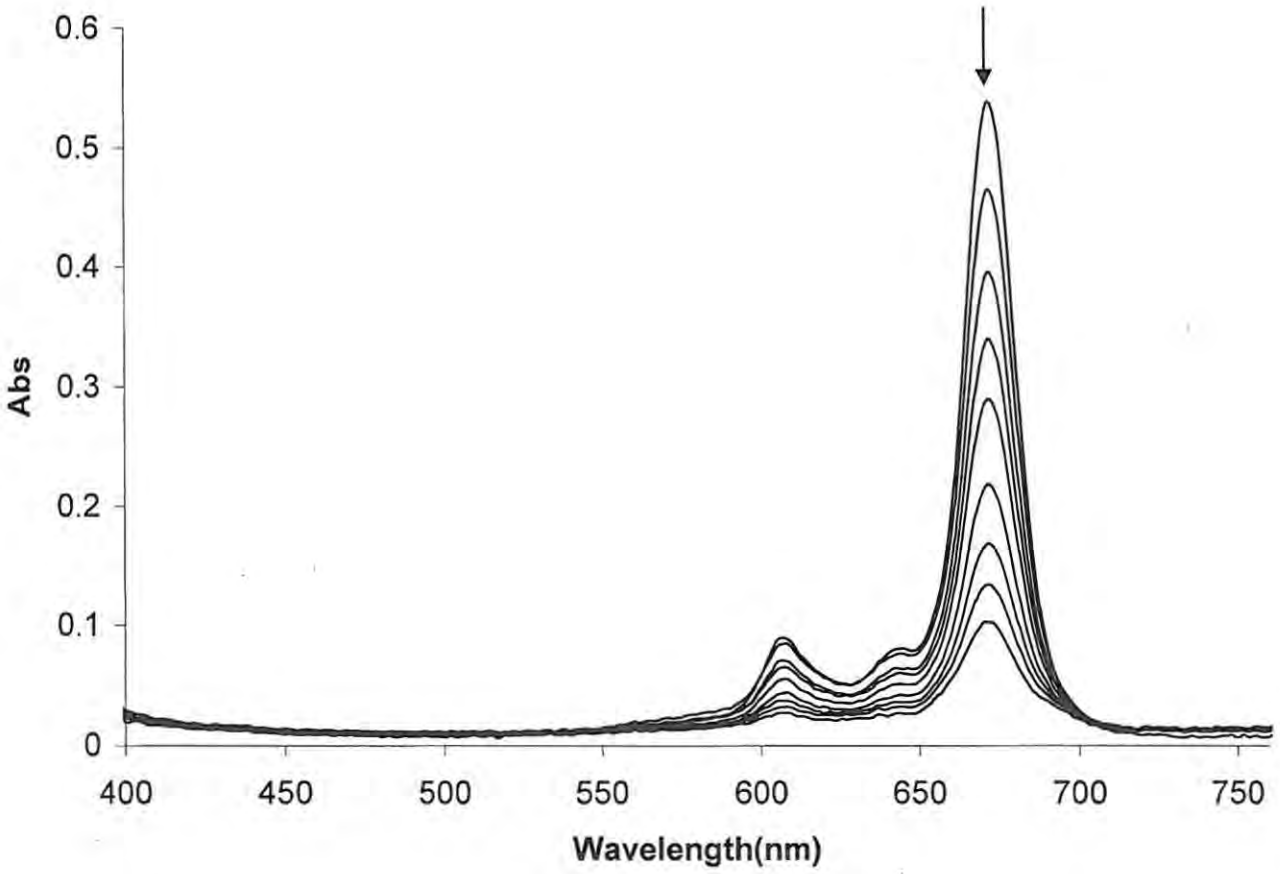

Figure 2.7. UV/vis spectra of **70** during the photobleaching process. Intial concentration used was 6.7×10^{-6} mol dm^{-3}.

An increase of quantum yields for photobleaching was observed when oxygen was bubbled through the solutions, as shown in figure 2.8. This was probably an indication of oxidative degradation which occurs due to singlet oxygen degrading the phthalocyanine macrocycle. A decrease in rate of photobleaching quantum yield was observed when DABCO (diazabicyclo-(2,2,2)-octane) was added as a radical scavenger, while when using d_6-DMSO as a solvent, an increase of the rate was also observed. Singlet oxygen is more stable in d_6DMSO, hence faster degradation. When nitrogen was bubbled through the solution, a decrease in rate of photobleaching quantum yield was also observed, showing that low or no oxygen reduces the rate at which the phhalocyanine macrocycle degrades. The reduction in rate in the presence of DABCO suggests that the degradation is not only a resulting singlet oxygen, but that radicals also play a part.

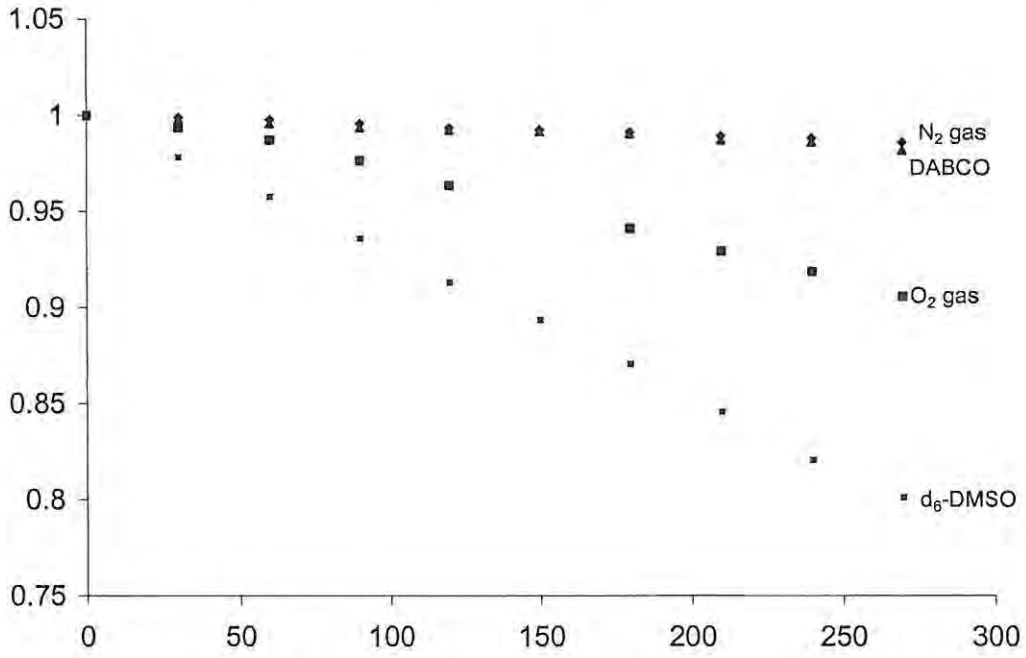

Figure 2.8. Photobleaching kinetic curves for complex **66** in air-saturated DMSO, deuterated DMSO, DABCO, Nitrogen and Oxygen.

The singlet oxygen interaction with the phthalocyanine is known to result in the macrocycle destruction of the phthalocyanine, resulting in formation of phthalimide as a photodegradation product [13].

2.3.2 Singlet Oxygen studies

The quantum yield of singlet oxygen photodegradation (Φ_Δ) of compounds in DMSO solution are presented in Table 2.4. Figure 2.10. shows the spectral changes observed during the photolysis of one of the ZnPc derivatives (**65**) in the presence of DPBF a singlet oxygen quencher.

The decrease of the DPBF maxima was monitored at ~ 417 nm. In all compounds little or no change in the spectra of the sensitizer was observed.

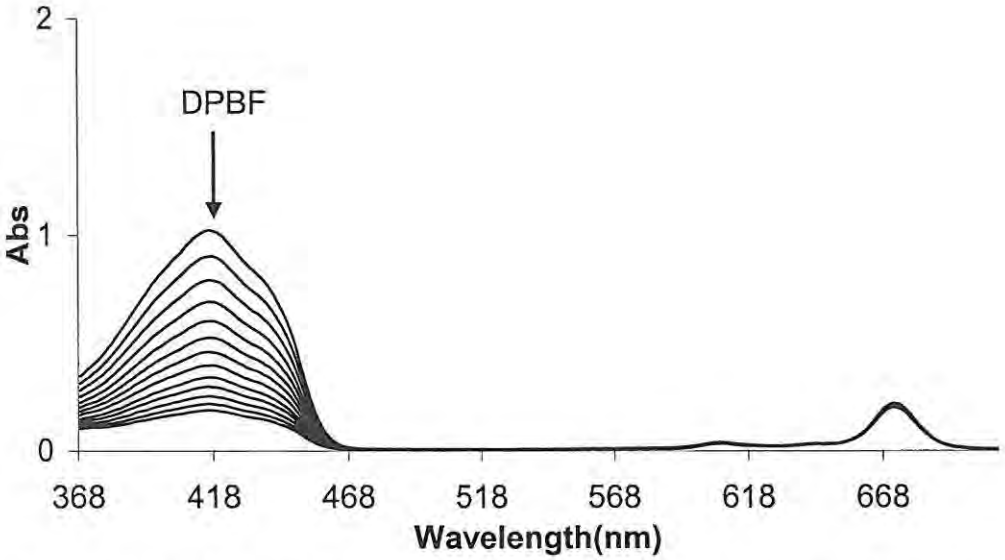

Figure 2.10. Spectral changes observed during photolysis of complex **65** in the presence of DPBF in DMSO. Initial [DPBF] = 1.8 x 10^{-3} mol dm^{-3} and [**65**] = 5.98 x 10^{-6} mol dm^{-3}

Low concentrations in the order of 10^{-6} mol. dm^{-3} were employed for the singlet oxygen studies to avoid aggregation and chain reactions that may occur [14].

For complexes **63, 64** and **65** relatively low Φ_Δ values were observed expected since porphyrazines generally have low Φ_Δ than phthalocyanines, also amine groups are known to quench singlet oxygen [15].

It can be seen in Table 2.4 that the MgPc complexes containing an increasing number of substituents e.g **66, 67** and **68** show an increase in singlet oxygen quantum yields (Φ_Δ) as the number of substituents increases (0.26, 0.30 and 0.50, respectively). This also the increase in the order of their Φ_p, which may confirm that since $^1O_2$ is involved in degrading molecules, the higher the Φ_Δ the higher the photobleaching.

Comparing complexes **66** and **69** values (as they contain different metal center, but same number of substituents) the higher Φ_Δ value for Zn complex **69** was observed (0.40) compared to the Mg complex (**66**) (0.26), this may probably due to the heavy atom effect, which results in the increase in triplet state quantum yield and lifetimes of Pc complexes.

Comparing complexes which also contain varying number of naphthaloxy substituents, complex **71** gave a significantly large value of Φ_Δ compare to complex **70** (that is, the more numbers electron-donating substituted groups, the higher singlet oxygen quantum yields (0.67 and 0.25 repectively for **70** and **71**).

Complexes **72** and **73** as they have the same number of substituents but differ in metal center, the singlet oxygen quantum yield value of the latter was significantly higher than that of the former (0.26 and 0.67 respectively), again reflecting the heavy atom effect.

All the singlet oxygen quantum yield values were within the literature values [16].

2.4 Photophysical studies

2.4.1 Triplet lifetime and quantum yield:

Singlet depletion curve for complex **71** is shown in Figure 2.10. Both the triplet lifetime and triplet quantum yield were determined by Laser flash photolysis for the selected compounds.

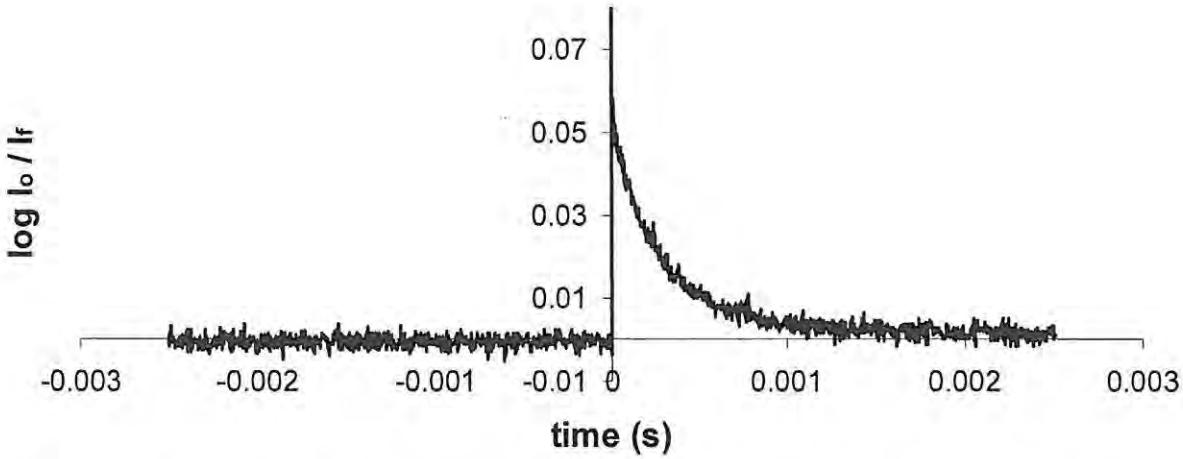

Figure 2.10. Singlet depletion curve for complex **71** showing monoexponential decay.

The triplet lifetime was determined by fitting the data to OriginPro 7.5. The triplet lifetimes (τ_T) for all the complexes were determined in DMSO. Both triplet quantum yields and triplet lifetime are listed in Table 2.5.

The largest τ_T value was observed for complex **68** (558 μs) and the smallest τ_T was observed for **72**. Complex **71** and **73** with the large Φ_Δ values of 0.67, had low τ_T of 230 and 250 μs, respectively. There is no direct correlation observed between Φ_Δ and τ_T as has been observed before [16]. Comparing **66, 67** and **68**, shows that the triplet life time (τ_T) increased with the number of substituents. For the triplet quantum yields, comparing complexes containing different central metal atoms, with the same number of substituents **72** and **73**, a larger triplet quantum yield was observed for the ZnPc (**73**) compared to the MgPc (**72**) (i.e 0.69 and 0 .43, respectively), due to the heavy atom effect of Zn.

When the number of the ring substituents are varied, the triplet quantum yields increases as the number of substituents increases as follows for **68** > **67** > **66**, as the τ_T and Φ_Δ values increase, accordingly.

Comparing porphyrazine complexes **63**, **64** and **65**, the long alky chain attached substituents (**64**) has higher triplet state lifetime (420 μs) compared to the benzene chain attached substituents (350 μs), and tertbutyl (360 μs) attached substituents.

Table 2.5. Triplet quantum yields and triplet lifetimes for zinc and magnesium phthalocyanine and porphyrazine complexes in DMSO.

Complex	$\lambda_{triplet}$ (nm)	Φ_T	τ_T (μs)	Φ_Δ
63	620	0.38	420	0.24
64	620	0.32	350	0.23
65	620	0.50	360	0.24
66	620	0.33	440	0.26
67	630	0.55	490	0.30
68	630	0.68	558	0.50
69	620	-	-	0.40
70	630	0.46	270	0.25
71	620	0.74	230	0.67
72	620	0.43	220	0.26
73	620	0.69	250	0.67

2.4.2 Fluorescence quantum yield

Figure 2.11. shows a typically normalized absorption and fluorescence spectra of the compounds in DMSO (using **66** as an example). The fluorescence data were recorded in DMSO solutions, with ZnPc being used as a reference (chapter 3.).

These are stokes shift of less than 20 nm, in general except for **68** (Table 2.6). These stokes shift trends suggests minor geometry differences between the ground and excited states, except for **68**.

Table 2.6. lists the fluorescence quantum yield values determined for complexes under study. It appears that ZnPc compounds have higher fluorescence quantum yields than the corresponding MgPc compounds, (**73** >**72**). However, within experimental error **69** and **66** have similar Φ_f.

The observed Φ_f values for **63** and **68** were quiet suprizing, since low values are observed (e.g 0.02 and 0.03 respectively). This could be a result of the quenching abilities of the substituents. Although these values seem so low, they are sufficient for fluorescence imaging applications. The Φ_f values for the complexes under study are within the range reported for complexes currently used for PDT [17,18].

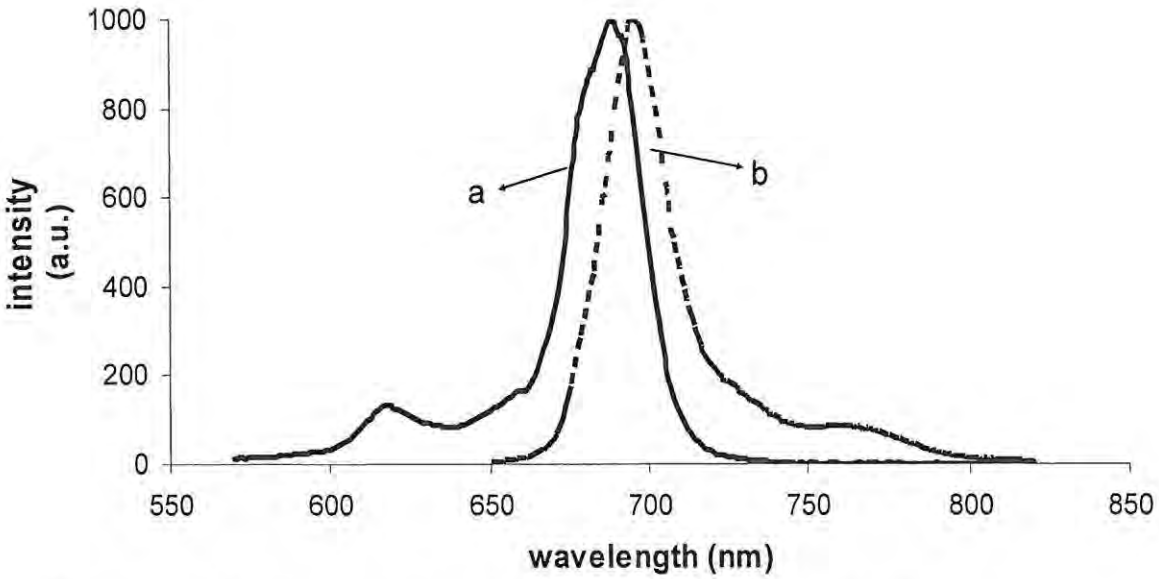

Figure 2.12. Fluorescence spectroscopy of the complex (**66**) where **a** = absorption spectra and **b** = emission spectra.

Table 2.6. Fluorescence data for zinc and magnesium phthalocyanines as well porphyrazine complexes in DMSO.

Complex	Stokes shift(nm)	Φ_f
63	7	0.02
64	7	0.22
65	12	0.14
66	10	0.14
67	7	0.18
68	37	0.03
69	16	0.12
70	8	0.18
71	7	0.18
72	9	0.20
73	9	0.26

References:

1. M. J. Cook, *The Chemical Record*, 2002, **2**, 225.
2. D. Wohrle, M. Eskes, K. Shigehara, A. Yamaha, *Synthesis*, 1993, 194.
3. H. Kliesch, A. Weitemeyer, S. Muller, D. Wohrle, *Liebigs. Ann*, 1995, 1272.
4. G. de la Torre and T. Torres, *J.Porphyrins Phthalocyanines*, 2002, **6**, 274.
5. N. Kobayashi, T. Ishizaki, K. Ishii, H. Konami, *J. Am. Chem. Soc*, 1999, **121**, 9096.
6. T. E. Youssef and M. Hannack, *J.Porphyrins Phthalocyanines*, 2002, **6**, 571.
7. N. Kobayashi, T. Ishizaki, K. Ishii, *J.Am.Chem.Soc*, 1999,**121**, 9096.
8. G. Schmid, M. Sommerhauer, M. Hannak in: Phthalocyanines in Properties and Applications, vol.3, C. C. Leznoff, A. B. P. Lever (Eds), VCH, 1999, New York, Chapter.1.
9. S. Angeloni and C. Ercolani, *J. Porphyrins Phthalocyanines*, 2000, **4**, 474.
10. M. Gouterman, in : D. Dolphin (Ed.), The Porphyrins, vol.3, Academic Press, New York, 1978.
11. R. Polley, T. G. Linben, P. Stihler and M. Hannack, *J.Porphyrins Phthalocyanines*, 1997, **1**, 169.
12. C. Jubert, A. Mohamadou, C. Gerard, S. Brandes, A. Tabard, J. –P, Barbier, *Inorg. Chem. Commun*, 2003, **6**, 900.
13. G. Winter, H. Heckmann, P. Hisch, W. Eberhardt, M. Hannack, L. Luer, H. J. Egelhaaf, D. Oelkrug, *J. Am. Chem. Soc*, 1998, **120**, 11662.
14. W. Spiller, H. Kliesch, D. Wöhrle, S. Hackbarth, B. Roder, and G. Schnurpfeil, *J. Porphyrins Phthalocyanines*, 1998, **2**, 145.
15. S. E. Maree and T. Nyokong, *J. Porphyrins Phthalocyanines*, 2001, **5**, 782.
16. G. Kostenich, T. Babushkina, A. Lavi, Y. Langzam, Z. Malik, A. Orestein, and B. Ehrenberg, *J. Porphyrins Phthalocyanines*, 1998, **2**, 382.
17. W. Bammler, C. Abels, and R. –M. Szeismies, Med. Laser Appl, 2003, **18**, 47.
18. E. G. Sakellariou, A. G. Montalban, H. G. Meunier, R. B. Ostler, G. Rumbles, A. G. M. Barrett, and B. M. Hoffman, *J. Photochem. Photobiol A : Chemistry*, 2000, **136**, 185.

3. EXPERIMENTAL

3.1 GENERAL APPARATUS

^{1}H-nuclear magnetic resonance (NMR) spectra were recorded on a Bruker EMX 400 NMR spectrometer. NMR spectra were obtained in the deuterated solvent specified, and are reported in parts per million (ppm, δ) downfield from a tetramethylsilane internal standard. UV-visible spectra were recorded on a Varian 500 UV/visible / NIR spectrophotometer. IR spectra (KBr pellets) were recorded with a Perkin Elmer Spectrum 2000 FTIR spectrometer. Maldi-TOF spectroscopy was also employed for analysing the compounds (Finnegan Madi-TOF mass spectroscopy). The light intensity was measured using a power meter (Lasermate).

SOLVENTS

N,N'-dimethylformamide (DMF) used for synthesis was dried over aluminium oxide and distilled before use. Dimethylsulphoxide (DMSO) was dried in alumina before use. Potasium carbonate, 2,3-dicyanobenzene, 1,4-dicyanohydroquinone, 1,8-diazabicyclo[5.4.0]undec-7-ene (DBU), 1,3-diphenylisobenzofuran (DPBF), diazabicyclooctane (DABCO), furan, butylthium, lithium bis(trimethylsilyl) amide ($LiN(SiMe_3)_2$) and trifluoroacetic acid were obtained from Sigma-Aldrich and used as received. All other solvents were distilled from the appropriate drying agents under a positive atmosphere. Alcohols were dried through generation of the alkoxide using magnesium and iodine. All other reagents were analytically or synthetically pure. ZnPc (Aldrich) was used as a standard for photochemical studies.

CHROMATOGRAPHY

Thin-layer chromatography (TLC) was performed using Merck GF_{254} silica gel plates with a 0.25 mm silica layer. Thin-layer chromatograms were developed

with solvent systems as indicated. The developed plates were visualized by using ultraviolet radiation (254 mm). Flash column chromatography was performed on Merck Kieselgel 60 (230 – 400 mesh) under a positive nitrogen pressure, in same cases.

3.2 PHOTOCHEMICAL AND PHOTOPHYSICAL METHODS

3.2.1 Singlet oxygen determination and photobleaching

Photochemical experiments were carried out in a spectrophotometric cell of 1 cm pathlength. For singlet oxygen determination, a typical procedure was as follows: a 2 ml air saturated DMSO solutions containing the MPz or MPc complexes under investigation (absorbance ~ 1 at the irradiation wavelength) and 1,3 diphenylbenzofuran (DPBF) (~3 x 10^{-5} mol dm^{-3}) were prepared in the dark, and introduced to the cell and photolysed in the Q band region of the dye with a General Electric Quartz line lamp (300 W). A 600 nm glass cut off filter (Schott) and a water filter were used to filter off ultraviolet and far infrared radiation. An interference filter (Intor, 650 nm, 670 nm or 700 nm with a bandwidth of 20 nm) was placed in the light path before the sample (Figure 3.1) under investigation for ZnPc complexes. The wavelength (close to that of the MPcs and MPzs) of the interference filter was chosen, depending on the absorption wavelength of the compound. The DPBF and Pc or Pz absorbances were both set to be ~ 1 and Q band irradiated by using appropriate inteference filter as explained above. DPBF absorption decay at ~ 416 nm was then monitored, while the Q band of the complexes remained unchanged. This is usually done by setting light intensity to be much lower than the one used for photobleaching purposes. The light intensity was measured with a power meter (Lasermate), the value was calculated using the equation 18. The values of Φ_Δ were calculated using Equation 19, with Φ_Δ^{ZnPc} = 0.67 [1] (singlet oxygen quantum yield for ZnPc standard in DMSO).

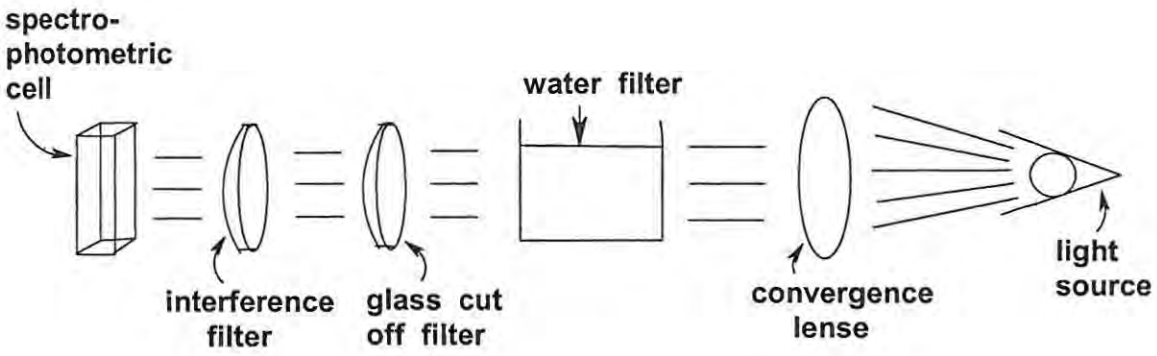

Figure 3.1 Set-up for singlet oxygen determination.

Experiments were also perfomed whereby the solutions were deaerated with N_2 gas, or saturated with O_2 in order to investigate the role of oxygen in the photodegradation process. The same set-up as described above was used for both the determination of quantumn yields of singlet oxygen and photodegradation except the fact that DPBF was employed for the former. And the light intensity used for photobleaching was much higher than that used for singlet oxygen purposes. Diazabicyclo-(2,2,2)-octane (DABCO) was used as a radical scavenger.

Calculation of α in equation 18 is shown in table 3.1, where T_{dye} is the transmittance of the dye, T_{filter} is the transmittance of the filter.

$$\alpha = \frac{\Sigma T_{filter}(1 - T_{dye})}{\Sigma T_{filter}}$$

Where α fraction of the overlap intergral of light for use in equation 18 and 19. For every new solution the α coefficient was determined and used for equation 19.

Table 3.1 Calculations of fraction of light (α) absorbed by the dye.

λ(nm)	T_{dye}	$1 - T_{dye}$	T_{filter}	$T_{filter}(1-T_{dye})$
680	0.70	0.30	0.08	0.02
690	0.65	0.35	0.87	0.31
			ΣT_{filter} = 0.95	$\Sigma T_{filter}(1-T_{dye})$ = 0.33

3.2.2 Triplet and fluorescence measurements.

Triplet state lifetimes and quantum yields were determined using a laser flash photolysis system. The excitation pulse was provided by a Nd-Yag (in frequency-doubled mode, providing 160 mJ, 80ns pulse of laser light at 10 Hz), pumping a Lambda-Phsik FL 2002 dye laser, Figure 3.2. A 75 W Xenon arc lamp provided the analysing light.

The Schematics of the system are shown in Figure 3.2. Triplet quantum yields were calculated using the singlet depletion method, equation 24 [2], and τ_T were determined by fitting data to OriginPro 7.5 Software .

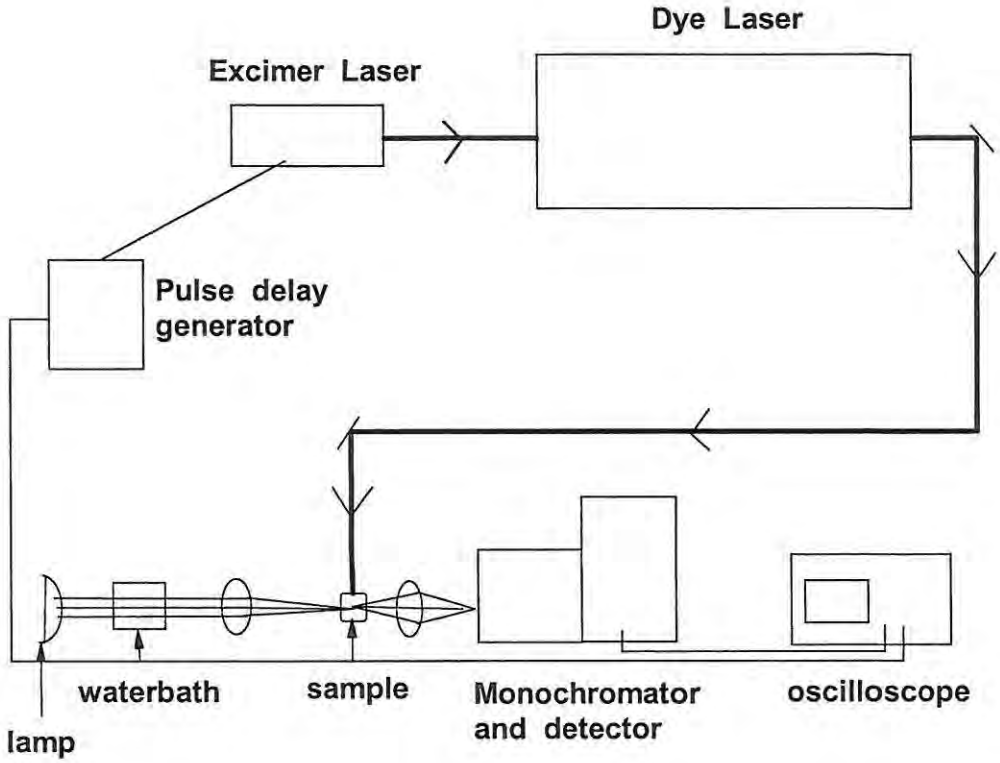

Figure 3.2 Set-up for triplet quantumn yield determinations.

Fluorescence (Φ_F) (equation 25), and triplet (Φ_T) (equation 24) quantum yields were calculated by a comparitive method using zinc phthalocyanine as a standard ($\Phi_F = 0.18$ [3] and $\Phi_T = 0.25$ [4]).

3.3 SYNTHESIS

3.3.1 Preparation of phthalonitrile precursors

The procedure were adopted from literature as follows: -

3.3.1.1 Synthesis of 1,4-hexyl furan (**43,** Scheme **2.3**) [5].

n–BuLi [3.5 M in hexane (50 ml)] was added to a solution of furan (**42**) (10 g, 0.15 mol) in dry THF (50 ml), under an atmosphere of dry argon at -78°C. The solution was allowed to warm to room temperature and stirred for 24 hr then cooled to -78°C and quenched with bromohexane (28.1 g, 0.1703 mol). The mixture was allowed to warm to room temperature and stirred for a further 24hr, then poured onto crushed ice (100 g) and extracted with diethyl ether (3x100 ml). The organic layer was then washed with water (50 ml), saturated brine (50 ml) and dried ($MgSO_4$), filtered and the solvents removed under reduced pressure to afford 1,4–hexylfuran (**43**). Yield = 62%

^{1}H NMR($CDCl_3$,400Hz): 1.5 – 1.6 (t, 6H, H_{-CH3}), 3.0-3.3 (m, 12H, H_{-CH2}), 3.5 – 4.0 (m, 8H, H_{-CH2}), 5.3-5.4 (s, 1H, H_{-Ring}), 5.5-5.6 (s, 1H, H_{-Ring}).

IR (KBr,cm^{-1}): ν = 1483 (long alkyl chain), 1288 (aryl ether).

3.3.1.2 Synthesis of 3,6-dihexyl -1,2-benzenedinitrile ether (Scheme **2.3**) [4].

Fumaronitrile (1.675 g, 0.0215 mol) was added to 1.4- hexylfuran (**43**) (8.75 g, 0.0371 mol) in the minimum amount of dry THF. The mixture was left in the fridge (T~5°C) for 14 days. After this time ^{1}H-NMR spectroscopy indicates a conversion to the adduct.

IR(KBr,cm^{-1}): ν = 2223 (C≡N str), 1495 (long alkyl chain), 1290 (aryl ether).

^{1}H-NMR ($CDCl_3$, 400 Hz):1.1-1.5 (t, 6H, H_{-CH3}), 3.2-3.3 (m, 12H, H_{-CH2}), 3.5-3.8(m, 8H, H_{-CH2}), 6.5-6.7 (m, 1H),7.1-7.3 (m, 1H).

3.3.1.3 Synthesis of 3,6-dihexyl -1,2-benzenedinitrile (**50**,Scheme **2.3**) [5].

The 3,6-dihxyl-1,2-benzenedinitrile was added to dry THF (250 ml) at -78°C and lithium bis (trimethylsilyl) amide 1.0M in THF (~ 45 ml) was added slowly. The dark solution was left stirring at -78°C for 0.5h, then left to warm to room temperature. The mixture was then poured over a saturated aqueous ammonium chloride and crushed ice (100 ml), and extracted with diethyl ether (3x25 ml). The organic layer was then washed with water (25 ml), saturated brine (25 ml) and dried ($MgSO_4$), filtered and the solvents removed under reduced pressure. The resultant mixture was separated by column chromatography over silica gel using dichloromethane/acetone (9:1) as a solvent to afford the crude product, which was treated with p-toluene sulfonic acid (25 mg) in methanol (50 ml) for 24hr. The resultant mixture was separated by column chromatography over silica gel using CH_2Cl_2/actetone (6:1) a eluent, and then recrystallized from ethanol to afford a colourless needles 1,4-hexylphthalonitrile (**50**).

Yield 53 %.

M.P: 61 - 63°C

^{1}H NMR ($CDCl_3$, 400 Hz): 1.15 – 1.75 (t, 6H, H_{-CH3}), 3.1 – 3.8 (m, 12H,H_{-CH2}), 4.2 –4.9 (m, 8H, H_{-CH2}), 5.2-5.5 (s, 2H, H_{-Ring}).

IR (KBr, cm^{-1}): 1467,1379 (long alkyl chain), 2135(C≡N str).

3.3.1.4 Synthesis of 3,6-dipentoxy-1,2-benzenedinitrile (**47**, Scheme **2.1**) [5,6].

3,6-bis(pentoxy)-1,2-benzenedinitrile was synthesized using reported procedure as follows:

A mixture of 3,6-dihydroxy-1,2-benzenedinitrile (**41**) (1.25 g, 0.007 mol) and K_2CO_3 (3.4 g, 0.0174 mol) in DMF (25 ml) was well stirred, 1-bromopentane (**45**) (2 ml) was added, and the solution was heated at 60°C for 48 h. At this time an additional portion of 2-bromopropane (0.5 ml) was added, and the solution was continuously heated at the same temperature for further 12 hrs. The reaction mixture was cooled to room temperature and poured into water (0.1 L) , and the solution was vigorously stirred. The resulting white solid was

filtered under reduced pressure and then recrystallized with hot MeOH to yield a white crystalline solid (**47**).

Yield 92 %

Mp. 205-210°C

^{1}H NMR ($CDCl_3$, 400 Hz) : 7.45(s , 2H , 6,7-benzene ring); 4.25 (t , 4H ,CH_2); 1.95-3.08(m, 4H , H_{-CH2}); 1.5-1.7 (m, 8H, H_{-CH2}), 1.09-1.15 (t , 6H , H_{-CH3}).

IR(KBr,cm^{-1}): ν = 2228 (C≡N str), 1496 (long alkyl chain), 1290 (C-O-C), 1200 , 1070 (Alky aryl ether), 961, 833 (substituted benzene ring).

3.3.1.5 Synthesis of 3,6-dinaphthaloxy-1,2-benzenedinitrile(**48**, Scheme **2.1**) [6,7].

A mixture of 3,6-dihydroxy-1,2-benzenedinitrile (**41**) (0.25 g, 1.6 mmol) and K_2CO_3 (3.4 g, 17.4 mmol) in DMF (25 ml) was well stirred, 1-chloronaphthalene (2 ml) was added, and the solution was heated at 120°C for 48 h. At this time an additional portion of 1-chloronaphthalene (0.5 ml) was added, and the solution was continuously heated at the same temperature for further 12 h. The reaction mixture was cooled to room temperature and poured into water (0.1 L), and the solution was vigorously stirred. The resulting light brown solid was filtered under reduced pressure and then recrystallized with hot MeOH to yield a white crystalline solid (**48**) (0.23 g, 0.6 mmol).

Yield 90 %

Mp. 205-210°C

^{1}H NMR ($CDCl_3$, 400 Hz) : 7.35-7.93(m , 14H , $H_{-naphthaloxy\ rings}$); 7.15(s, 2H, $H_{-benzene\ ring}$).

IR(KBr,cm^{-1}): ν = 2225 (C≡N str), 1315 (C-O-C), 961, 833 (substituted benzene ring).

3.3.1.6 Synthesis of 4,7-dipentoxy-1,3-diiminoisoindoline (**49**, Scheme **2.2**) [6,7].

3,6-bis(pentoxy)-1,2-benzenedinitrile (**47**) (1.13 g, 3.8 mmol) was suspended in DMF, and the mixture was heated to dissolve the suspension. Through the reaction mixture ammonia gas was bubbled until it was concentrated. The reaction mixture was cooled to room temperature and the resulting light brown solid was filtered under reduced pressure and then recrystallized with hot MeOH to yield a white crystalline solid as 4,7-bis(isopentoxy)-1,3-diiminoisoindoline (**49**).

IR(KBr,cm^{-1}): 3228 (N-H str) , 1262 (C-O-C)1375, 1052, 717.

3.3.1.7 Synthesis of 4-nitrophthalonitrile (**55**, Scheme **2.4**)

A 4-nitrophthalonitrile (**55**) was synthesized synthesized by the following method:

Synthesis of 4-nitrophthalimide (**53**, Scheme **2.4**)

Phthalimide (**52**) was synthesized from phthalic acid following literature [8] and converted to **53** as follows:

Fuming nitric acid (30 ml) was added slowly to the concentrated sulphuric acid (180 ml) and the mixture is cooled in an ice bath. When the temperature of the mixed acids reaches 12°C phthalimide (**52**) (50.0 g, 0.3 mol) was stirred in as quickly as possible while the temperature is mentained between 10°C and 15°C using ice-bath. The solution is then allowed to reach room temperature and left to stand overnight. The yellow solution obtained is poured on ice (1.1 kg) while rapidly stirring the solution to yield a beige suspension, which is removed by filtration under reduced pressure. The beige solid is washed with ice-water (6 x 150 ml) to yield 4-nitrophthalimide (**53**) (25.9 g, 0.1 mol)

Yield 40%

Mp. 197-200°C

^{1}H NMR ($CDCl_3$) 8.72 (d, 1H, H_{ring}), 8.68(dd, 1H, H_{ring}), 8.09(d, 1H, H_{ring}), 7.96(s, 1H, H_{NH}).

IR(KBr,cm^{-1}): 1780(s) and 1720(s)(Co-NH-CO), 1536(vs) (NO_2 assym.), 1349(vs) (NO_2 sym).

Synthesis of 4-nitrophthalamide (**54**, Scheme **2.4**).

4-nitrophthalimide (**53**) (20 g, 0.1 mol) was stirred in 25% aqueous ammonia solution (300 ml) for 24h, after this time a further 100 ml 25% aqueous ammonia solution was added and stirred for a further 24 hrs. The yellowish product was filtered off and washed with water (3 x 200 ml) to yield the 4-nitrophthalamide (**54**) (18.7 g, 0.09 mol).

Yield 89 %

Mp. 180-183°C

^{1}H NMR($CDCl_3$) : 8.42 (d, 1H, H_{ring}) 8.24 (dd, 1H, H_{ring}) 7.89 (d, 1H, H_{ring}).

IR(KBr,cm^{-1}) : 3340(NH_2 str), 1679(C=O str), 1615(NH_2).

Synthesis of 4-nitrophthalamide (**55**,Scheme **2.4**).

A freshly distilled thionyl chloride (70 ml, 0.07 mol) was added while stirring at 0°C to dry DMF(100 ml) in a nitrogen atmosphere. After 2 hrs , dry 4-nitrophthalamide (**54**) (17.0 g, 0.081 mol) was added. The mixture was stirred for 5h at 0°C and then at room temperature overnight before it was added to ice water (approx 500 ml), filtered and washed with H_2O (6 x 100ml). After recrystallizing twice from MeOH, light yellow 4-nitrophthalonitrile (**55**) was obtained (8.5 g, 0.05 mol).

Yield 60%

Mp.144-147°C

^{1}HNMR($CDCl_3$): 8.69(1H, d, Ar-H), 8.62(1H, dd, Ar-H), 8.11(1H, d, Ar-H),

IR(KBr,cm^{-1}) 2242(s)(C≡N), 1542(vs)(NO_2 assym), 1359(vs)(NO_2 sym).

3.3.2 Synthesis of Maleonitrile derivatives

3.3.2.1 Synthesis of octanoyl chloride (**56**, reaction 3.1.)

An acid chloride has to be synthesised from an appropriate carboxylic acid. The method was adopted from reference [9] and used for the synthesis as follows:

Thionyl chloride (8,3 g, 7.0 mmol) was heated gently at 50-60°C . At this time an octanoic acid (8.6 g , 6 mmol) was added to it dropwise for over 30-40 min, while on the other hand HCl and SO_2 were released from the solution as by products, leaving octanoyl chloride (**46**).

$$\mathbf{RCOOH + SOCl_2 \xrightarrow{\text{(excess)}} RCOCl + SO_2 + HCl}$$
$$\mathbf{46}$$

$\mathbf{R = CH_3(CH_2)_6}$

Reaction 3.1 Synthesis of octanoyl chloride (**46**)

3.3.2.2 Synthesis of 1,2-dicyano-1,2-dioctanoylamide (**59**, Scheme **2.5**).

Diaminomaleotrile (**44**) (3.2g, 3mmol) was suspended in dry DMSO (10 ml). and added the suspension of octanoyl chloride (**56**) in DMSO. The reaction was stirred for 12 hrs at room temperature being monitored by TLC until one spot appeared. The product was precipitated in H_2O (20 ml). The precipitate was filtered and washed with 10 % HCl to protonate the amino-groups in the maleonitrile. The filtered product was washed with H_2O (20 ml) and dried. The dried product was purified by flash column chromatography to give (**59**). IR spectra showed intense bands corresponding to C-N and C=O bond stretches.

Yield 67%

IR(KBr, cm^{-1}): ν = 3436 (N-H str), 3295, 2234 (C≡N str), 1726, 1671 and 1676 (C=O), 1512, 1465, 1410.

^1H NMR (d_6-DMSO, 400 Hz) : 10.4-10.5 (s, 1H, H_{-NH}); 3.5-1.15 (m, 24H, $H_{-long\ alkyl\ chain}$); 0.9-0.8(t, 6 H, H_{-CH3}).

3.3.2.3 Synthesis of 1,2-dicyano-1,2 dibenzoylamide (**60**, Scheme **2.5**).

The method was adopted from literature [9] as follows:

In a closed vessel, a mixture of diaminomaleonitrile (**44**) (0.1 g, 0.9 mmol) and benzoyl chloride (**57**) (0.27 g, 1.5 mmol) in DMF (20 ml) was vigorously shaken for 10-15 minutes. The colour of the solution drastically changed from brown to red and then to redish-pink precipitate. H_2O was added to the product and the mixture centrifuged (6 x 10 ml), then dried to produce (**60**) .

Yield 40%

IR (KBr,cm^{-1}): ν = 3435 (N-H str), 2357(C≡N) , 1677 (C=O), (substituted benzene ring).

^1H NMR (d_6-DMSO, 400 Hz) : 11.99-12.05(s,1H,H_{-NH});10.20-10.50(s,1H,H_{-NH});7.05-7.80(m,10H, $H_{-benzene\ ring\ substituents}$)

3.3.2.4 Synthesis of 1,2-dicyano-1,2-di-tertbutylacetylamide (**61,** Scheme **2.5**)

The method was also adopted from literature [9] as follows:

A mixture of diaminomaleonitrile (**44**) (0.1 g, 0.9 mmol) and tertbutylacetyl chloride (**58**, 0.32 g , 3.2 mmol) in DMF (20 ml) was vigorously stirred for 2-3 hr. The colour of the solution drastically changed from brown to dark pink then to yellow and then to a redish precipitate. Water was added H_2O to the product, the mixture centrifuged (6 x 10 ml), then dried, to produce (**61**).

Yield 65 %

IR (KBr, cm^{-1}): ν = 3460 (N-H str), 3253, 2359 (C≡N str), 1682 (C=O str), 1352(w) (tertbutyl peaks), 985.

^{1}H NMR ($CDCl_3$, 400 Hz) : 11.98-12.02 (s,1H, H_{-NH}); 10.20-10.30 (s,1H,H_{-NH}); 2.80-2.85 (m,2H,H_{CH2}); 2.10-2.55 (m,2H,H_{CH2}) 0.90-1.05 (t,18H,H_{-CH3}).

3.3.3 Synthesis of unsusbtituted subphthalocyanine (26, Scheme 2.6)

The unsubstituted sub-phthalocyanine (**26**) was synthesised by the following reported procedures [10-13] as follows:

Dicyanobenzene (**25**) (0.4 g, 3.5 mol), was suspended in 1-chloronaphthalene/DMSO (1:1) (50 ml). The reaction mixture was stirred for 5-10 min at room temperature. The mixture was then cooled to 0°C in ice-bath and BCl_3 (0.15 g, 1.0 mmol) was added dropwise under nitrogen, and the mixture allowed to warm up to room temperature. The reaction mixture was then heated to 220°C for 1hr, the product turned from yellow brown to deep violet. The solvent was removed and the resulting violet product was Soxhlet extracted for 24 hr with petroleum ether (80-100°C) and then for 2hr with toluene.

The obtained brown product was recrystallized from ethanol and washed with petroleum ether to yield a deep purple sub-phthalocyanine (**26**)

Yield = 75 %

UV/vis(nm, DMF): λ_{max} = 573, 568, 526, 310, 275

^{1}H NMR(400 MHz, $CDCl_3$) : 6.25-6.47 (s, 6H, H_{Sub-Pc}), 4.40-5.55 (s, 6H, H_{Sub-Pc}).

IR(KBr,cm^{-1}):ν = 1618, 1447, 1381, 1281, 1192, 1129, 953, 876, 752, 623.

3.4 Synthesis of zinc nitrophthalocyanines (62) and porphyrazines by ring enlargement of subphthalocyanine (63-65), Scheme 2.7

All these complexes were synthesized according to the literature methods [14] by dissolving unsubstituted SubPc (**26**) (1,287 g, 2.9 mmol) in the mixture of

freshly distilled DMSO:1-chloronaphthalene (4:2) (6ml). Then 4-nitrophthalonitrile (**54**) (0.173 g, 0.0009 mmol), **59** (0.306 g, 0.7 mmol), **60** (0.330 g, 0.001 mmol), or **61** (0.30 g, 0.8 mmol), to be used for ring expansion were dissolved in the freshly distilled DMSO:1-chloronaphthalene (4:2) (6 ml) in the presence of DBU (0.1 g, 0.65 mmol) for each reaction. The reaction mixtures were heated up to 130°C depending on how sensitive the reaction components were to the heat, then zinc(II) acetate dehydrate (0.11 g, 0.5 mmol) in the DMSO: 1-chloronaphthalene solvent mixture was added dropwise to the heated mixtures for over a period of 1hr. The reaction mixtures were refluxed at 130°C for approximately 0.5 hr - 1 hr. Then 1-chloronaphthalene was distilled off and the product mixtures in DMSO were precipited in H_2O, and centrifuged over methanol. The products were dried off to yield Pc (**62**) and Pzs (**63-65**).

Complex 62

Yield = 60%

UV/vis(nm, DMF): λ_{max} = 671, 606, 561, 344.

IR(KBr,cm^{-1}): ν = 1578(NO_2 assym), 1469, 1317, 2927, 3067, 3157 (Aromatic peak)(w).

Complex 63

Yield 34 %. Anal : Calcd. For $C_{42}H_{26}N_{10}O_2Zn$: C(65.67), H(3.41), N(18.24). Found : C(65.01), H(4.02), N(17.96). IR(KBr,cm^{-1}): ν = 717.7 (substituted benzene ring), 1263.2, 1375.1 (Aryl-N-) 1614 (C=O str). ^{1}HNMR (d_6-DMSO, 400 Hz): 9.37-9.52 (m, 6H, $H_{-1,4Pc}$); 8.21-8.30 (m, 6H, $H_{-2,3Pc}$); 11.89-12.05 (s,1H,H_{-NH});10.40-10.55(s,1H,H_{-NH})7.45-8.20 (m,10H, $H_{-benzene\ ring\ substituents}$).

UV/vis (DMSO): λ_{max} = 672, 603, 335, 263 nm.

Complex 64

Yield 45 %. Anal : Calcd. For $C_{44}H_{46}N_{10}O_2Zn$: C(65.06), H(5.71), N(17.24). Found : C(64.91), H(5.89), N(17.66). IR(KBr,cm^{-1}): ν = 1624 (C=O str), 1436.3 , 1408.0 (long alkyl chain), 894.7 , 760.9 (substituted benzene ring), 1309.9

(Aryl-N-). ^{1}H NMR (d_6-DMSO, 400 Hz) : 9.30-9.38 (m, 6H, $H_{-1,4Pc}$); 8.20-8.35 (m, 6H, $H_{-2,3Pc}$); 12.65-12.85 (s, 1H, H_{-NH}); 10.30-10.50(s, 1H, H_{-NH}); 1.10-2.75 (m, 24H, $H_{-long\ alkyl\ chain}$); 0.70-0.92 (t, 6H, H_{-CH3}).
UV/vis (DMSO): λ_{max}(nm) = 672, 605, 342, 265.

Complex 65

Yield 38 %. Anal : Calcd. For $C_{40}H_{38}N_{10}O_2Zn$: C(63.53), H(5.07), N(18.52). Found : C(63.01), H(4.89), N(17.16). IR(KBr,cm^{-1}): ν =1372(w) (tertbutyl peaks), 995, 1610 (C=O str). ^{1}H NMR (d_6-DMSO, 400 Hz): 8.60-8.80 (m, 6H, $H_{-1,4Pc}$); 7.40-7.60 (m, 6H, $H_{-2,3Pc}$); 12.85-12.92 (s,1H,H_{-NH}); 10.40-10.60 (s,1H,H_{-NH}); 2.40-2.50 (m,4H, H_{CH2}); 1.70-1.90 (t,18H,H_{-CH3}). UV/vis (DMSO): λ_{max}(nm) = 672, 605, 337, 263.

3.5 Synthesis of unsymmetrically substituted zinc and magnesium phthalocyanines by statistical condensation of dinitriles

*3.5.1 Synthesis of di-1,4-pentoxy (66), tetra-1,4,9,12-pentoxy (67) and octa-1,4,5,8,9,12,13,16-pentoxy (68) phthalocyaninato Mg(II) (*Scheme **2.8***)*

A suspension of magnesium turnings (0.7 ,0.03mol) in *n*-butanol (50 ml) was heated at reflux for 8-24 hrs using a small chip of iodine to initiate the reaction. To the resulting magnesium butoxide suspension was added **49** (1.10 g; 3.0 mmol) and 1,2-dicyanobenzene (**25**, 1.152 g, 9.0 mmol). The solution rapidly turned yellow, then bright green, and finally settled as a deep blue/green color within 1-2 hrs. The reaction mixture was kept at reflux under nitrogen atmosphere for 18 hrs. The butanol was removed by vaccum distillation, and residue taken up in $CHCl_3$ and filtered to remove the insoluble MgPc formed as a by product. The filtrate was concentrated and Soxhlet extracted with EtOAc / Hexane (1:1) to afford the product as a mixture, which was later further purified by Soxhlet extraction using different solvent mixtures, i.e MeOH / CH_3Cl (1:1) for **66**, EtOAc / Hexane (2:1) for **67**

and EtOAc / Acetone (3:4) for **68**, depending on the polarity of each compound from the product mixture.

Complex 66

Yield 33 %. Anal : Calcd. For $C_{42}H_{36}MgN_8O_2$: C(71.14), H(5.12), N(15.80). Found:C(73.01), H(4.92), N(15.52).

IR(KBr,cm^{-1}):ν=2228 (N-Hstr),1470,1382,1326 (long-alkylchain); 1252(C-O-C), 1085, 1052, 880 (substituted aromatic ring); 796(s) (substituted aromatic ring). ^1H NMR (d_6-DMSO, 400 Hz): 9.30-9.40 (br s,6H, $H_{-1,4Pc}$); 8.20-8.50 (m, 2H, $H_{-2,3Pc}$); 7.50-7.90 (m, 6H, $H_{-2,3Pc}$); 0.8-2.7 (m,16H,$H_{-long\ alkyl\ chain}$); 0.30-0.40 (t, 6H, H_{-CH3}).

UV/vis (DMSO): λ_{max} = 673, 624, 345 nm. Maldi-TOF $[MH]^+$ found : 709.098 , Calculated : 708.053.

Compound 67

Yield 19 %. Anal : Cald. For $C_{52}H_{56}MgN_8O_4$: C(70.86), H(6.40), N(13.71). Found : C(70.56), H(6.14), N(13.07). IR(KBr,cm^{-1}): ν = 2225 (N-H str), 1436, 1408 (long alkyl chain), 1230 (C-O-C), 1055, 1055, 1032 (alkyl ether), 897, 701(substituted benzene ring), 1311(Aryl-N-). ^{1}HNMR (d_6-DMSO, 400 Hz) : 9.52-9.38 (m, 4H, $H_{-1,4Pc}$); 8.34-8.20 (m, 4H, $H_{-2,3Pc}$); 7.60-7.75 (m, 4H, $H_{-2,3Pc}$); 1.15-4.23 (m, 32H, $H_{-long\ alkyl\ chain}$); 0.73-0.92 (t, 12H, H_{-CH3}).

UV/vis (DMSO): λ_{max} = 693, 622,347 nm.

Compound 68

Yield 15 %. Anal : Calcd. For $C_{72}H_{96}MgN_8O_8$: C(70.54), H(7.89), N(9.14). Found : C(70.89), H(8.01), N(9.30). IR(KBr,cm^{-1}): ν = 2229 (N-H str),1373 (long alkyl chain), 1333 (Aryl-N-) ,1226 (Alkyl ether), 1205 (-O-C), 723 (substituted benzene ring). ^{1}H NMR (d_6-DMSO, 400 Hz) : 7.52-7.89 (m, 8H, $H_{-3,2Pc}$); 1.10-4.30 (m, 64H, $H_{-long\ alky\ chain}$); 0.51-1.00 (t, 24H, H_{-CH3}). UV/vis (DMSO): λ_{max}(nm) = 696, 625, 343.

3.5.2 Synthesis of di-1,4-pentoxy phthalocyaninato Zn(II) (**69**, Scheme **2.8**).

The magnesium complex (**66**) was dissolved in neat trifluoroacetic acid (10-15 ml) and stirred at room temperature for 1 hr. The solution was poured over ice and neutralized with concentrated aqueous NH_3. The resulting precipitate was filtered and washed with water and MeOH. A large excess of zn(II) acetate was added to a mixture, chromatography by $CH_3OH/CHCl_3$ (1:l2) gave pure compound (**69**).

Yield 23 %. Anal : Calcd. For $C_{42}H_{36}N_8O_2Zn$: C(67.24), H(4.84), N(14.94). Found: C(68.01), H(4.87), N(14.52). IR(KBr,cm^{-1}): ν = 1451, 1410 (longalkychain), 1093, 1021, 952 (C-O str), 700, 800. ^1H NMR (d_6-DMSO, 400 Hz) : 9.40-9.70 (br s, 6H, $H_{-1,4Pc}$); 8.40-8.90 (m, 2H, $H_{-3,2Pc}$); 1.30-5.06(m,6H,H_{-CH2}); 0.80-1.00(t,6H,H_{-CH3}). UV/vis (DMSO): λ_{max}(nm) = 673, 624, 345.

3.5.3 Synthesis di-1,4-naphthaloxy(70) and tetra-1,4,9.12-naphthaloxy (71) phthalocyaninato Mg(II) (Scheme **2.9***)*

A mixture of 1.2-dicyanobenzene (**25**) (0.650 g, 9.0 mmol) and 1,4–dinaphthaloxyphthalonitrile (**48**, 0.170 g, 3.0 mmol) in butanol, was heated in the presence of magnesium butoxide and a small chip of iodine. The solution rapidly turned yellow, then deep green, and finally settled as a deep blue green within 8–12 hr. The reaction mixture was kept at reflux for 24 hr. The butanol was removed by blowing nitrogen gas to the solution while heating to evaporate the solvent (BuOH), and the residue was Soxhlet extracted with $CHCl_3$ and the insoluble MgPc formed as a by product. The resulting residue was concentrated and chromatographed to get the product as a mixture. The mixture was Soxhlet extracted with EtOAc / MeOH (1:1) for **70** and EtOAc / Hexane (3:2) for **71** as isolated products.

Compound 70

Yield 27 %. Anal : Calcd. For $C_{52}H_{28}MgN_8O_2$: C(76.06), H(3.44), N(13.65). Found : C(76.00), H(3.59), N(13.14). IR(KBr,cm^{-1}): ν =1310.4 (Aryl-N-) , 1287.8 (Aryl ethers) , 870.3 (substituted benzene ring) . ^1H NMR (d_6-DMSO, 400 Hz) :

9.75-9.85 (s , 6H, $H_{-1,4Pc}$); 8.01-8.33 (d , 8H, $H_{-2,3Pc}$); 7.25-7.73 (m,7H,H- $_{Naphthaloxy\ ring\ substituents}$); 7.10-7.22 (m, 7H,H- $_{Naphthaloxy\ ring\ substituents}$).

UV/vis (DMSO): λ_{max} (nm) = 696, 673, 606,347.

Compound 71

Yield 22 %. Anal : Calcd. For $C_{72}H_{40}MgN_8O_4$: C(78.28), H(3.65), N(10.14). Found : C(77.99), H(3.62), N(9.89). IR(KBr,cm^{-1}): ν =1310.4 (Aryl-N-) , 1287.8 (Aryl ethers) , 870.3 (substituted benzene ring). ^{1}H NMR (d_6-DMSO, 400 Hz): 9.83-9.95 (s,4H,$H_{-1,4Pc}$); 8.15-8.32 (s, 4H, $H_{-2,3Pc}$); 8.47-8.95 (s, 4H, $H_{-2,3Pc}$), 8.05-7.0 (m, 28H, $H_{-Naphthaloxy\ ring\ substituents}$). UV/vis (DMSO): λ_{max}(nm) =738, 697, 347 nm.

3.5.4 Synthesis of di-1,4-hexyl phthalocyanato Mg(II) (**72**,Scheme **2.10**)

A mixture of 1.2-dicyanobenzene (**25**, 0.288 g, 9.0 mmol) and 1,4–hexylphthalonitrile (**50**, 0.204 g,3.0 mmol) in butanol was heated, in the presence of magnesium butoxide, using a small chip of iodine to initiate the reaction. The solution rapidly turned yellow, then bright green, and finally settled as a deep blue green within 3– 4 hr. The reaction mixture was kept under reflux for 18 hr. The butanol was removed by blowing nitrogen gas to the solution meanwhile heating to evaporate the solvent (BuOH), and the residue was Soxhlet extracted with $CHCl_3$ and the insoluble Mg removed as a by-product. The resulting solution was concentrated by removing the solvent and chromatographed to get the desired product (**72**).

R_f = 0.3

Yield 49 %. Anal : Calcd. For $C_{44}H_{40}MgN_8$: C(74.94), H(5.72), N(15.89).

Found: C(73.06), H(4.92), N(15.68). IR(KBr cm^{-1}): 1483 (long alkyl chain), 1329 (Aryl-N-), 724 (substituted benzene ring). ^{1}HNMR (d_6-DMSO, 400 Hz) : 9.40-9.50 (m, 6H, $H_{-1,4Pc}$); 8.20-8.30(m, 6H, $H_{-2,3Pc}$); 7.60-7.70(d, 2H, $H_{-2,3Pc}$); 4.40-4.50 (s, 2H, H_{-CH2}); 4.20-4.30 (s, 2H, H_{-CH2}); 2.60-2.70 (m, 4H, H_{-CH2}); 2.21-2.30 (m, 4H, H_{-CH2}); 2.00-2.10 (d, 4H, H_{-CH2}); 1.60-1.80 (s, br, 2H, H_{-CH2}); 1.00-1.50 (m, 6H, H_{-CH2}); 0.80-0.90 (t, 6H, H_{-CH3}). UV-vis (DMSO): λ_{max}(nm): 672, 640, 605, 345.

3.5.5 Synthesis of di-1,4-hexyl phthalocyanato Zn(II) (**73**, Scheme **2.10**).

The complex mono(1,4)–hexylmagnesiumphthalocyanines (**72**) (0.09 g, 0.15 mmol) was dissolved in neat triflouroacetic acid (10-15 ml) and stirred at room temperature for 1 hr. The solution was poured over ice and neutralized with concentrated aqueous NH_3. The resulting precipitate was filtered and washed with water and MeOH. Then chromatographed with $CH_3OH/CHCl_3$ (1:3) as an eluent to give compound (**73**).
Yield 42 %. Anal : Calcd. For $C_{44}H_{40}N_8Zn$: C(70.82), H(5.40), N(15.02). Found : C(73.01), H(4.99), N(15.16). IR(KBr cm^{-1}): 1487 (long alkyl chain) , 1332 (Aryl-N-) , 726 (substituted benzene ring). ^1H NMR (d_6-DMSO, 400 Hz) : 9.60-9.70 (m, 6H, $H_{-1,4\text{-Pc}}$); 8.00-8.50 (m, 6H, $H_{-2,3\text{-Pc}}$); 7.80-7.90 (d, 2H, $H_{-2,3\text{-Pc}}$); 5.20-5.40 (s, 2H, H_{-CH2}); 4.80-4.90 (m, 2H, H_{-CH2}); 4.50-4.70 (s, 2H, H_{-CH2}); 2.50-2.54 (m, 4H, H_{-CH2}); 2.30-2.40 (d, 4H, H_{-CH2}); 1.80-2.10 (s, br, 4H, H_{-CH2}); 1.40-1.50 (m, 6H, H_{-CH2}); 0.90-1.20 (t, 6H, H_{-CH3}).
UV-vis (DMSO): λ_{max}(nm): 672, 638, 605, 341.

Summary of the synthesized porphyrazine (Pz) and phthalocyanine (Pc) complexes, represented by Figure **3.3.**

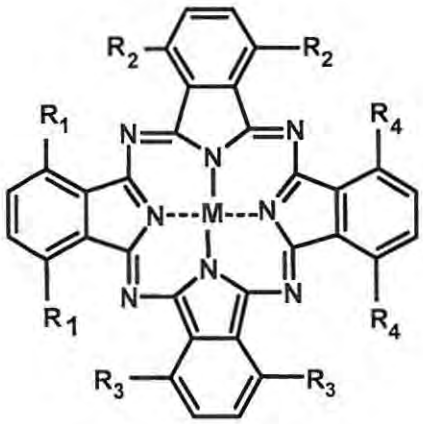

Pc

Pz

Pz complexes

62 $R_3 = NO_2$, $R_1, R_2, R_4, R_3', R_4' = H$, $M = Zn$

63 $R_1 =$ 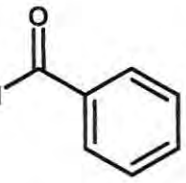 $R_2 = R_3 = R_4 = H$

64 $R_1 =$ 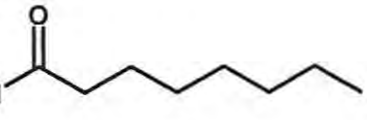 $R_2 = R_3 = R_4 = H$

65 $R_1 = R_2 =$ 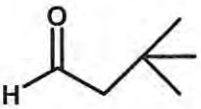 $R_3 = R_4 = H$

Pc complexes

66 $R_1 =$  $R_2 = R_3 = R'_3 = R'_4 = H$ $M = Zn$

67 $R_1 = R_2 =$  $R_3 = R_4 = H$ $M = Mg$

68 $R_1 = R_2 = R_3 = R_4 =$  $M = Mg$

69 $R_1 =$  $R_2 = R_3 = R'_3 = R'_4 = H$ $M = Zn$

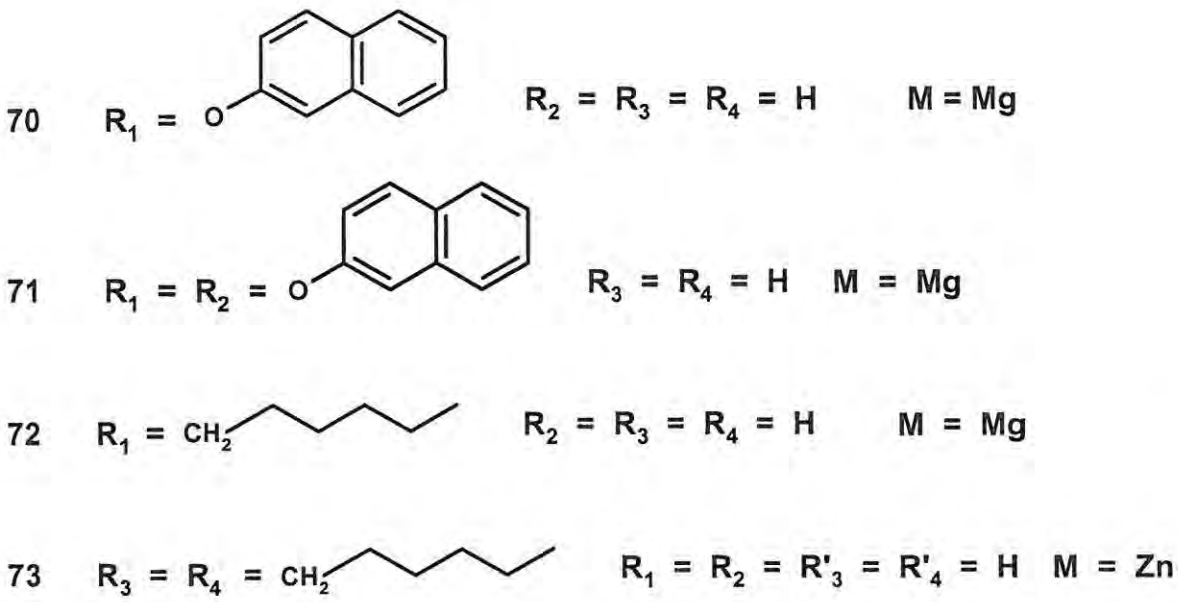

Figure 3.3 A representation of zinc and magnesium phthalocyanine and porphyrazine complexes synthesized.

References:

1. N. Kuznetzova, E. Makarova, S. Daskevich, N. Gretsova, V. Negrimovsky, O. Kaliya, E. Luk'yanet's, *Zh. Obshch. Khim*, 2000, **70**, 140.
2. J. C. Dalton and N. J. Turro, *Mol. Photochem*, 1970, **2**, 133.
3. R. P. Linstead. *J. Chem. Soc.* 1984, **136**, 1016.
4. N. A. Kuznetsova, N. S. Gretsova, E. A. Makarova, S. N. Dashkevich, V. M. Negrimovskii, O. L. Kaliya, and E. A. Luk'yanets, *Russ. J. Gen. Chem*, 2000, **70**, 133.
5. C. Bryant, M. J. Cook, T. G Ryan, and A. J. Thorne, *Tetrahedron*, 1996, **52**, 809.
6. D. Wohrle, M. Eskes, K. Shigehara, A. Yamada, *Synthesis*, 1993, 194.
7. A. Weitemeyer, H. Kliesch, D. Wohrle, *J.Org.Chem.*, 1995, **60** , 4903.
8. Practical Organic Chemistry including Qualitative Organic Analysis, I. Vogel, 3rd Edition, 1945, pg 797.
9. R. P. Linstead, *J. Chem. Soc*, 1934, 1016.
10. T. P. Forsyth, D. Bradley, G. Williams, A. G. Mantalban, C. L. Stern, A. G. M. Barrett , and B . Hoffman, *J.Org.Chem.* 1998, **63**, 331.
11. P. Matlaba, T. Nyokong, *Polyhedron,* 2002, **21**, 2463.
12. H. Ali, S. K. Sim, J. E. van Lier, *J.Chem. Research* (S) (1999) 496.
13. N. Kobayashi, R. Kondo, S. -I. Nakajima, T. Osa, *J. Am.Chem. Soc.* 1990, **112**, 9640.
14. A. Weitermeyer, H. Kliesch, D. Wohrle, *J. Org. Chem*, 1995, **60**, 4900.

4. CONCLUSION AND FUTURE WORK

Various methods were employed to obtain a number of substituted phthalocyanine derivatives, in order to study the effect of different substituents on the photophysical and photochemical properties.
The syntheses are easy, two different methods were used, namely the statistical condensation route and the so called subphthalocyanine route.
Several new compounds including alkyl, phenoxy and amide substituted macrocycles which showed very interesting physical as well as chemical characteristics have been synthesized, and these compounds may prove valuable in fields of study that reaches beyond this specific field.
However, a significant experience was obtained in our group on the synthesis as well as purification of these new compounds which requires extensive cleaning procedures to get the desired product.
The solubility as well as a shift of the Q-band towards the infrared region, with increase in electron donating groups of the compounds were observed.

In the present study the efficiency of phthalocyanine Mg and Zn complexes with di-, tetra- and octa- alky phenoxy substituted and amide substituted porphyrazines in sensitization of singlet oxygen were examined for the first time. It was observed that the increase in electron donating character of the alky phenoxy phthalocyanine macrocycle periphery leads to an increase in singlet oxygen quantum yields.
The amide substituted phthalocyanine macrocycle resulted in decrease in singlet oxygen quantum yield, this is probably due to the enhanced excited states reductive quenching by amide in DMSO. Complexes have singlet oxygen quantum yield ranging from 0.23 to 0.67 .

In terms of photostability, it was shown that Zn and Mg complexes undergo a photobleaching process which is mediated more likely by oxidation of the phthalocyanine ring. The complexes are relatively stable to photodegradation with quantum yields of photobleaching ranging in the

10^{-5}. However, all the complexes showed good potential as phototherapy drugs.

Future work could include the use of other available long alkyl, phenoxy and amide groups on the macrocyclic ring, the improvement of the used method and other methods for synthesis. An interesting study could also be an extensive electrochemical study of the effects of the different electron-withdrawing and electron-donating groups on these phthalocyanine derivatives. A study of the effect of substituents of these complexes in a cellular environment can also be useful.